ESTIMATING EROSION OF CRETACEOUS-AGED KIMBERLITES IN THE REPUBLIC OF SOUTH AFRICA THROUGH THE EXAMINATION OF UPPER-CRUSTAL XENOLITHS

A THESIS SUBMITTED IN PARTIAL FULFILLMENT OF THE REQUIREMENTS FOR THE DEGREE OF

MASTERS OF SCIENCE

AT

RHODES UNIVERSITY

BY

EMILY KATE HANSON

JANUARY 2007

ABSTRACT

The estimation of post-emplacement kimberlite erosion in South Africa through the study of upper-crustal xenoliths is relatively unexplored; however the presence of these xenoliths has been recognized for well over 100 years. Post-emplacement erosion levels of a small number of South African kimberlite pipes have been inferred through the study of the degree of country-rock diagenesis, the depth of sill formation, the depth of the initiation of the diatreme and fission track studies. Through these studies, several estimates were proposed for the Group I Kimberley kimberlites. Although the 1400 m estimate of erosion remains widely accepted today, this estimate relies on the presence of Karoo-like basalt xenoliths in the Group I Kimberley kimberlites, as their presence proves that basalt existed in the Kimberley area when the kimberlites were emplaced. Basaltic xenoliths were described during the early stages of mining in Kimberley, though only one of these descriptions suggests that the 'basaltic' boulders correlate with the Karoo basalts. Because of the discrepancy between these early documentations of upper-crustal xenoliths and because the occurrence of Karoo-like basalt xenoliths in the Group I Kimberley kimberlites is under question, a re-investigation of the erosion levels and the upper crustal xenolith suites in South African, Cretaceous-aged kimberlites, including Melton Wold, Voorspoed, Roberts Victor, West End, Record Stone Quarry, Finsch, Markt, Frank Smith, Pampoenpoort, Uintjiesberg, Koffiefontein / Ebenheuyser, Monastery, Kimberley (Big Hole), Kamfersdam , Jagersfontein, Kaal Vallei, De Beers, Bultfontein, Lushof, Britstown Cluster, Hebron and Lovedale, was conducted.

This study presents the analytical results for upper-crustal sandstone and basalt xenoliths collected from dumps, excavation pits and borehole core at the above-mentioned kimberlites, and demonstrates that they correlate with stratigraphic units of the Karoo Supergroup on the basis of mineral and geochemical compositions. These upper-crustal xenoliths are incorporated into kimberlites and down-rafted to levels below their stratigraphic position during kimberlite emplacement, consequently recording the broad stratigraphy into which each kimberlite is emplaced. Therefore, the Cretaceous lateral extent of the Karoo Supergroup is inferred and post-emplacement erosion estimated by reconstructing the stratigraphy based on upper-crustal xenolith suites for each kimberlite and calculating the total thickness of the now-eroded units.

The distribution of sandstone xenoliths indicates that during the Cretaceous the lateral extent of the Dwyka, Ecca and Beaufort Groups encompassed all of the examined kimberlites, while the 'Stormberg' Group was constrained to an area outlined by the Voorspoed and Monastery kimberlites. Similarly, basalt xenoliths occur in all of the Group II and transitional (143 – 100 Ma) kimberlites but only in the Group I (90 – 74 Ma) kimberlites that lie within close proximity to the western outcrop margin of the outcrop area of the Drakensberg Group basalts (Lesotho Remnant), namely Monastery, Jagersfontein and Kaal Vallei. This trend implies an eastward-retreat of the inland erosion front of the Karoo basalts between 140 and 90 Ma and subsequent erosion of the underlying sedimentary units. It also suggests that a thicker succession of Karoo strata was present at the time of Group II and transitional kimberlite emplacement and that there has been more post-emplacement erosion in these kimberlites than the younger Group I kimberlites, except for Monastery, Jagersfontein and Kaal Vallei. Estimates are unique to each kimberlite as they are dependent on both stratigraphic location, elevation and present country rock, and range from approximately 1000 – 2500 m for the older kimberlites and less than 700 m to 1400 m for the younger kimberlites.

Furthermore, the upper-crustal xenoliths found at the Group I Kimberley kimberlites and the coinciding trend of basalt erosion demonstrate that Karoo basalts were eroded from the Kimberley area by the time the Group I Kimberley kimberlites erupted (~85 Ma). Therefore, basalts are omitted from the Group I Kimberley kimberlites post-emplacement erosion estimate, and the upper Beaufort Group is considered the upper limit of the stratigraphy that was present at the time of the eruption of the Group I Kimberley pipes. Therefore, the erosion estimates decrease from a previous estimate of 1400 m down to 400 to 1100 m, where 850 m is considered a dependable intermediate estimate.

TABLE OF CONTENTS

LIST OF FIGURES

LIST OF TABLES

ACKNOWLEDGMENTS

My thanks and gratitude must be extended to several people:

De Beers Consolidated Mines Ltd. and RESCOM for funding and for the use of their facilities

J. Robey is thanked several times over for his assistance in the field, and for inspiring this project in collaboration with J. Ward

R. Scholz, L. Urban, J. Markram, R. Van Buren and W. de Jager for their help at De Beers, with the GIS databases and in searching for historical documents

J. Hepple and his staff for thin section preparation, sample preparation and for the time spent mending equipment

J. Abdy who kindly helped with sample crushing and preparation

M. Skinner for ever challenging discussions, as well as H. Tsikos, S. Bütner, S. Prevec, R. Prevec and V. Mitha for their assistance with various details

A. Goddard in sincerely thanked and acknowledged for her help with essentially everything

My deepest gratitude must also be extended to my advisor, J. Moore, my co-advisor E. Bordy, and J. Marsh. Thank you venturing into the field, for the sometimes difficult XRF sessions, for the numerous pieces of advice and criticisms, for wading through drafts of this text and for all of your time and energy. Thank you.

1. INTRODUCTION

1.1 INSPIRATION FOR THE PRESENT STUDY

Hawthorne's (1975) original kimberlite model and proposition of 1400 m of post-emplacement erosion in the Kimberley area (South Africa) are commonly quoted figures in Kimberlite Geology. Although the model and estimate are based on additional parameters besides the occurrence of basalt xenoliths in the kimberlite pipes, the presence of Karoo basalts in the Kimberley area at the time of emplacement of the Group I kimberlites (~85 Ma) remains a critical supporting argument for this erosion estimate (e.g., Clement, 1982; Field and Scott Smith, 1999b). However, the only published evidence for the presence of Karoo basalts remains the citations of a 70 ft (~20 m) rounded basalt boulder in the Kimberley mine (Matthews, 1887); a large floating reef described as a "xenolith of diabase, covering and area of 3,000 square feet (~900 m)," with fractures and veinlets in filled by calcite and zeolites (Wagner, 1914, p. 23), and an "amygdaloidal rock" (Williams, 1932, pg. 259); which have been interpreted as Karoo basalt by Williams (1932), Hawthorne (1975) and Clement (1982). However, when considered as observational statements, these documentations do not unequivocally qualify the above described xenoliths as Karoo basalt, but simply suggest that they are diabase (dolerite) and/or amygdaloidal 'rocks' and are therefore not indisputably of Karoo age.

In order to achieve 1400 m of post-emplacement erosion in the Kimberley area, the presence of Karoo basalts at ~85 Ma is essential. As stated above, the strongest evidence for or against the occurrence of Karoo basalts at ~85 Ma is the presence or absence of Karoo basalt xenoliths within the younger Kimberley kimberlites. However, since the original descriptions of the in-situ floating reefs and xenoliths, no Karoo-like basalts have been observed during mining operations of the Group I Kimberley pipes, nor at the dumps of earlier operations (Robey, pers. comm. 2006). The lack of recent records of Karoo basalt xenoliths therefore suggests the following possibilities:

1. The 'amygdaloidal rocks' or 'diabase' were incorrectly classified, and were actually xenoliths of Ventersdorp Supergroup basalts or Karoo-age intrusives (i.e., dolerites) respectively, which are prevalent in the Kimberley area, indicating that no Karoo basalts were present at ~85 Ma.

2. The xenoliths were interpreted correctly, but the small volume of Karoo basalt xenoliths within the Group I Kimberley pipes signifies that at most, a thin veneer of basalt covered the area at ~85 Ma.

Regardless of the interpretation, it is apparent that previous approximates overestimate the amount of erosion that has occurred since ~85 Ma (Robey and Ward, pers. comm. 2006). As a result, the Hawthorne (1975) model and the erosion patterns of South Africa's kimberlites as a whole must be reconsidered and new estimates generated using a simple and tangible method.

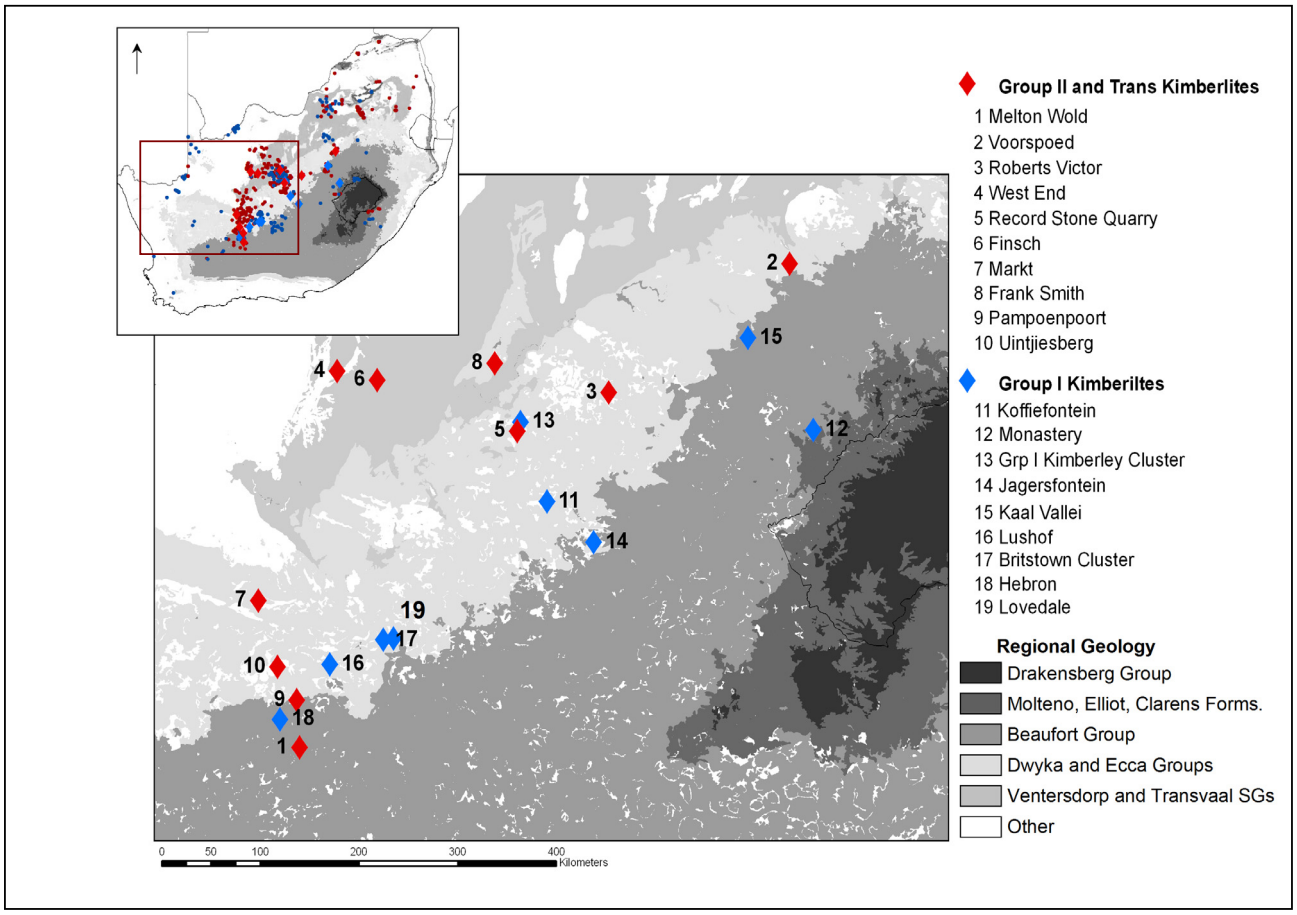

Figure 1.1: Map of the study area showing the kimberlites included in the study (Group II and transitional kimberlites – Red; Group I kimberlites – Blue) and the regional geology. Map constructed from the 1:250,000 Geological Maps, Geological Survey of South Africa; De Beers GIS database (unpubl.).

1.2 PURPOSE

Upper-crustal xenoliths have been poorly documented at kimberlite pipes in southern Africa. Therefore, one of the goals of this project is to provide documentation of these xenoliths at the kimberlites included in this study. In doing so, it is also possible to comment on post-emplacement erosion levels of these kimberlites.

A relatively unexplored and simple concept that can be applied to estimates of post-eruption kimberlite pipe erosion is the analysis of the crustal xenolith suites that occur within each kimberlite pipe. As kimberlites are emplaced, the ascending kimberlitic-magma samples rock fragments from the mantle and lower-crust, while upper-crustal fragments are incorporated into the kimberlite as infill. These fragments are preserved as xenoliths within the kimberlite body, and as a result, provide a record of the stratigraphic units into which the kimberlite was emplaced. By analysing these upper-crustal xenoliths and correlating them with known stratigraphic units (e.g., groups, formations), these xenoliths can provide insight into the general stratigraphic succession that was present at the time of kimberlite emplacement. Therefore, if a crude palaeo-stratigraphy is constructed for a given kimberlite pipe based on the xenolith suite, the thickness of this palaeo-stratigraphy can be broadly estimated, and thus the amount of erosion inferred. This method is based purely on the presence or absence of xenoliths that correlate with known stratigraphic units that are no longer preserved in the immediate proximity of the kimberlite pipe, and is therefore considered a tangible method of estimating erosion.

The purpose of this project is to apply this erosion estimate concept to a series of kimberlites across central South Africa (Figure 1.1). Except for West End and Finsch which intrude the basement complex, the kimberlites included in this study intrude into remnants of the Karoo Supergroup (KSG) and occur within both the main Karoo Basin and the projected extent of Karoo-province volcanism. Therefore, the upper crustal-xenoliths are analysed in order to correlate them with either the sedimentary units or the basalts of the KSG based on mineral and geochemical compositions respectively.

The kimberlite pipes were selected to cover a large enough geographic area and age range, approximately 143 to 70 Ma, to provide a representative sample of the xenolith suites regardless of either age or location. By analysing the xenolith suites of each of these kimberlites, it is possible to comment on the original depositional extent of each of the major Karoo Supergroup sedimentary units. Furthermore, the spatial and temporal distribution of basalt xenoliths may be utilized to approximate the extent of Karoo basalts at approximately 120 Ma and 85 Ma, based on xenoliths found in the older and younger kimberlites, to

determine if Karoo basalts were present at the time of kimberlite eruption, or if they had been removed prior to the time of the kimberlite emplacement. Ultimately, the results of the xenolith analyses may be utilised to generate erosion estimates for each of the kimberlites studied and to re-evaluate the Hawthorne (1975) model for post-emplacement erosion levels of the Group I Kimberley kimberlite cluster (KKC).

1.3 GEOLOGICAL SETTING

The study area extends across the central portion of the main Karoo Basin from Lesotho to Victoria West (South Africa), and includes 23 kimberlites ranging in age from approximately 143 to 70 Ma (Figure 1.1) (Table 1a). Xenoliths were collected and analysed from 17 of these locations, namely Melton Wold, Voorspoed, Roberts Victor, West End, Record Stone Quarry / Wimbledon, Finsch, Markt, Frank Smith, Pampoenpoort, Uintjiesberg, Koffiefontein / Ebenheuyser, Monastery, Kimberley[1], Jagersfontein, Kaal Vallei, DeBeers[1] and Bultfontein[1]. The other 6 locations, Kamfersdam[1], Lushof[2], Britstown cluster[2], Hebron[2] and Lovedale[2], were only visited to confirm the absence of basalt xenoliths. Brief descriptions of these kimberlites are provided in Table 1a.

Regional geology of the study area includes the sedimentary Dwyka, Ecca, Beaufort and 'Stormberg' Groups of the Late Palaeozoic-Early Mesozoic KSG, with the Drakensberg Group basalts occurring to the east in Lesotho, while Archaean Ventersdorp Supergroup (VSG) lavas, Proterozoic Transvaal Supergroup and Cenozoic Kalahari Group sedimentary rocks outcrop in the northwest (Figure 1.1). The sedimentary units of the KSG dominate the study area, and are the present surface country rock for all of the kimberlites except for Finsch and West End, which intrude the dolomites of the Transvaal Supergroup (Table 1a). The KSG sedimentary units continue at depth in the south and south-eastern parts of the study area (e.g., Catuneanu *et al.,* 1998); while the basalts of the VSG occur at shallow depths in the Kimberley area and extend towards the north and northwest (e.g., Hawthorne, 1975). In the cratonic environment, the KSG or VSG units rest on the Archaean basement granite gneiss, while the KSG in the off-craton areas is directly underlain by the Proterozoic Namaqua Metamorphic Complex (Skinner *et al.,* 1992) or the Cape Supergroup.

[1] The Kimberley, De Beers, Bultfontein and Kamfersdam kimberlites make up the KKC
[2] These kimberlites will be referred to as the LBH pipes

Kimberlite Pipes Sampled	Abrv	Age	Grp	Cratonic Environment	Exposed Facies (kimberlite type)	Country Rock (relative position within group)	Diamondiferous / Mined
Melton Wold	MW	143 ± 14[1]	II t	Off-craton	Diatreme (VK)	Beaufort (basal)	No
Voorspoed	V	131 ± 1.7[2]	II	On-craton	Diatreme (VK)	Ecca (middle)	Yes
Roberts Victor	RV	127.3[3]	II	On-craton	Diatreme (VK)	Ecca (lower)	Yes
West End	WE	118[4]	II	On-craton	Root (MK)	Transvaal Supergroup	Yes
Record Stone Quarry / Wimbeldon	RSQ	118[4]	II	On-craton	Root (MK)	Ecca (basal)	Yes
Finsch	FN	118.4 ± 2.2[1]	II	On-craton	Diatreme (VK)	Transvaal Supergroup	Yes
Markt	MK	116.8 ± 1[5]	II	On-craton	Root (MK)	Ecca (basal)	No
Frank Smith	FS	116.2 ± 3[1]	II	On-craton	Diatreme (VK)	Ecca (basal)	Yes
Pampoenpoort	PP	103.2 ± 0.7[5]	I t	Off-craton	Root (MK)	Ecca (upper)	No
Uintjiesberg	UJ	100.7 ± 1.4[1]	II	Off-craton	Diatreme (VK)	Ecca (middle)	No
Koffiefontein / Ebenheuyser	KF	90.4[6]	I	On-craton	Diatreme (VK)	Ecca (middle)	Yes
Monastery	M	88 ± 4[3]	I	On-craton	Diatreme (VK)	Molteno (upper)	Yes
Kimberley (Big Hole)	BH	87 ± 1[4]	I	On-craton	Diatreme (VK)	Ecca / Dwyka Contact	Yes
Jagersfontein	JG	85.6 ± 1[1]	I	On-craton	Diatreme (VK)	Ecca (upper)	Yes
Kaal Vallei	KV	84.9 ± 0.9[7]	I	On-craton	Diatreme (VK)	Ecca (upper)	Yes
De Beers	DB	84.3 ± 3[3]	I	On-craton	Diatreme (VK)	Ecca / Dwyka Contact	Yes
Bultfontein	BF	84 ± 0.9[7]	I	On-craton	Diatreme (VK)	Ecca / Dwyka Contact	Yes
KIMBERLITES PIPES VISITED							
Kamfersdam	**KKC**	86.9[6]	I	On-craton	Diatreme (VK)	Ecca / Dwyka Contact	Yes
Lushof	**LBH**	78.3[6]	I	Off-craton	Diatreme (VK)	Ecca (upper)	No
Britstown Cluster	*LBH*	74.4 ± 0.8[5]	I	On-craton	Root (MK	Ecca (upper)	No
Hebron	*LBH*	74[4]	I	Off-craton	Diatreme (VK)	Beaufort (basal)	No
Lovedale	*LBH*	74[4]	I	On-craton	Root (MK)	Ecca (upper)	No

[1]Smith *et al.,* 1985
[2]Phillips *et al.,* 1999
[3]Allsopp and Barret, 1975
[4]De Beers database (unpubl.)
[5]Smith *et al.,* 1994
[6]Davis, 1977
[7]Kramers *et al.,* 1983

Table 1a: Brief description of the kimberlites included in the present study, abbreviations used for sample numbering. Exposed kimberlite type from the De Beers GIS database (unpbl.) with terminology after Sparks *et al.* (2006); country rock information obtained from 1:250,000 Geological Maps, Geological Survey of South Africa, maps: 2726, 2822, 2824, 2826, 2922, 2924, 3022, 3122

2. NEAR-SURFACE KIMBERLITE EMPLACEMENT AND XENOLITH INCORPORATION

2.1 KIMBERLITE EMPLACEMENT MODELS

Several models attempt to describe the mechanism responsible for the near-surface emplacement of typical South African kimberlite bodies (Field and Scott Smith's (1999a) class 1), although the exact nature of kimberlite formation remains contentious. At present, there are three dominant schools of thought:

1. The dynamic-volcanism model (Sparks *et al.,* 2006) is based on a modern understanding of volcanic and magmatic processes and is the most recent approach to kimberlite emplacement.
2. The magmatic fluidization model (e.g., Dawson, 1971; Clement, 1975, 1982; Field and Scott Smith, 1999b; Skinner and Marsh, 2004) based on magma degassing is a commonly quoted and accepted theory for kimberlite eruption
3. The phreatomagmatic model (e.g. Lorenz, 1973, 1975, 1985, 1993; Lorenz *et al.,* 1999) is based on the interaction of the kimberlitic-magma with groundwater and is often criticized as this process is not considered necessary for the 'explosion' of kimberlites (see Sparks *et al.,* 2006).

The primary differences between the models lie in the mechanism required for magma eruption, either degassing or groundwater interactions, and the nature of pipe initiation and formation, from the bottom upwards or from the top downwards.

2.1.1 Dynamic Volcanism Model

Recently, Sparks *et al.* (2006) applied a modern understanding of the physical processes of volcanism to develop a four-stage conceptual model of kimberlite emplacement (Figure 2.1). In this model, pipe formation is initiated from the top downwards by near surface explosive expansions resulting from the high volatile content of the kimberlite magma. In stage I, the initial cratering stage, kimberlite magma ascends to the Earth's surface via narrow fissures. Within a few hundred metres below the surface, the explosive pressure of the magma, due to the volatile content, exceeds the atmospheric pressure causing explosive surface cratering and the initiation of pipe formation. The crater widens and deepens from the top downwards during stage II. As the pipe increases in size, under-pressures result in rock-bursts, which vary with factors such as lithology and can lead to undermining of overlying rocks and slumping of the pipe wall and inner crater, all of which

contribute to the widening and deepening of the pipe. At this stage, pipes are sometimes emptied allowing pieces of wall rock to fall deep into the expanding pipe.

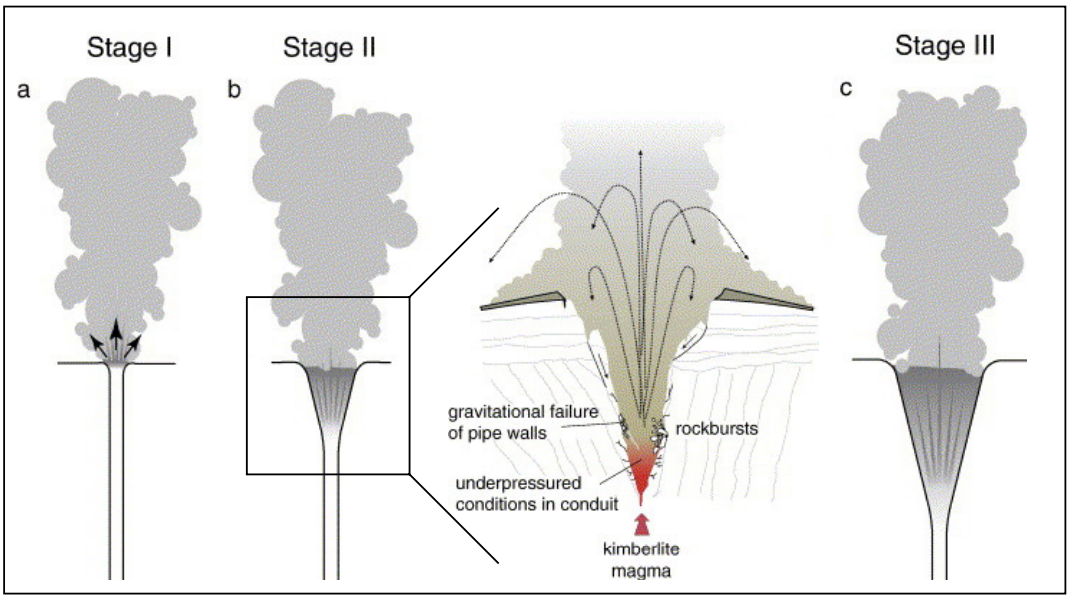

Figure 2.1: First three stages of the dynamic volcanism model. a) Initial cratering and diatreme formation stage is characterized by overpressured, choked flow of the magma. b) As the crater widens and deepens the exit pressure equalizes to the atmospheric pressure, during this time there are rock bursts and slumping of the wall rock due to under-pressures. c) Gas exit velocity decreases due to the increased size in the diatreme and pressure-adjusted conditions are achieved. Modified after Sparks *et al.* (2006).

The transition from stage II to III, the infilling stage, is likely to be gradual with alternating phases of emptying and filling. As the pipe continues to widen and deepen, the gas exit velocity decreases as under-pressures increase and material that would have been ejected in stage II becomes trapped within the pipe. During this stage, breccias and volcanoclastic kimberlite (VK)[3] are preserved at the outer margins of the kimberlite. Eventually, magma supply rates and degassing decrease allowing the development of magmatic kimberlite (MK)[4] at the base of the pipe through late-stage welding processes. After eruption has ceased and the hot volcanoclastic deposits are emplaced within the pipe, the magma body begins to cool, a process that may take tens to hundreds of years. During the cooling period, stage IV, the circulation of meteoric water results in hydrothermal

[3] Sparks *et al.* (2006) adopt the term volcanoclastic kimberlite (VK) to describe the kimberlite that underwent explosion during emplacement. VK is the equivalent of tuffisitic kimberlite or tuffisitic kimberlite breccia (TK, TKB) in other models

[4] Sparks *et al.* (2006) apply the term magmatic kimberlite (MK) to intrusive kimberlite, which dominates the root zone, and was previously termed hypabyssal kimberlite (HK) (e.g. Clement, 1982; Field and Scott Smith, 1999b)

alteration and serpentinization of the kimberlite magma and low temperature alteration occurs as thermal equilibrium with the surrounding environment is achieved (Sparks *et al.,* 2006). Unlike the other models discussed below, the model of Sparks *et al.* (2006) is not dependant on country-rock composition, the presence of competent cap rocks or the occurrence of abundant groundwater.

2.1.2 Magmatic Fluidization Model

Variations of this model are based on the degassing concept, and consider near-surface kimberlite eruption a result of magma pulses and the near-surface fluidization of volatile-rich magma through explosive degassing. Field and Scott Smith (1999b) present the most recent fluidization model, which is based on the original models proposed by Dawson (1971), Clement (1975, 1982) and Clement and Reid (1989). In the Field and Scott Smith (1999b) model for the emplacement of southern African kimberlites, embryonic pipes are generated through multiple magma pulses (Figure 2.2). As the magma ascends along joints in the country rock, the volatiles migrate and concentrate at the front of the magma. When the ascending magma reaches a barrier, such as a dolerite sill, there is a hiatus in the upward movement of the magma. During this time, increased pressure in the magma causes fracturing and brecciation of the country rock until the barrier is breached allowing the magma to continue its ascent until it reaches another barrier where the process is repeated. As the magma rises by exploiting weaknesses in the country rock, the magma column increases in size and volatiles are exsolved.

When the magma reaches the final barrier, or 'cap rock', the continued exsolution of volatiles increases the volatile pressure and fractures the cap rock, which subsequently decreases the capping pressure. When the volatile pressure exceeds the lithostatic pressure, there is an explosive breakthrough and cratering at the surface followed by magma degassing whereby fluidization of the magma and authigenic brecciation of the country rock along the margins of the embryonic pipe occurs. After breaching the surface, the magma continues to ascend while the degassing front descends causing erosion and collapse of the country rock, which enlarges the base of the crater, excavates the diatreme from the top downwards and allows for the incorporation of country rock fragments into the fluidized magma. Finally, the system cools rapidly, quenching the vapour phases, and material is ejected to form a pyroclastic eruption which infills the crater as pyroclastic kimberlite (PK). In this model, the diatreme infill, tuffisitic kimberlite breccia (TKB), is the part of the magma column that underwent fluidization, whereas the hypabyssal kimberlite (HK), present in the root zone, is

formed by magma that did not experience degassing or fluidization, and thus the transition between the two is the preserved degassing front. Therefore, the textural and mineralogical differences found in the different types of kimberlitic rocks are a manifestation of the different stages of volatile exsolution and fluidization (Skinner and Marsh, 2004).

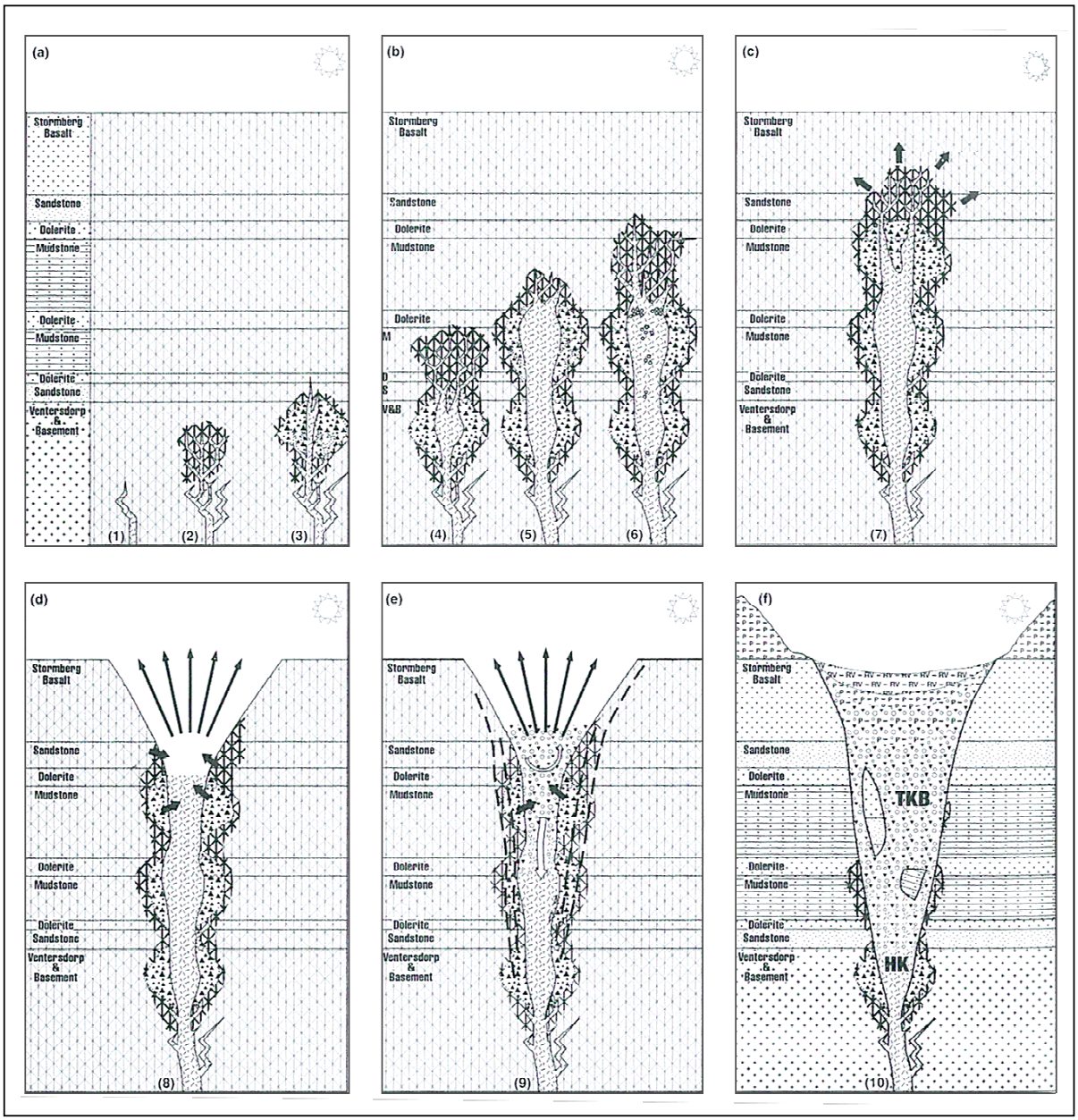

Figure 2.2: Magmatic fluidization model showing the development of the embryonic pipe and diatreme. Note the necessity for dolerite sills and a competent capping rock. Symbols as follows: thickened joint lines = fracturing of country rock due to rising magma; solid triangles = breccia with country rock clasts; arrows = volatile movement into country rock; white arrow = fluidization; short black arrows = implosion; thick dashed lines = gradual widening of the diatreme; inverted triangles = small, angular country rock xenoliths; dashes = HK. After Field and Scott Smith (1999b).

According to Field and Scott Smith (1999b), there is a correlation between the type and shape of the kimberlite pipe and the nature of the country rock into which the kimberlite is emplaced. To generate the typical Cretaceous southern African kimberlite (Figure 1.1), intermittent layers of country rock with different lithological strengths, such as sedimentary units intruded by dolerite sills, and a competent capping rock, such as basaltic lava, are required. Therefore, the magmatic fluidization model relies on the presence of Karoo basalts at the time of kimberlite emplacement. Specific temperatures and pressures, which occur approximately 2 km below the original surface, are also required for the initial expansion through degassing and formation of diatreme facies kimberlite (Dawson, 1971; Skinner and Marsh, 2004).

2.1.3 Phreatomagmatic Model

Lorenz (1973, 1975) pioneered the phreatomagmatic model for South African kimberlites, which attributes the near-surface explosion of kimberlite magma to interactions with groundwater such as a large aquifer, or surface water that may occur as a lake, river or shallow sea (Lorenz, 1985). According to Lorenz *et al.* (1999), kimberlite magma ascends via narrow fissures where it interacts with near-surface groundwater causing several small, short-lived explosions that brecciate and fragment the country rock ultimately generating an explosion crater. This explosion also results in a fine fragmentation of the melt and decoupling of water from the melt by means of evaporation, which then expands and fragments the melt further. With continued magma pulses and water supply into the brecciated rocks, further explosions at the top of the kimberlite dyke, or the root zone, act to fragment the country rock more and allow deeper penetration of the groundwater and the downward migration of the explosion interface. Over time, an increase in mass deficiency, caused by the mass ejecting explosions, causes failure in the overlying rocks and a concurrent subsidence of these rocks into the root zone, producing a pipe-shaped diatreme. Growth of the diatreme continues in this manner as long as the kimberlite magma ascends along the fissures and groundwater remains within the system. Eventually, as the groundwater supply is depleted, the eruptions cease and the ascending magma intrudes the diatreme to form dykes and plugs. The site of the final explosions is preserved as the root zone, the top of which marks the transition from hypabyssal (HK) to diatreme facies or tuffisitic kimberlite breccia (TKB).

This model accounts for the high percentage of country rock xenoliths found within kimberlite bodies, as the shapes and abundance of these clasts are indicative of explosive

crushing processes (Lorenz *et al.,* 1999). Here, the xenoliths are incorporated into the kimberlite magma as result of brecciation, fragmentation and eventual down-slumping of the country rock. However, this model has often been discounted for the South African type kimberlites because interactions between water and juvenile gases are not considered a requisite for kimberlite emplacement (e.g. Field and Scott Smith, 1999b; Sparks *et al.*, 2006). Some researchers believe that phreatomagmatism was possibly a contributing factor in the emplacement of some of the southern African kimberlites (Clement and Reid, 1989), but phreatomagmatism is mainly ascribed to the Canadian setting, as groundwater interactions can account for the flared shape observed in most of the Canadian pipes (Field and Scott Smith, 1999b).

2.2 Incorporation, Distribution and Nature of Xenoliths

Four main types of xenoliths, or foreign inclusions, ranging in size from microscopic fragments to large 'floating reefs', occur within kimberlite bodies: those derived from the upper mantle; those entrained from the lower crust; fragments from the immediate wall rock; and upper crustal xenoliths of earlier formations that were present near-surface at the time of kimberlite emplacement and were subsequently removed by post-emplacement erosion (e.g. Wagner, 1914; Williams, 1932; Dawson, 1980). The upper crustal xenoliths are of primary interest for this project because they crudely reflect the original stratigraphic succession through which the kimberlite erupted (Williams, 1932; Hawthorne, 1975; Clement, 1982). Furthermore, they provide an indication of the extent of the stratigraphic units from which the xenoliths were derived at the time of kimberlite emplacement.

It is apparent that these xenoliths were incorporated into the kimberlite magma at a level below their stratigraphic position. However the means by which they were brought down to such depths is dependant on kimberlite emplacement mechanisms, and thus varies with different emplacement models. According to Wagner (1914) and Williams (1932), fractured country rock must have collapsed into the "fractured crust" where the fragments were eventually carried by the erupting magma. Through the up-and-down movement within the magma, sinking occurred due to differences in specific gravity and water movement, and the rock fragments were carried to depths of 800 m (Williams, 1932) to 1.5 - 2 km (Clement, 1982) below their stratigraphic position. Similarly, Clement (1982) attributes xenolith distribution to buoyant mixing and downward sinking prior to the final crystallization of the pipe.

The models discussed above all require that upper crustal xenoliths are incorporated into the kimberlite magma by means of collapse due to erosion, fragmentation or under-pressure. The main difference between these models lies in whether the country rock collapses directly into the magma (Field and Scott Smith, 1999b) such that the distribution of the fragments is dependant on mixing processes within the magma as well as density of the fragments (e.g., Clement, 1982), or if the fragments subside into an open diatreme (Sparks *et al.*, 2006) and are carried down by gravitational forces. In the magmatic fluidization model, the size of the fragments that sink, as well as the depth to which they sink, is dependant on the degree of degassing the magma experiences. It is therefore probable that the depth of xenolith down-rafting varies from pipe to pipe. While the larger and denser blocks tend to sink, the smaller and less dense fragments are carried upwards by the fluidized system (Field and Scott Smith, 1999b). Conversely, in the dynamic volcanism model the country rocks are able to collapse and fall to depth in an open crater (Sparks *et al.*, 2006) where, presumably, they are later entrained by the rising magma and redistributed in the kimberlite pipe.

Regardless of the means by which upper crustal xenoliths are incorporated and distributed within the kimberlite magma, observations show that they are most prevalent in the diatreme zone (TKB or VK), and that large floating reefs are generally concentrated towards the perimeter (Hawthorne, 1975; Clement, 1982). Although most of the larger reefs are down-rafted from their stratigraphic position, a small percentage of these reefs were apparently displaced upwards by the magma (Williams, 1932). The large floating reefs, such as those found in the KKC and Finsch pipes, occur as either amalgamated columns of brecciated and fragmented rocks of one or more types, or as discrete and competent blocks of a single rock type displaying little to no internal disruption. Like the latter, smaller xenoliths are also known to be well-preserved with little thermal or chemical alteration, thus implying that the magma temperatures were relatively low during xenolith entrainment (Williams, 1932). Skinner and Marsh (2004) also cite the relatively pristine nature of the xenoliths as evidence that the xenoliths were incorporated into the diatreme facies kimberlite (DKF, composed of TKB or VK) during the formation of the diatreme system.

Xenoliths found towards the base of the diatreme or in the root zone (HK or MK) are predominantly derived from the upper mantle or local country rock (Clement, 1982). According to some researchers, upper crustal xenoliths are not found at such depths as the transportation of the crustal xenoliths requires motion that only occurs in the fluidized system (e.g., Skinner, pers. comm. 2006). Although the intrusions of a small number of kimberlites appear devoid of upper crustal xenoliths, sedimentary and dolerite fragments have been noted

in low abundances within the hypabyssal / magmatic facies of most of the Kimberley kimberlites (Clement, 1975, 1982). This confirms that xenoliths can be down-rafted to such levels and incorporated in both the root zone and intruding bodies during kimberlite emplacement. The xenoliths found within the HK / MK are generally restricted to 0.5 to 10 cm , very rarely up to 1 m in diameter, while microscopic fragments are rare and no large reefs are known (Clement, 1982).

2.3 Previous Citations of Upper Crustal Xenoliths

The presence of these upper crustal xenoliths has been recognized for well over 100 years, and early reports of Karoo Supergroup xenoliths in South African kimberlites include those presented by Matthews (1887), Du Toit (1906), Rogers and Du Toit (1909), Harger (1913), Wagner (1914) and Williams (1932). Most accounts are based on observations of features such as colour, grain size, fracture and amygdale composition, and focus on the upper units, such as the Beaufort and 'Stormberg' Group sandstones and Drakensberg Group basalts.

2.3.1 Kimberlites Included in Present Study

Karoo SG Sedimentary Rock Xenoliths

Beaufort Group mudstones, siltstones and sandstones have been observed at Melton Wold (Mambali, 1998), Voorspoed, Roberts Victor, Finch, Koffiefontein, Monastery, Jagersfontein and the KKC pipes. At Voorspoed (V), Roberts Victor (RV), Koffiefontein (KF), Monastery (M), Jagersfontein (JG) and the KKC they occur as "red, sandy mudstones" (Williams, 1932), as well as "white sandstones" and "large rounded sandstones" at RV and JG, "purplish shale" at KF and "olive green shale" at the KKC (Wagner, 1914). The Finsch xenoliths are more variable, with red, purple, yellow, black and green mudstones and shales, and white to buff sandstones all interpreted as originating from the Beaufort Group (Visser, 1972; Clement, 1982). Results of a geochemical study of the sandstone xenoliths in the KKC pipes suggest that they were mostly derived from the Ecca Group and lower portion of the Beaufort Group (Rambula, 2005). Furthermore, several fossils were found within the kimberlite xenoliths of Kimberley, including fish, endothiodont reptiles and plants that are unique to the Beaufort-aged sedimentary units (Wagner, 1914). As a result, Beaufort Group shales and sandstones were definitely present in the Kimberley area at ~85 Ma.

Citations of 'Stormberg'-like xenoliths are restricted to red and reddish-brown shales found at the Voorspoed, Jagersfontein and KKC pipes and are interpreted as originating from

the ‘Red Beds’ (Elliot Formation) (Wagner, 1914, Williams, 1932). However, the red, sandy mudstones with smooth fractures and ‘Cave sandstones’ (Clarens Formation) present in the KKC pipes and interpreted as originating from the ‘Stormberg’ Group by Wagner (1914) were later interpreted as oxidized Beaufort Group rocks by Williams (1932).

Karoo Basalt Xenoliths

Except for Roberts Victor, Record Stone Quarry, Pampoenpoort, Kaal Vallei and the LBH kimberlites, Karoo-like basalts were noted at all of the kimberlites included in the present study by previous researchers. The lack of recorded occurrences of basalt xenoliths in the above listed kimberlites may be attributed to either lack of documentation on these pipes, in the case of RV, RQS, PP and KV, or the absence of Karoo basalts at the time of kimberlite emplacement, a likely scenario for the LBH pipes.

Early qualifications that the basalt xenoliths are in fact of Karoo affinity were predominantly based on macroscopic observations, petrographic descriptions and amygdale composition. For example, V, MK, FS, UJ, KF and JG contain vesicular basalts with zeolite amygdales that Wagner (1914) suggests are “petrographically identical” to the Karoo basalts. These statements are based on previous accounts and descriptions of vesicular and amygdaloidal lavas in the V, KF, JG (Harger, 1913), FS (Du Toit, 1906) and UJ (Rogers and Du Toit, 1909) kimberlites. The basalts in the MK and UJ are described as dark in colour, usually amygdaloidal, with vesicles filled with zeolites, they are usually weathered, and are petrographically most similar to the Drakensberg Group basalts (Rogers and Du Toit, 1909).

In addition to the above records, Williams (1932) also notes the presence of amygdaloidal basalts that are “petrographically similar” to the Karoo basalts in the WE, M (described by Harger, 1913) and KKC pipes. Recent geochemical studies of basalt xenoliths collected from the MW, V and UJ kimberlites indicate that the basalts are from Drakensberg Group as they are geochemically similar to the Lesotho Formation basalts (Letsale, 1998; Mambali, 1998; Roberts, 1997). The Finsch basalt xenoliths are grayish-green to red-brown, amygdaloidal or massive, and vary from microscopic fragments to large floating reefs up to 600 m below the present surface (Clement, 1982).

As previously mentioned, the most controversial of these observations is the presence of Karoo-like basalts in the KKC because no basalts, other than Ventersdorp, have been observed recently at these kimberlites. Careful review of the documentation of the igneous and volcanic xenoliths observed during early mining operations reveals that the original descriptions of these xenoliths in the KKC do not provide any indication that they are similar

to the Karoo basalts, e.g. amygdaloidal texture or zeolite amygdales. While Matthews (1887) and Wagner (1914) both cite the presence of basaltic fragments or amygdaloidal diabase in the KKC, neither implies that they correlate with the Karoo basalts.

> "Huge masses of igneous rock were likewise quite common in the upper levels of the Kimberley pipes. Matthews (1887), for example, refers to an enormous rounded boulder of basalt with a diameter of 70 ft, which was found in the Kimberley Mine. Similarly, the well known 'island' in the De Beers Mine was nothing else than a xenolith of diabase, covering an area of 3,000 square feet, and extending to a depth of almost 800 feet" (Wagner, 1914, p. 23).

Here, Wagner (1914) refers to diabase, which can be considered a Karoo dolerite, as well as a basaltic boulder. Matthews' (1887) description of these accidental inclusions, and specifically of this basaltic boulder, is as follows:

> "They ['erratic boulders'] consisted for the most part of dark and light coloured shales, whinstone or basaltic boulders, and large masses of fine grained micaceous sandstones containing fragments of coal and the remains of fossil reptiles…Several remarkable detached boulders were found…There was one isolated basaltic boulder, nearly round, of gigantic proportions. It almost filled up two claims…and measured 70 feet in diameter…It was much decomposed, and large flakes or layers frequently fell away into neighboring claims…The upper portion of this stone in the yellow ground had a yellow, and the lower portion in the blue a blue tint…
>
> The floating reef proper in the Kimberley mine…was formed of a light olive-gray coloured laminated shale, with a few rounded stones and angular pieces of basaltic rock, as well as occasional fragments of fine grained sandstone" (Matthews, 1887, p. 147-148).

Note that Matthews (1887) never refers to an amygdaloidal texture when describing the basaltic fragments and boulders that he observed, and that whinstone refers to dolerite, basalt or any other fine-grained, dark igneous rock. Later reports on the country rock found at the Kimberley mines describe the near-surface rocks as a basic igneous series of basalts and dolerites, probably Karoo in age (Rastall, 1906). In all likeliness, Rastall (1906) is referring to the dolerite dykes and sills that occur at shallow depths in Kimberley. Similarly, there are contradictory descriptions of the xenoliths found in the KKC. For example, several samples classified as basalt by Becker (1904) were later described as olivine or quartz diabase by Lindgren (1905)[5]. Lindgren's (1905) descriptions suggest that the samples are likely Ventersdorp Supergroup lavas. Because of the common interchanging of 'dolerite', 'diabase' and 'basaltic' in respect to basic igneous rocks, Matthews' (1887) account of basaltic fragments should not be construed as 'amygdaloidal basalts'.

[5] Samples 74,898, 75,899, 74,900, 75,941, 75,945 75,950 in Becker (1904) and Lindgren (1905)

Furthermore, Wagner (1914) lists a series of kimberlites that contain "fragments of vesicular basalt with zeolite amygdales" (p. 24) that are considered petrographically identical to the Stormberg series lavas [Drakensberg Group]. While Voorspoed, Koffiefontein, Jagersfontein, Frank Smith, Untjiesberg and Markt are included in this list, the KKC are not mentioned. Therefore, according to Wagner (1914), Karoo basalts xenoliths do not occur in the KKC, and therefore the basalts were not preserved in the Kimberley area when the KKC pipes were emplaced.

On the other hand, Williams (1932) states that there are amygdaloidal xenoliths in the Kimberley pipes and that they are in fact of Karoo affinity, and considers their presence proof that the entire Karoo Supergroup (i.e., the Dwyka, Ecca, Beaufort, 'Stormberg' and Drakensberg Groups) occurred in the Kimberley area.

> "In the Kimberley and adjacent Orange Free State pipes and fissures the common inclusions are dolerite, black Dwyka shale, melaphyre (amygdaloidal diabase), quartzite, quartz-porphyry, gneiss and granite and of formations now eroded, *i.e.,* Beaufort sandstones, grey and blue Ecca shales, sandstones of the Stormberg series, and an amygdaloidal rock corresponding to the amygdaloidal lava of the Drakensberg" (Williams, 1932, p. 259).

In reference to xenoliths from formations now eroded, Williams (1932) lists the Jagersfontein, Voorspoed, Kimberley, Newlands, Frank Smith, Crown, West End, Postmasburg and Monastery mines as having xenoliths with pipe amygdales, thus showing that "the area that must have been covered by these lavas [Stormberg Series, Drakensberg volcanic beds]" (p. 274).

In contradiction, in an earlier reference to "rubble" inclusions in the Kimberley pipes, Williams (1932) lists melaphyre with little to no Ecca or Beaufort fragments in the Kimberley mine; Beaufort sandstone, Dwyka shale and melaphyre in the De Beers mine; Dwyka shale, Beaufort sandstone and dolerite in the Bultfontein mine; and shale, dolerite and Beaufort sandstone in the Wesselton mine (p. 93). Here, no reference is made to basaltic inclusions. If another quote presented by Williams (1932) is considered, it is apparent that he differentiates between diabase and dolerite, which are both dark coloured igneous rocks that are the intrusive equivalent of basalt:

> "In Dutoitspan, Bultfontein and Wesselton mines, these inclusion [xenoliths] appear from the surface to the lowest workings, and are composed of a mixture of Beaufort sandstones, Ecca shales, quartzites, dolerite and diabase" (Williams, 1932, pg. 270).

Prior to the above statement, A. Williams (1932) cites Gardner Williams' earlier descriptions of the 'amygdaloidal diabase':

> "The mass of country rock [De Beers mine] continued from the surface to a depth of about 800 feet, and was composed of olivine diabase of amygdaloidal structure, Ecca shale and Beaufort sandstone. Gardner Williams was of the opinion that the olivine diabase rock found as an inclusion in the kimberlite was the same rock that he afterwards met at a depth of 244 feet when sinking the first De Beers main rockshaft. This particular rock has since been called melaphyre, and in the Kimberley district is one of the country rocks surrounding the kimberlite pipes. Later investigations proved conclusively that the huge inclusion was composed of melaphyre, sandstone and shale, and that the melaphyre was identical with the melaphyre which surrounded the pipe…" (Williams, 1932, p. 269-270).

Presumably, the rocks intersected at depth are the Ventersdorp Supergroup lavas which are found in the Kimberley area at depths of approximately 75 – 220 m (250 – 700 ft) (Rastall, 1906), and the 'olivine diabase of amygdaloidal structure' referred to as melaphyre is actually part of the Ventersdorp Supergroup (see Harger 1909, p. 154). Therefore, the reference to dolerite and diabase in Williams' (1932) above statement should be read as 'Beaufort sandstones, Ecca shales, quartzite and dolerite melaphyre' where the dolerite is from the near-surface Karoo dolerite sills preserved in the Kimberley area. Williams (1932) also describes the large floating reef in the Dutoitspan mine, known as Mount Ararat, as a mass of diabase (see p. 178; 271-272). In this case, Williams believes that the floating reef was uplifted by plastic magma, suggesting that Mount Ararat was composed of Karoo dolerite.

The question still remains as to the reference to the "amygdaloidal rock corresponding to the amygdaloidal lava of the Drakensberg" (Williams, 1932, pg. 259) in the Kimberley pipes. According to Hawthorne (1975), the lavas described by Williams (1932) are identifiable by their colour, the presence of zeolite and calcite pipe amygdales so there is little doubt that they are of Karoo origin. Even so, if one considers earlier descriptions of xenoliths in the KKC (*e.g.* Matthews, 1887; Wagner, 1914) and recognizes that Williams' (1932) text is, for the most part, a compilation of this work, then it is apparent that Williams may have misinterpreted previous citations of igneous xenoliths. Because Williams (1932) is the only author who cites the presence of amygdaloidal, Karoo-like basalts in the Kimberley pipes, other than more recent researchers such as Hawthorne (1975) and Clement (1982) who refer Williams (1932) when discussing the basalt xenoliths, it is unlikely that basalts were present in Kimberley approximately 85 Ma when the KKC erupted.

2.3.2 Kimberlites Not Included in Present Study

The red sandy mudstone xenoliths described above were also noted in the Lace / Crown Kimberlite (located in the Free State) by Williams (1932). Vesicular and amygdaloidal basalt xenoliths were also reported in the Lace / Crown, Riet Gat (Victoria West area), Newlands (Rogers and Du Toit, 1909; Harger, 1913; Wagner, 1914; Williams, 1932) and Darleston kimberlites (Ward, pers. comm. 2006).

2.4 Application to Present Study

Early citations of upper crustal xenoliths provide both a historical database with which the results of the present study can be compared, and evidence that it is possible to correlate the xenoliths with units of the KSG. If the xenolith correlations discussed above are correct, then several assumptions can be made, including: 1) Karoo basalts covered the study area until at least ~85 Ma, when the KKC were emplaced; 2) Hawthorne's erosion estimate is inadequate for the KKC kimberlites. However, except for sandstone xenoliths from the KKC and basalt xenoliths from MW, V and UJ, no mineralogical or geochemical examinations of these xenoliths have been utilized to correlate the xenoliths with the stratigraphy of the Karoo Supergroup. Therefore, one of the primary objectives of this project is to re-examine previous accounts and descriptions of these xenoliths and to use more objective methods to identify the source of each of the analyzed samples.

3. SANDSTONE XENOLITHS: OVERVIEW OF THE KAROO SUPERGROUP SEDIMENTARY UNITS AND CORRELATION OF THE SANDSTONE XENOLITHS

3.1 SEDIMENTARY UNITS OF THE KAROO SUPERGROUP: A DEPOSITIONAL, LITHOLOGIC AND PETROGRAPHIC OVERVIEW

3.1.1 INTRODUCTION

The KSG consists of sedimentary and igneous sequences preserved in several basins throughout southern Africa from the Late Carboniferous through the Early Jurassic. Deposition of the predominantly clastic sedimentary units of the KSG began at approximately 300 Ma (Visser, 1997) and continued for 120 million years, until sedimentation was disrupted by the initiation of continental flood basalt volcanism at 183 Ma (Duncan *et al*., 1997), resulting in the formation of the Drakensberg Group (Figure 2.2).

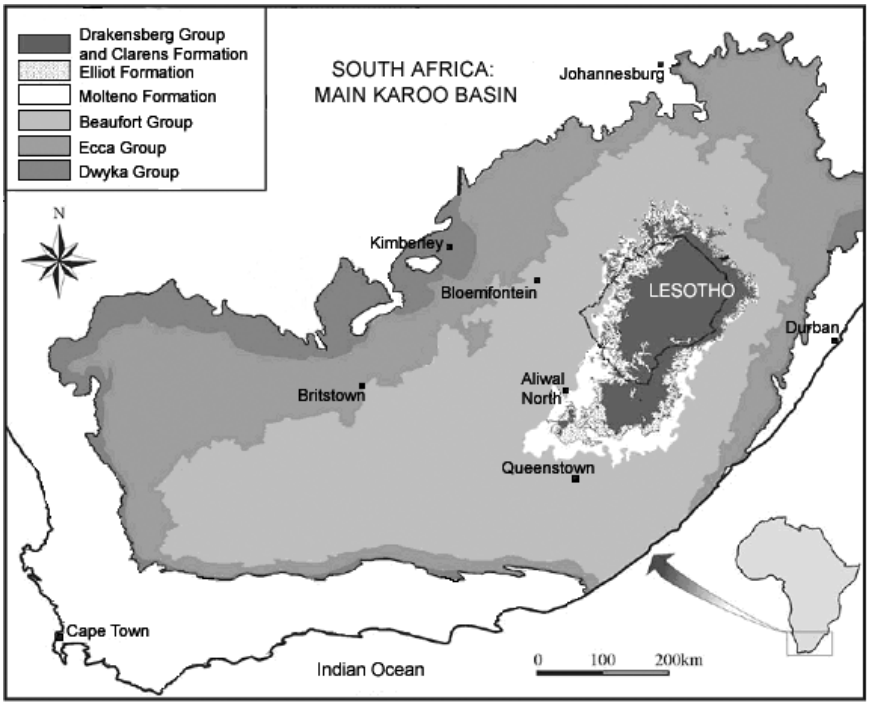

Figure 2.1: Geological map of the main Karoo Basin (after Catuneanu *et al.,* 1998; Bordy *et al*., 2004).

Lithostratigraphic units in the KSG include, from the base, the Dwyka and Ecca Groups, the Adelaide and Tarkastad Subgroups of the Beaufort Group and the Molteno, Elliot and Clarens Formations of the "Stormberg" Group (Johnson, 1994) (Figs. 2.1, 2.2). The present outcrop area of these lithostratigraphic units within the main Karoo Basin, an area of approximately 600,000 km^2 (Cole, 1992), represents eroded remains of the original

deposition area (Figure 2.1). Pre-erosion cumulative thickness of the Karoo sedimentary units varies between 10,000 m (Johnson *et al*., 1996) and 12,000 m (Cole, 1992). Ignoring the shift of the depositional axis, the total maximum thickness of the entire succession is estimated to be about 20,000 m (Johnson, 1991).

Following is a brief discussion of the development of the main Karoo Basin as well as a detailed description of the Dwyka, Ecca and Beaufort Groups and the Molteno, Elliot and Clarens Formations.

3.1.2 DEVELOPMENT OF THE MAIN KAROO BASIN

The main Karoo Basin is considered a retro-arc foreland basin as it is associated with a magmatic arc and fold-thrust belt (Cape Fold Belt) system (e.g., Cole, 1992; Johnson, 1991; Catuneanu *et al.,* 1998). Although the evolution of the basin remains a topic of debate, the foreland-basin evolution model presented by Catuneanu *et al.* (1998) indicates that the stratigraphy of the Karoo sedimentary units was influenced by foreland-basin tectonics from the initiation through to the termination of sedimentation.

The retroarc foreland basin evolved in relation to the subduction of the palaeo-Pacific plate under the Gondwana plate during the Late Carboniferous and continued into the Early Jurassic (Cole, 1992, Catuneanu *et al*., 1998). During this time, the basin developed into proximal foredeep and distal forebulge environments (Catuneanu *et al*., 1998). The basic premise of the model generated by Catuneanu *et al.*. (1998) is as follows:

Sedimentation was controlled by first-order cycles of orogenic loading and unloading overprinted by second-order sequence events. In the first order orogenic loading phase, represented by the Late Carboniferous to the Middle Triassic Dwyka, Ecca and Beaufort Group rocks, accommodation was mainly confined to the proximal foredeep and to a lesser extent to the distal forebulge region. In the subsequent first-order unloading phase, represented by the Late Triassic to Early Jurassic Molteno, Elliot and Clarens Formations, uplift decreased the accommodation in the foredeep and increased accommodation in the area of the previous forebulge, which transformed into a foresag (Catuneanu *et al.*, 1998; Bordy *et al*., 2005).

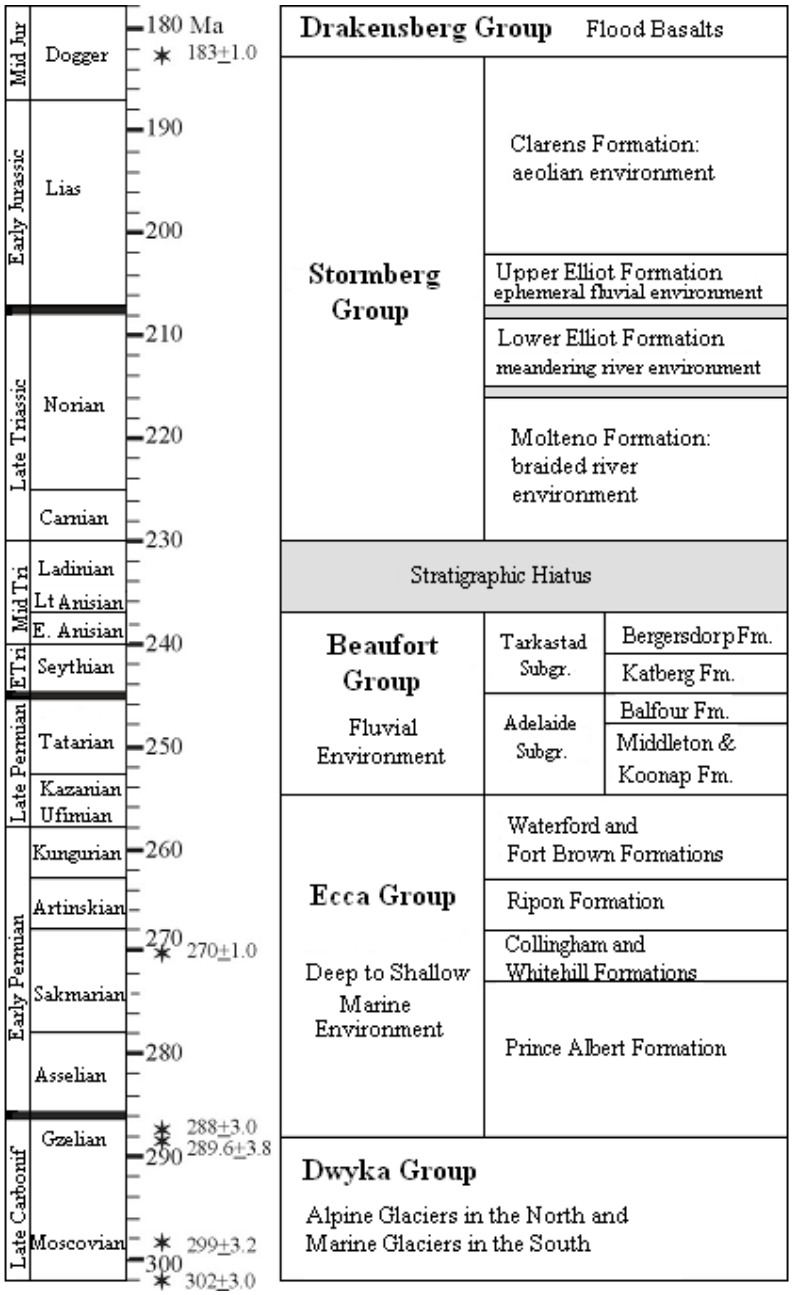

Figure 3.2: Lithostratigraphy of the Karoo Supergroup within the southeastern portion of the main Karoo Basin. Unpublished illustration provided by E. Bordy. (Based on: Catuneanu and Elango, 2001; Catuneanu *et al*, 2002; Bordy *et al*., 2004 with radiometric ages based on Bangert *et al.,* 1999; Turner, 1999; Catuneanu *et al*., 2002; Duncan *et al*., 1997; Rubidge, 1995; Smith and Kitching, 1997).

However, this broad trend is complicated by second-order cycles generated by tectonic 'paroxysms' or orogenic pulses and subsequent orogenic quiescence, which trigger stages of tectonic loading and unloading that manifest in distinct sedimentary packages and

unconformities throughout the KSG (Catuneanu *et al*., 1998). In addition, climatic changes, eustatic sea level fluctuations and localized factors such as differential basement tectonics also influence the development of retro-arc foreland basins and lateral distribution of available accommodation space (Catuneanu, 2004).

3.1.3 DWYKA GROUP

3.1.3a Geological Overview

The Late Carboniferous Dwyka Group, comprising glacially derived tillite, shale and minor sandstone, is the basal member of the Karoo Supergroup (Johnson, 1991; Cole, 1992; Visser *et al*., 1997) (Figure 2.1). Sedimentation of the Dwyka Group began approximately 300 Ma ago and culminated at 290 Ma with ice sheet regression (Bangert *et al*., 1999). In the southern portion of the main Karoo Basin, the glacial deposits disconformably or paraconformably overlie the Witteberg Group of the Cape Supergroup (Veevers *et al*., 1994; Johnson, 1991). North of 33˚S, Dwyka sedimentary rocks rest unconformably on undulating pre-Karoo surfaces underlain by older stratigraphic units such as the Ventersdorp Supergroup lavas (Visser *et al*., 1976-77). Because of the basal contact with the irregular pre-Karoo surfaces, measured thickness of the Dwyka Group is locally variable (Johnson, 1994). However, on a regional scale, the Dwyka Group thins from a maximum thickness of 700 m (Johnson, 1991) to 800 m (Visser *et al*., 1990; Johnson, 1994) in the foredeep basin in the south down to 80 – 100 m in the north, and locally down to 30 m in the Kimberley – Britstown area (Visser *et al*., 1976-77).

Dwyka Group sedimentary rocks were deposited in a glacial environment, with glacio-fluvial, deltaic and lacustrine deposits in the north and glacio-marine deposits in the south (Visser, 1986; Cole, 1992; Catuneanu *et al.*, 1998). Glacial pavement, provenance and basement palaeo-topography studies indicate initial ice flow directions from the northeast to the southwest, followed by east to west and ending with southeast to northwest trend (Visser *et al*., 1976-77; Visser *et al*., 1997).

3.1.3b Lithology

The Dwyka Group sedimentary rocks consist of tillite, shale and sandstones, with tillite being the dominant lithology (Johnson, 1976). According to Visser (1997) and Visser *et a*l. (1997), these lithologies represent deglaciation sequences that are characterised by sharp basal contacts with a basal tillite overlain by mudrock, sandstone, siltstone, shale and subordinate conglomerate of variable thickness. In the northern parts of the basin, moraine

deposits are preserved as a basal tillite overlain by a stratified terminal zone successions with lenses of diamictite, sandstone and shale (Visser, 1986; Visser *et al*., 1976-77).

Tillite: According to Visser *et al.* (1976-77) and Johnson (1976, 1991, 1994), tillite present in the Dwyka Group is dark blue-grey to green-black and weathers to a yellowish or olive-grey colour. It is composed of poorly sorted pebble- to cobble-sized clasts suspended in a fine argillaceous to sandy matrix. Larger clasts tend to be rounded and are sometimes facetted and striated. The matrix is poorly sorted and ranges from mud to sand with angular to rounded grains of (in descending order) quartz, feldspar and rock fragments. The tillite is usually massive, though it can be crudely stratified or bedded.

Sandstone: Sandstone occurs as intercalated units within the tillite and as well-developed units towards the top of the Dwyka Group (Johnson, 1976; Visser *et al*., 1976-77). Visser *et al*. (1976-77) report that the sandstones are greenish-grey to brown, fine- to medium-grained, poorly to moderately sorted and micaceous with subrounded grains. They are composed of quartz, feldspar, chert, quartzite and lava fragments cemented by calcite. Trough cross-bedding, slumping and bioturbation are present (Table 3a).

Shale: Dwyka Group shale is typically varved, blue-green to green-brown units with 0.15 mm to 50 mm thick laminae (Visser *et al*., 1976-77).

Other: Visser *et al*. (1976-77) report limestone lenses up to 1 m thick in the Britstown-Kimberley area. These units are dark grey to black with cross-bedding and oolitic structures. Chemically precipitated and replacement carbonates are most abundant with minor stromatolitic limestone in the Prieska area. The limestone units formed by replacement contain small, less than 0.5 cm in diameter, fragments of quartz and feldspar. Volcanic tuff beds also occur in some areas of the Dwyka Group (Cole, 1992).

3.1.3c Provenance

Johnson (1991) shows that the Dwyka Group sandstones plot in the transitional continental provenance field of monocrystalline quartz, feldspar and total lithic fragments (Qm:F:Lt) diagrams (Figure 2.3A). However, this study is limited to the analysis of a single sample, and thus the provenance of the Dwyka Group sandstones is likely more widespread.

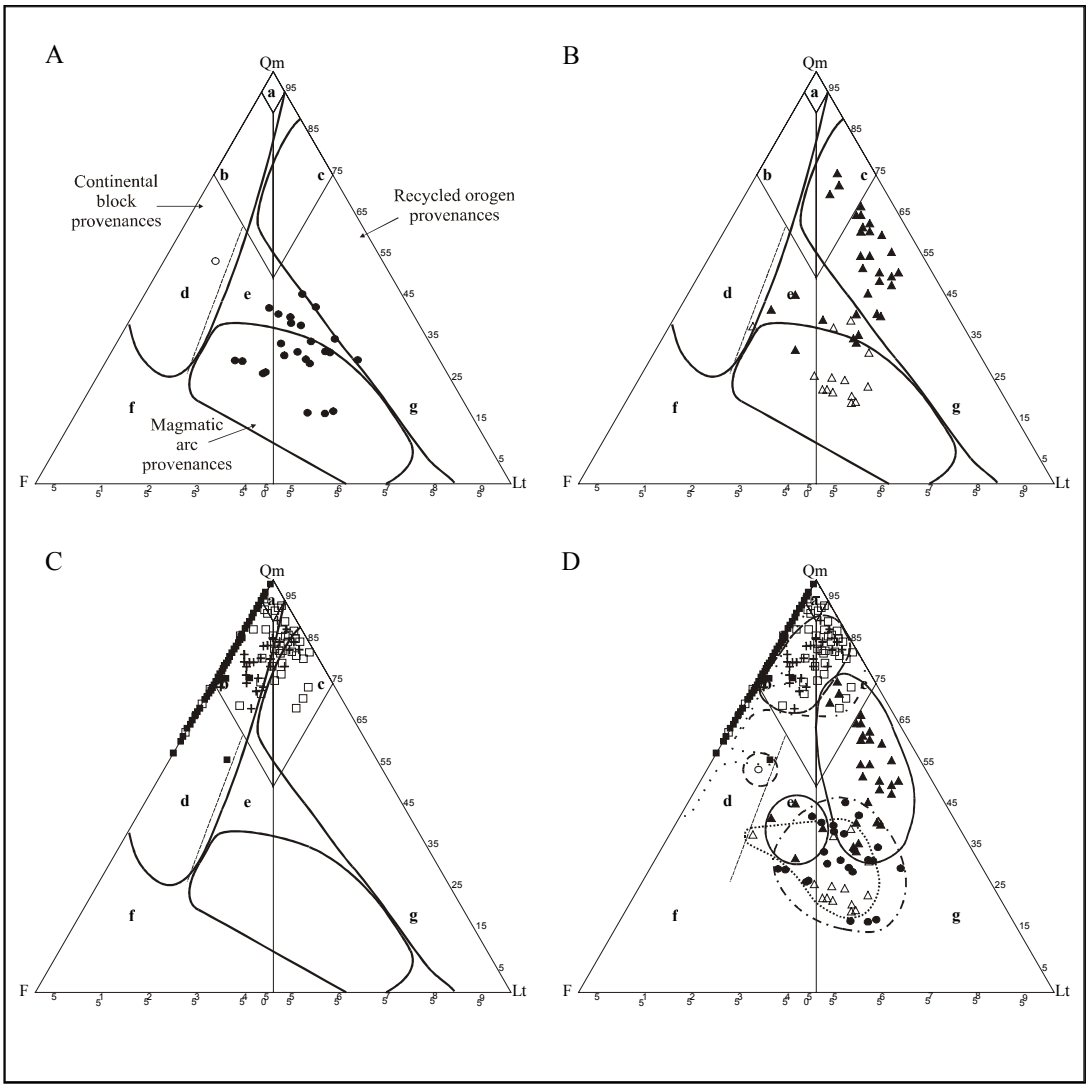

Figure 3.3: Ternary diagrams showing KSG sandstone point-counting data presented in previous studies. A) Dwyka Group (○) (Johnson, 1991) and Ecca Group (●) (Kingsley, 1977; Johnson, 1991; Fiedler and Adelmann, 1998); B) Beaufort Group, Adelaide Subgroup (Δ) (Johnson, 1991; Haycock *et al.*., 1997; Fiedler and Adelmann, 1998); Tarkastad Subgroup (▲) (Johnson, 1991; Hancox, 1998; Haycock *et al*., 1997); C) 'Stormberg' Group, Molteno Formation (+) (Eriksson, 1984; Johnson, 1991; Hancox, 1998); Elliot Formation (□) (Eriksson, 1984; Johnson, 1991; Bordy *et al*., 2004); Clarens Formation (■) (Eriksson, 1984; Johnson, 1991). D) Compilation of all data with inferred fields for each of the stratigraphic units used for correlation purposes. Qm:F:Lt (monocrystalline quartz : feldspar : total lithic fragments). Classification: a- quartz arenite, b- subarkose, c- sublitharenite, d- arkose, e- lithic arkose, f- arkosic arenite, g- litharenite, after Pettijohn *et al*. (1987). Provenance Fields after Dickinson *et al*. (1983).

3.1.4 ECCA GROUP

3.1.4a Geological Overview

The sedimentation of the Ecca Group began approximately 290 Ma with ice sheet retreat and continued throughout most of the Permian (Bangert *et al*., 1999). The transition from Dwyka to Ecca Group sedimentation was gradual and generated a conformable, diachronous contact that youngs to the north (Cole, 1992). Sedimentary units of the Ecca Group thin to the north, with a maximum thickness of 3,000 m in the foredeep in the south and thinning to less than 900 m in the forebulge region in the north (Johnson, 1976; Johnson, 1994; Johnson *et al*., 1996).

With the exception of the uppermost and northern formations, the Ecca Group was deposited in a marine environment. For example, the basal units were deposited in a deep water, reducing environment with submarine fans (Catuneanu *et al*., 1998). However, with oceanic regression, the environment evolved into a shallow marine and eventually a continental fluvial setting, especially in the distal, northern portion of the basin. This transition gave rise to distal to proximal submarine fan, regressive marine, delta front and eventually fluvial facies assemblages (Smith, 1990; Cole, 1992; Veevers *et al*., 1994; Catuneanu *et al*., 1998; Rubidge *et al*., 2000).

3.1.4b Lithology

The Ecca Group sedimentary units include shale, mudstone and coal with inter-dispersed siltstone, sandstone and minor conglomerate (Johnson, 1994; Johnson *et al*., 1996). Shale and mudstone are the predominant rock types and the abundance of sandstone increases upward in the succession. In the proximal region there are coarsening upward sequences, while in the upper distal region fining and coarsening upward sequences occur; however the broad grain-size trend of the Ecca Group is coarsening upward (Johnson, 1994; Johnson *et al*., 1996; Catuneanu *et al*., 1998). Tuffaceous layers and chert bands also occur throughout the succession (Johnson, 1976).

Sandstone: The Ecca Group sandstones are dark grey to light grey in colour (Johnson, 1976), very fine- to fine-grained (Johnson, 1976; Visser *et al*., 1976-77) and rarely medium-grained (Van Lente *et al*., 2003). They are grain-supported with matrix contents ranging from 10% (Fielder and Adelmann, 1998) to 20% to 30% (Johnson, 1976). Sedimentary structures such as ripple cross-lamination, horizontal bedding and planar cross-stratification occur (Rubidge

et al., 2000). Some sandstones have a mottled appearance, with calc-silicate dominated pale spots set in a dark matrix (Johnson, 1976).

Siltstone: In the Britstown-Kimberley area, Ecca Group siltstones are greenish and bluish grey with ripple cross-lamination (Visser *et al*., 1976-77). In the south, the siltstones are dark, organic rich and are characterized by fine horizontal laminations (Rubidge *et al*., 2000).

Shale and Mudstone: The argillaceous units are dark grey, medium grey, black, bluish-green and olive-grey. They are compositionally variable with micaceous, pyritic and carbonaceous varieties (Johnson, 1976; Visser *et al*., 1976-77; Rubidge *et al*., 2000). In the Kimberley and Britstown area, Visser *et al*., (1976-77) observed illite and chlorite as the dominant clay minerals as well as calcite, minor quartz and feldspar. According to Johnson (1976), the Ecca Group shales and mudstones are typically laminated and less commonly massive, and throughout the Group, the mudstones are characterized by 'platy' or 'flaky' weathering. Varved sequences also occur where the fine layer tends to be thicker than the coarse layer.

Other: As previously mentioned, other rock types within the Ecca Group include tuffs and chert. The tuffs are yellowish to greyish yellow (Johnson, 1976) and are rhyodacitic in composition (Viljoen, 1990). Chert occurs as interbedded layers within the shale and mudstone units (Johnson, 1976). Large, 10-15 cm in diameter, dark brown and black calcareous nodules or concretions are also prevalent within the Ecca Group. These nodules are roughly spherical and usually contain a shale fragment nucleus (Johnson, 1976; Rubidge *et al*., 2000).

3.1.4c Sandstone Petrography

Petrographic analyses indicate the sandstones are lithicarkoses and ultralithofeldspathic and feldspathic litharenites (Johnson, 1991; Fiedler and Adelmann, 1998) (Figure 2.3A). Quartz mainly occurs as well-rounded monocrystalline grains or long, sharp slivers that are unstrained with no inclusions. Grain boundaries tend to be concavo-convex and overgrowths are common (Kingsley, 1977; Fiedler and Adelmann, 1998). Plagioclase is the dominant feldspar, followed by potassium feldspar, microcline and myrmecite (Johnson, 1991). Plagioclase grains exhibit albite and lesser pericline twinning and occur as oligoclase or albite (Kingsley, 1977), whereas potassium feldspars are characterized by Carlsbad twinning (Fiedler and Adelmann, 1998). Both are fresh to strongly

altered, where alteration occurs as calcite, clay or sericite replacements. Rock fragments include (in ascending order) sedimentary, including chert, and metasedimentary, metamorphic and volcanic fragments (Johnson, 1976; Fiedler and Adelmann, 1998). Argillite and shale are the dominant sedimentary rock fragment types and are characterized by irregular grain boundaries that conform to surrounding grains. The metamorphic fragments are predominantly subrounded mica schists (Kingsley, 1977) and the volcanic fragments are large, lath-shaped feldspars set in a finer-grained, partially altered groundmass (Fiedler and Adelmann, 1998). The heavy minerals present are zircon, rutile, garnet, apatite and tourmaline with occasional sphene and epidote (Kingsley, 1977; Fiedler and Adelmann, 1998) (Table 3a).

3.1.4d Provenance

Qm:F:Lt data of the Ecca Group plot within the recycled orogen and transitional magmatic arc provenance fields (Johnson, 1991; Fiedler and Adelmann, 1998) (Figure 2.3A). The Ecca Group in the southern part of the basin was most likely derived from the Cape Fold Belt as well as an active magmatic arc (Veevers *et al*., 1994; Fiedler and Adelmann, 1998). The interbedded volcanic tuffs resulted from volcanism near the palaeo-Pacific plate margin (Cole, 1992).

3.1.5 BEAUFORT GROUP

3.1.5a Geological Overview

The Late Permian - Middle Triassic Beaufort Group consists of fluvial and lacustrine strata (Johnson, 1994; Haycock *et al*., 1997) (Figure 2.2). According to Rubidge *et al*. (2000), the Ecca-Beaufort contact is conformable and diachronous (youngs to the north), and can be associated with the gradual regression of the Ecca-sea. The upper contact is unconformable as a stratigraphic hiatus associated with erosion of the Beaufort Group sediments occurred prior to the deposition of the overlying Molteno Formation (Veevers *et al*., 1994).

Currently the Beaufort Group succession covers an area of 150,000 (Smith, 1990) to 200,000 km^2 in South Africa (Catuneanu *et al*., 2005) (Figure 2.1). The preserved thickness of the southern units is 6000 to 7000 m (Johnson, 1994; Johnson, 1976; Veevers *et al*., 1994) and rapidly thins northward to 700 m in the Free State (Johnson, 1994) and 500 m at the northern end of the basin (Smith, 1990). The Beaufort Group is subdivided into the basal Adelaide and the upper Tarkastad Subgroups (Johnson, 1976; Johnson, 1994).

Adelaide Subgroup

The Adelaide Subgroup was deposited in the Late Permian (Johnson *et al*., 1996) and it is the thicker of the two units, ranging from south to north from 5,000 to 800 m (Johnson, 1976). Adelaide Subgroup sedimentary rocks were deposited in a fluvio-lacustrine environment in which the proximal environments were dominated by lakes and high-energy braided systems that graded into lower energy, high-sinuosity meandering channels, whereas the distal regions were characterized by meandering rivers with wide semiarid flood plains (Johnson *et al*., 1996; Catuneanu *et al*., 1998; Rubidge *et al.*, 2000).

Tarkastad Subgroup

The unconformably overlying Tarkastad Subgroup is Early to Middle Triassic in age (Johnson *et al*., 1996). The deposits are relatively thin, thinning from 1,900 m in the south to 850 m in the north (Johnson, 1976). During the early stages of deposition, uplift along the southern margin of the basin introduced coarser material and re-generated the fluvial systems (Cole, 1992). Sediments were deposited by braided, low-sinuosity rivers that again graded into meandering systems with associated flood plains (Johnson, 1991; Johnson *et al*., 1996).

3.1.5b Lithology

Adelaide Subgroup

Lithological units present in the Adelaide Subgroup include sandstone, siltstone and mudstone as well as pebble lags (Rubidge *et al*., 2000) organized in fining-upward sequences with basal erosive surfaces. According to Haycock *et al*. (1997) and Rubidge *et al*. (2000), the coarsest units occur within the northern deposits.

Sandstone: The sandstone units range from light olive to light grey, greenish grey, bluish grey and yellowish and are very fine- to coarse grained (Haycock *et al*., 1997; Johnson, 1976; Catuneanu *et al*., 1998). Some sandstones, such as those found in the Palingkloof Member, are moderately sorted (Haycock *et al*., 1997). Trough cross-stratification, horizontal stratification and ripple cross-lamination structures occur within the different facies (Rubidge *et al*., 2000).

Siltstone and Mudstone: The siltstones and mudstones are pale blue-grey, olive, dark green and occasionally greyish red to reddish purple. They are predominantly massive, though horizontal lamination and ripple cross-lamination also occur. Post-depositional structures

include wrinkle marks and mudcracks (Johnson, 1976; Johnson, 1994; Veevers *et al*., 1994; Haycock *et al*., 1997; Rubidge *et al*., 2000).

Other: Reddish-brown calcareous concretions of various sizes, some of which are fossil-bearing, occur within the fines (Rubidge *et al*., 2000). Ashflow tuffs with pumice lapilli have also been reported (Veevers *et al.,* 1994).

Tarkastad Subgroup

The Tarkastad Subgroup is dominated by sandstone with lesser silt and mudstones (Haycock *et al*., 1997). However, mudstone abundance tends to increase away from margins of the basin (Johnson, 1976). Like the Adelaide Subgroup, the Tarkastad Subgroup sedimentary rocks occur as a series of fining-upward successions that may be construed as a single fining-upward sequence (Johnson, 1976; Catuneanu *et al*., 1998).

Sandstone: Tarkastad Subgroup sandstones are light olive to grey, pale blue-grey, brownish grey, greenish grey and very light grey in colour. Grain sizes range from fine to coarse, with the average grain size being coarser than that of the Adelaide Subgroup sandstones (Haycock *et al.,* 1997). Proximal sandstones are characterized by horizontal and trough cross-stratification; whereas the distal samples are dominantly planar cross-stratified or horizontally bedded (Johnson, 1976; Haycock *et al*., 1997).

Siltstone and Mudstone: Siltstone and mudstone units are less abundant than in the Adelaide Subgroup; however red mudstones are more prevalent (Veevers *et al*., 1994). Other colours include medium greenish grey and bluish grey with lesser pale blue and dark grey (Johnson, 1976; Johnson, 1994; Haycock *et al*., 1997).

Other: Small concretions, 10 to 130 mm in diameter, occur throughout the Tarkastad Subgroup sedimentary rocks (Haycock *et al*., 1997).

3.1.5c Sandstone Petrography

Adelaide Subgroup

Adelaide Subgroup sandstones are classified as ultralithofeldspathic and are similar in composition to the Ecca Group sandstones (Johnson, 1991). The lower Adelaide Subgroup sandstones are indistinguishable from those of the upper Ecca Group (Fiedler and Adelmann,

1998). Like the Ecca Group sandstones, monocrystalline quartz is usually well-rounded (Fiedler and Adelmann, 1998), although grains with undulose extinction are dominant (Kingsley, 1977). Compositionally, plagioclase is more abundant than potassium feldspar and both are fresh to strongly altered to calcite, clay or sericite (Fiedler and Adelmann, 1998). The high percentage of lithic fragments is dominated by felsic, volcanic fragments (Johnson, 1976; Fiedler and Adelmann, 1998; Johnson, 1991). Heavy minerals found within the Adelaide Subgroup sandstones are similar to those in the Ecca Group sandstones and include zircon, rutile, garnet, apatite and tourmaline with occasional sphene and epidote (Kingsley, 1977; Fiedler and Adelmann, 1998) (Table 3a).

Tarkastad Subgroup

Lithic sandstones represent the most abundant sandstone type within the Tarkastad Subgroup (Johnson, 1991). Quartz content increases up-sequence at the expense of feldspar (Johnson, 1991). Quartz grains are sub-angular to subrounded with low to high sphericity and secondary overgrowths are common. Plagioclase and orthoclase, the dominant feldspars, are fresh to strongly altered to sericite and kaolinite (Haycock *et al*., 1997). Lithic fragments are dominated by felsic grains of a fine-grained quartz and feldspar mosaic (Johnson, 1976). Accessory minerals include biotite, muscovite, epidote, zoisite, chlorite, zircon and rutile. Calcite cement occurs within some of the sandstone units (Haycock *et al*., 1997) (Table 3a).

3.1.5d Provenance

The Cape Fold Belt acted as the major provenance for the entire Beaufort Group succession with other inputs from the magmatic arc further south, the cratonic highlands in the northeast (Johnson *et al*., 1996), and the Proterozoic Maurice Ewing Bank basement in the southeast (Haycock *et al*., 1997). Provenance of the Adelaide Subgroup is similar to the Ecca Group. Adelaide Subgroup sandstones plot within the transitional magmatic arc and dissected arc fields of Qm:F:Lt diagrams (Figure 2.3B). With transition into the Tarkastad Subgroup, the provenance shifts into the dissected arc and transitional recycled orogen fields (Johnson, 1991) (Figure 2.3B). The transition in provenance is likely related to uplift and folding of the Cape Supergroup (Johnson, 1976; Johnson *et al*., 1996).

3.1.6 'STORMBERG' GROUP

3.1.6a Geological Overview

The informal 'Stormberg' Group was deposited throughout the Middle Triassic and Early Jurassic (Johnson *et al*., 1996) following a mid-Triassic sedimentary hiatus (Cole, 1992; Veevers *et al*., 1994), thus the basal contact is characterized by an unconformable, first-order sequence boundary (Bordy *et al*., 2005).

On a regional scale, the sedimentary units thin to the north, with the cumulative thickness ranging from 1100 m in the south to 200 m in the north (Veevers *et al*., 1994). Other regional trends include grain-size fining towards the northern part of the basin and relatively homogenous lateral facies (Catuneanu *et al*., 1998; Bordy *et al*., 2004).

The fluvial and aeolian deposits of the "Stormberg" Group are subdivided into the Molteno, Elliot and Clarens Formations (Figure 2.2), which are preserved in and around Lesotho (Figure 2.1).

Molteno Formation

The mid-Triassic to the Late Triassic Molteno Formation, which unconformably overlies the Beaufort Group, is the basal formation of the "Stormberg" Group and is comprised of fluvial sedimentary rocks (Turner, 1983; Veevers *et al*., 1994). This formation ranges from 450 m to 600 m in the south (Visser, 1984; Johnson, 1991; Johnson, 1994; Veevers *et al*., 1994; Hancox, 1998) and thins to 0 m thick in the north (Visser, 1984; Johnson, 1994). Subdivisions of the formation include the unconformity-bound lower Bamboesberg and Indwe Sandstone members as well as an upper unnamed sequence (Bordy *et al*., 2005).

Molteno times were characterized by a humid and temperate, though seasonally warm, climate (Bordy *et al*., 2005). During this time, renewed uplift along the basin margins (Smith, 1990) resulted in the development of perennial, high-energy, bed-load dominated braided fluvial systems that drained an alluvial plain (Turner, 1983; Cole, 1992; Hancox, 1998; Bordy *et al*., 2005).

Elliot Formation

Unconformably overlying the Molteno Formation (Bordy *et al*., 2005), the Elliot Formation, or 'red beds', represents the middle portion of the "Stormberg" Group. This unit is also characterized by fluvial and lacustrine sedimentary rocks, which were deposited from the Late Triassic to the Early Jurassic (Gauffre, 1993). It is slightly thinner than the Molteno

with a maximum thickness of 500 m in the south (Visser, 1984; Johnson, 1994), rapidly thinning to 20 m in the north where it oversteps the Molteno Formation and directly overlies the Beaufort Group (Visser, 1984; Veevers *et al*., 1994).

The Elliot Formation was initially deposited by moderately meandering rivers with extensive flood plains in an increasingly warmer and drier climate (Cole, 1992; Veevers *et al*., 1994, Bordy *et al*., 2005). The increasing aridity lead to the formation of ephemeral fluvial systems with playa lake deposits in the Early Jurassic (Smith, 1990; Bordy *et al*., 2005).

Clarens Formation

The Clarens Formation is the uppermost sedimentary unit of the 'Stormberg' Group, and thus the Karoo Supergroup, and it conformably overlies the Elliot Formation. According to Johnson (1976), the lower, uneven contact varies between sharp, gradational or intertongued. Accumulation of up to 300 m (Visser, 1984; Johnson, 1991) of Clarens Formation sandstones in a shallow basin that thins rapidly to the north (Beukes, 1970) occurred during the Early Jurassic (Johnson, 1991; Johnson, 1994). With a south-north extent of approximately 300 km, the remnants of the Clarens Formation are small relative to the size of the main Karoo Basin. The upper contact of the Clarens Formation is defined by the appearance of the basalts of the Drakensberg Group, although sheets and lenses of sandstones and shale continue into the lowermost basalt formations (Beukes, 1970).

The final phase of Karoo sedimentation occurred in a semi-arid to arid environment (Beukes, 1970; Eriksson, 1986). Aridity increased during the middle of the Clarens resulting in a progression from massive and lenticular shallow-water deposits towards dune, wadi-channels and playa-lake deposits representative of a wet desert environment (Beukes, 1970; Eriksson, 1986; Smith, 1990). The final phase of deposition was marked by an increase in humidity and concomitant increase in shallow-water deposits (Beukes, 1970).

3.1.6b Lithology

Molteno Formation

Rock types present in the Molteno Formation occur in small-scale fining-upward successions of matrix-supported conglomerate and pebbly sandstone overlain by coarse sandstone, finer sandstone, mudrocks and coal (Turner, 1983; Hancox, 1998).

Sandstone: Molteno sandstones are characterized by a glittering appearance (Johnson, 1976). They are typically light grey to yellowish grey, olive grey and yellowish brown (Johnson, 1976; Catuneanu et al., 1998; Bordy et al., 2005). Grain sizes range from medium- to very coarse-grained, though some fine-grained units also occur (Eriksson, 1984; Eriksson, 1987; Bordy et al., 2005). Finer-grained components are subangular to subrounded, and roundedness tends to increase with grain size (Johnson, 1976). The sandstones tend to be grain-supported with moderately poor sorting (Eriksson, 1984). Basal sandstones are usually massive; while cross-bedding, horizontal bedding and cross-lamination occur in the upper part of the fining-upward successions (Johnson, 1976; Catuneanu et al., 1998).

Mudstone: Mudstone colours range from pale olive, reddish to medium dark grey (Johnson, 1976, Johnson, 1994).

Elliot Formation

The Elliot Formation can be separated into Lower (LEF) and Upper (UEF), both of which are comprised of sandstones, siltstones and mudstones.

Sandstone: These rocks are typically yellowish grey to dusky yellow or pale red to red (Johnson, 1976; Eriksson, 1987). The sandstones in the LEF are dominantly medium-grained and moderately sorted; while the UEF sandstones range from medium- to very fine-grained and are better sorted (Bordy *et al.,* 2005). Angularity of the grains seems to be inversely related to sorting, as roundedness decreases with increased sorting (Eriksson, 1984). Silica cement is common within the Elliot Formation (Bordy *et al*., 2005). Dominant sedimentary structures include horizontal-lamination and trough-cross bedding (Johnson, 1976).

Mudstone and Siltstone: Siltstone units tend to be light red to pink, while mudstones are pale to dark red, greyish red and greenish-grey, or less commonly yellowish grey, light olive grey or pale olive (Johnson, 1976; Johnson, 1994). They are usually massive and quartz-rich (Eriksson, 1987).

Clarens Formation

Sandstones and coarse siltstones are the major rock types in the Clarens Formation, with the former predominating (Johnson, 1976). Sandstones generally fine upwards with the transition from wadi-channel to dominantly aeolian environments (Veevers *et al*., 1994).

Sandstone: The sandstones of the Clarens Formation are unique in comparison to the rest of the Karoo sedimentary rocks in their relatively uniform and massive appearance (Johnson, 1976). Colours include white, cream, yellowish grey, very pale orange and pink. They are dominantly very fine- to fine-grained and subrounded to subangular; though subordinate medium- to coarse-grained sandstones occur (Beukes, 1970; Johnson, 1976; Eriksson, 1984; Johnson, 1994). The sandstones that are moderately well-sorted tend to be grain-supported, while those that are poorly sorted are matrix-supported and less abundant (Eriksson, 1984) (Table 3a).

3.1.6c Sandstone Petrography

Molteno Formation

The Molteno Formation sandstone units are quartzitic (Eriksson, 1987), and can be classified as sub-lithic arenites to quartz arenites, sub-arkoses and quartz-rich feldspathic wackes (Eriksson, 1984; Johnson, 1991; Bordy *et al.*, 2005) (Figure 3.3C). Monocrystalline quartz grains often contain small vacuoles, enclose zircon and rutile grains or contain mica inclusions (Bordy *et al.,* 2005) and commonly exhibit undulose extinction (Eriksson, 1984). Polycrystalline quartz grains are dominantly composed of less than four crystals, grains with more than four crystals rarely occur and the individual crystals are irregular and non-equigranular (Bordy *et al*., 2005). Plagioclase is the dominant feldspar type (Eriksson, 1984) and lithic fragments are dominantly mudstone followed by chert or metamorphic fragments (Bordy *et al*., 2005). Decimetre-sized clasts of Witteberg Group quartzites and large feldspar crystals also occur (Turner, 1983). According to Eriksson (1987), significant red colouration caused by hematite can be seen in a large percentage of the upper Molteno Formation sandstones under thin section. The hematite occurs as a diffuse microcrystalline stain of the interstitial material, thin coatings of grain surfaces and/or discrete crystals. Other heavy and accessory minerals found in the Molteno Formation sandstones include zircon, hornblende, riebeckite, sphene and garnet (Eriksson, 1984) (Table 3a).

Elliot Formation

Elliot Formation sandstones are classified as sub-lithic arenites to quartz arenites and sub-arkoses with the lower units dominated by quartzo-lithic sandstones and the upper by quartzo-feldspathic sandstones (Johnson, 1991; Bordy *et al*., 2004, 2005). The detrital quartz grains are subrounded to rounded, although angular grains with conchoidal surfaces often occur in the upper sandstones (Eriksson, 1985; Bordy *et al*, 2005). Like the Molteno Formation, the polycrystalline grains predominantly contain less than four, irregular, non-equigranular crystals (Bordy *et al*., 2004; 2005). Feldspar occurs as plagioclase with lesser microcline (Eriksson, 1984; Bordy *et al*., 2004; 2005). The plagioclase is albite twinned and the microcline is characteristically cross-hatched and is typically fresher than the plagioclase, which is altered to clay and mica. Lithic fragments are similar to those in the Molteno Formation, with mudstones dominating followed by chert and metamorphic fragments (Bordy *et al*., 2004; 2005). Heavy minerals are more abundant in the Elliot Formation and include rounded to subrounded zircon, garnet, green hornblende, rare sphene and riebeckite (Eriksson, 1984; 1985; Bordy *et al*., 2004; 2005). Hematite, similar to that observed in the Molteno Formation, also occurs within the Elliot Formation. However the colour is less vibrant, the hematite crystals are better developed and the diffuse microcrystalline stain is more prevalent (Eriksson, 1987) (Table 3a).

Clarens Formation

Clarens Formation sandstones are classified as quartz-rich feldspathic wackes (Eriksson, 1984) and feldspathic sandstones (Johnson, 1991) (Figure 2.3D). Monocrystalline quartz grains are rounded to well-rounded, and sutured polycrystalline quartz grains are common. Heavy minerals tend to be subrounded to rounded and include titanite, epidote, apatite, andalusite, zircon and garnet, which is more angular than the other heavy minerals (Beukes, 1970). Like the underlying sandstones of the 'Stormberg' Group, hematite occurs as stains, coatings, blebs and crystals, and according to Eriksson (1987) all of the Clarens Formation sandstones host hematite blebs and crystals. The matrix of the Clarens Formation sandstones is dominantly illite with lesser kaolinite, montmorillonite and chlorite (Beukes, 1970).

3.1.6d Provenance

The Cape Fold Belt represents the dominant provenance for the "Stormberg" Group sedimentary rocks; however the provenance changes from quartzose recycled orogen to

transitional continental throughout the sedimentary succession (Johnson, 1991; Johnson *et al*., 1996).

Both the Molteno and Elliot Formation sandstones plot within the quartzose recycled orogen or the recycled orogen field of the Qm:F:Lt diagram (Figure 2.3C). It is most likely that the southern and south-western strata of the Cape Fold Belt acted as the primary provenance (Johnson, 1991, Bordy *et al*., 2005).

According to Bordy *et al*. (2004; 2005), the provenance of the Elliot Formation changes up-sequence. The provenance of the lower Elliot Formation was a southerly and south-westerly source dominated by an assortment of sedimentary, metamorphic, and igneous rocks. However, the upper part of the Formation was sourced from the west from a granite-gneiss dominated basement and sedimentary rocks. The Clarens Formation sandstones plot in the transitional continental provenance field on Qm:F:Lt diagrams (Johnson, 1991) (Figure 2.3C). Johnson (1991) believes they may represent re-worked Karoo, specifically Beaufort Group sedimentary rocks.

Table 3a: Summary of the Sandstone Petrography of the KSG Sedimentary Groups

Group		COMPOSITION	Colour	Matrix or Grain Supported	Grain Roundness*/ Sortedness**	Grain Size***	Quartz		Feldspar		Lithics		Accessory Minerals	Other
							Qm	Qp	Type	Nature	Type	Nature		
'Stormberg' Group	Clarens Formation	Quartz-rich feldspathic wackes[1,11] and feldspathic sandstone[2]	White, cream, yellowish gray, pale orange, pink [1,2,3,4,5]	Grain supported[5] Matrix Supported[5]	MW sorted[5] P sorted[5]	VFG to FG, minor MG to CG[1,2,5]	SR-SA, subordinate R and A, undulose extinction very rare[11]		Plagioclase[11]	Dominant feldspar, 5-25 % total mineral [11]	Limited occurences[11]		Zircon, hornblende (common)[11]; titanite, epidote, apatite, andalusite (SR to R) [1]; garnet (SA)[1] and sphene (rare) [11]; hematite[5]	Sandstones are submature[1] Matrix = illite ± kaolinite, chlorite, mont-morillonite[1]
	Elliot Formation	Sub-lithic arenites to quartz arenites[9]; quartzo-lithic and quartzo-feldspathic sandstones[6]	Yellowish gray to dusky yellow, pale red to red[2,5]		M sorted6,[10] More WR[5] MW sorted[6,10] Less WR[5]	MG[6,10] lesser VFG to FG[6,10]	SR to R, minor A with conchoidal surfaces[5,6]	<4 non-equi-granular crystals dominant [6,10]	Plagioclase [6,10,11,12] Microcline [6,10,11,12]	Albite twinned, clay and mica alteration[6,10] Cross-hatched, less altered[6,10]	Mud-stones > Chert > Metamorphic[6,10]		Zircon, garnet, green hornblende, rare sphene and riebeckite (all SR to R)[6,10,11,12] Hematite[5]	Silica cement is common[6] Hematite as diffuse stain and well developed crystals[5]
	Molteno Formation	Sub-lithic arenites to quartz arenites, sub arkoses, quartz-rich feldspathic wackes[6,9,11]	Light gray to yellowish gray, olive gray, yellowish brown[2,3,6]	Grain supported[11]	More WR[2], MP sorted[11] SA to SR[2], MP sorted[11]	MG to VCG [6,11,13] Lesser FG[6,11,13]	Undulose exinction[11], vacuoles, mica inclusions, enclosed zircon or rutile common[6]	<4 non-equigranular crystals dominant, >4 crystals rare[6]	Plagioclase [11]	Dominant feldspar[11]	Mud-stones > Chert > Metamorphic[6,10]		Zircon, hornblende, riebeckite, sphene, garnet[11], hematite[5]	Glittery appearence[2] Large quartzite fragments and feldspar grains[3]
Beaufort Formation	Tarkastad Subgroup	Lithic sandstone[9]	Light olive to gray, pale blue-gray, brownish-grey and very light-gray[2,3,14]			FG to CG[2,14]	SA to SR, low to high spherocity, overgrowths common[14]		Plagioclase and orthoclase[9]	Dominant feldspar types, fresh to strong sericite and kaolinite alteration[9]	Igneous[2]	Felsic, fine-grained quartz and feldspar mosaic, most abundant[2]	Biotite, muscovite, epidote, zoisite, chlorite, zircon, rutile[9]	Calcite cement present within some sandstones[9]
	Adelaide Subgroup	Ultralitho-feldspathic sandstones[9]	Light olive to light gray, greenish gray, bluish grey, yellowish[2,14]		MW sorted (some units)[14]	VFG to CG, avg finer than Tark-astad[2,14]	WR, grains with undulose extinction dominant[8]		Plagioclase > K-feldspar[8]	Fresh to strongly calcite, clay or sericite altered[8]	Igneous[7,8,9]	Felsic, dominant[7,8,9]	Zircon, rutile, garnet, apatite, tourmaline, ± sphene ± epidote[8,15]	Compositionally indistinguishable from Ecca sandstones[8,9]
Ecca Formation		Lithic arkoses, ultralitho-feldspathic, feldspathic litharenites[8,9]	Dark gray to light gray[2]	Grain supported, 10%[8] to 20-30% matrix[2]		VFG to FG[2,16], rarely MG[17]	Mainly unstrained, no inclusions, concavo-convex contacts, overgrowths common[8]		Plagioclase >	Oligoclase or albite, fresh to calcite, clay or sericite altered[8]	Sedi-mentary >	Dominantly argillite and shale	Zircon, rutile, garnet, apatite, tourmaline[8]	Some sandstones have a mottled appearence[2]
									K-feldspar >	Carlsbad twinning, fresh to altered[8]	Metasedimentary > metamorphic > Chert <			
									Microcline > Myrmecite	Least abundant[8]	Volcanic	Large feldspar laths in a FG partially altered groundmass[2,8]		
Dwyka			Greenish-grey to brown[16]		P to MW sorted, SR grains[16]	FG to MG[16]		Chert, quartzite[16]			Volcanic			Micaceous, calcite cement[16]

*Roundedness		**Sortedness		***Grain Size	
WR	Well Rounded	W	Well	VFG	Very Fine Grained
R	Rounded	MW	Moderately Well	FG	Fine Grained
SR	Subrounded	MP	Moderately Poorly	MG	Medium Grained
SA	Subangular	P	Poorly	CG	Coarse Grained
A	Angular			VCG	Very Coarse Grained

1 Beukes, 1970
2 Johnson, 1976
3 Catuneanu *et al*., 1998
4 Johnson, 1994
5 Eriksson, 1987
6 Bordy *et al*., 2005
7 Johnson, 1976
8 Fiedler and Adelmann, 1998
9 Johnson, 1991
10 Bordy *et al*, 2004
11 Eriksson, 1984
12 Eriksson, 1985
13 Eriksson, 1987
14 Haycock *et al*, 1997
15 Kingsley, 1977
16 Visser *et al*., 1976-77
17 Van Lente *et al*., 2003

3.2 Sampling and Analysis of Sedimentary Samples

3.2.1 Sampling of the Sedimentary Xenoliths

Samples were collected from coarse-material kimberlite dumps and excavation pits, at the surface of unmined kimberlites, and at Finsch samples were also collected from borehole core. The coarsest-grained sandstones found were collected from each kimberlite, as well as any sedimentary xenoliths with unique characteristics, such as green, purple or red colouring or fossils.

The samples were considered in thin section and the freshest, coarsest-grain samples were chosen for analysis. As a result, the sandstone xenoliths from some kimberlites, such as Melton Wold, Frank Smith, Markt and Uintjiesburg, were not analyzed because they were altered to such a degree that the individual grains could not be classified. In total, 37 samples were analyzed from Voorspoed (5), Roberts Victor (5), RSQ (1), Finsch (7), Pampoenpoort (2), Koffiefontein (1), Monastery (3), Kaal Vallei (2), Big Hole (2), Jagersfontein (4), De Beers (2) and Bultfontein (3).

3.2.2 Analytical Methods

The purpose of analyzing the sandstone xenoliths is to identify the source of the samples by correlating the xenoliths with the stratigraphic units of the Karoo Supergroup based on the results of both qualitative and quantitative analyses. Qualitative methods include the careful recording of variations in sedimentary features such as trends in grain-size variation with roundedness and sorting, the nature of polycrystalline quartz grains, feldspar types, heavy mineral assemblages and the occurrence of hematite. Colour was also determined as certain colours appear to be diagnostic of certain stratigraphic units, *e.g.* reddish sandstones are more common in the Elliot Formation (Eriksson, 1984).

The quantitative methods applied in this study include grain-size determination and point-counting to establish mineral percentages and provenance. Because grain size as an independent attribute is not considered a critical factor in the correlation of the Karoo sedimentary rocks, *i.e.* all of the stratigraphic units are characterized by sandstones with a range of grain-sizes, grain-size studies simply involved measuring several select grains, in thin section, along the long axis.

Point-counting was used to determine the mineral composition of the samples, the relative abundance of each mineral component, and the nature of the provenance. The Gazzi-Dickinson point-counting method, as described by Ingersoll *et al*. (1984), was applied for the

following two reasons: first, it maximizes source-rock data while minimizing time; and second, it overcomes the problem of grain-size differences and enables comparison between samples with different grain-sizes.

Grain-size differences between samples could not be avoided because the material available for sampling was restricted to the sandstones that were trapped by the kimberlites during emplacement. As a result, it was not possible to collect samples with a specific, pre-determined grain-size from each study location. With the Gazzi-Dickinson method, the effects of grain-size differences are reduced by counting sand-sized crystal components of larger lithic fragments as individual grains. It should be noted that mineral abundances in coarse-grained samples are skewed with the Gazzi-Dickinson technique by lowering lithic values and elevating all other values (Ingersoll *et al*., 1984). However, the sandstones analyzed in this study were relatively fine-grained, and very few, if any, of the lithic fragments were large enough to have their components counted as single entities, so it can be assumed that the problem of skewedness is minimal.

3.2.3 Methodologies in Point Counting

Number of Grains

The number of grains used for point counting should be large enough to generate precise and accurate results, but should be small enough to make the study efficient. According to Galehouse (1971), 300 counts per sample is ideal because probable error is sufficiently low at the 95% confidence level. Graphical data presented by Galehouse (1971) also shows that any increase in accuracy resulting from counting a larger number of grains would not justify the extra time needed to conduct the study (Johnson, 1991). As a result, in this study 300 grains were counted per sample.

Classification of Grains

Grains were classified as quartz, feldspar, lithic fragment or accessory mineral based on optical and textural properties, while matrix and cement were omitted from the counting. Monocrystalline and polycrystalline quartz grains were distinguished and the polycrystalline grains were ultimately grouped with the lithics. Lithic fragments were further classified as volcanic, metamorphic or sedimentary, and feldspar grains as plagioclase, microcline, perthite, K-feldspar and untwinned. Untwinned feldspars were identified by the presence of

alteration, and may be underestimated as any unaltered and untwined feldspar grain was likely classified as quartz (see Table 3b for the classification scheme).

Table 3b: Grain classification scheme for point counting analyses

	Grain Type	Description and Means of Classification
Qm*	Monocrystalline Quartz	Single quartz crystals with straight or undulose extinction and no alteration, sometimes containing vacuoles and inclusions
F*	Total Feldspar	All feldspar grains regardless of type or degree of alteration, subclassified as plagioclase, K-feldspar, microcline or other
Lt*	Total Lithic Fragments	Li + Ls + Lm + Qp
Qp	Polycrystalline Quartz	Quartz grains containing more than one crystal, including chert; with either straight, semi-sutured or sutured contacts; and equi- or non-equi-granular crystal sizes
Li	Igneous Fragments	Lithic fragments containing (in this case) felsic crystals, dominantly quartz and fresh to strongly altered feldspar, with straight contacts
Ls	Sedimentary Fragments	Lithic fragments that are argillic or muddy in nature and sometimes conform to surrounding grains. According to Pettijohn *et al.,* (1987) and Johnson (1991), these are often mistaken for matrix and thus can be underestimated.
Lm	Metamorphic Fragments	Lithic fragments with crystals exhibiting an elongated fabric and/or sutured contacts
Acc	Accessory Minerals	Monomineralic grains other than quartz and feldspar, includes micas, chlorite, calcite, epidote, garnet, rutile, tourmaline, zircon, opaque, hematite, sphene, hornblende and titanite

*groupings used for ternary diagrams

3.2.4 Analysis of Quantitative Data

Monocrystalline Quartz – Feldspar – Total Lithics (Qm:F:Lt) ternary diagrams were utilized for classification purposes, to determine the provenance and to compare and correlate

the results with previous studies of the Karoo Supergroup sandstones. The point counting data were recalculated as Qm, F, and Lt normalized to 100 and free of 'other' minerals. By generating these plots, it was possible to loosely assign each sample to a specific Karoo Supergroup unit with a degree of confidence.

However, the correlation process is complicated by three factors. First, because of the semi-quantitative nature of the point counting method, each researcher / point-counter is likely to exhibit biases causing slight discrepancies between the results from each study. Second, the previous data used to generate the sandstone composition fields, with which the xenoliths are compared, is based on samples collected throughout the main Karoo Basin, all of which are isolated from the current study area where the majority of the younger Karoo formations are not found in situ. The mineralogical compositions for each formation (and study locality) are expected to vary throughout the main Karoo Basin as a result of localized depositional factors, including sediment transportation modes and distances from the source areas. The above problems were reduced by generating the Qm:F:Lt fields for each of the stratigraphic units from data collected by multiple researchers. Nevertheless, they are still evident on the Qm:F:Lt diagrams, especially the sub-field of the Tarkastad Subgroup produced from Haycock *et al.*'s (1997) study of the unit in southern Kwazulu-Natal which is distinctly separated from the main field resulting from the data collected by Johnson (1991) and Hancox (1998) (Figure 3.3; 3.4).

The third factor to consider when analyzing and correlating the point counting data is the overlap of the fields on the Qm:F:Lt diagram (Figure 3.3; 3.4). Because of this overlap, other petrographic characteristics are also considered when assigning a xenolith to a specific stratigraphic unit. Nevertheless, some of the formations, such as the Ecca Group and Adelaide Subgroup as well as the Molteno, Clarens and Elliot Formations, had to be grouped together because of the high degree of petrographic similarities between them.

When all of these factors are considered, it is evident that limitations exist in the methods adopted for correlating each xenolith with a specific stratigraphic unit of the Karoo Supergroup. However, this method attempts to utilize all of the published and some unpublished petrographic data that is currently available for the stratigraphic units, and thus, the results generated are considered consistent and reliable with the highest possible degree of confidence to date.

TABLE 3C: **SANDSTONE XENOLITH POINT COUNTING RESULTS ***

Sample			**Quartz**		**Feldspar**						**Lithics**				**Accessory**												**Normalized****		
	Figure 3.4																												
	Number	Symbol	Qm	Qp	Total	Plagioclase	Microcline	Perthite	K-Feldspar	Untwinned	Total	Sedimentary	Igneous	Metamorphic	Total	Biotite	Muscovite	Chlorite	Epidote	Garnet	Rutile	Tourmaline	Zircon	Opaques	Hematite	Other***	**Qm**	**F**	**Lt**
V2-08	1	Δ	63.0	6.0	22.5	x	x			x	2.0	x			6.5					x		x	x	x	x	C	67	24	9
V4-13	2	Δ	78.5	9.0	9.0	x	x			x	1.5	x			2.0		x		x	x				x	x		80	9	11
V4-14	3	Δ	37.0	30.0	30.0	x	x			x	1.0		x	x	2.0	x	x			x			x	x	x		38	31	32
V5-15	4	Δ	79.0	3.3	9.7	x	x			x	2.7	x			5.3			x		x	x	x	x	x	x		83	10	6
V5-17	5	Δ	32.3	24.0	37.3	x	x	x		x	4.0	x	x		2.3	x	x						x	x	x		33	38	29
RV1-04	6	■	38.0	13.3	33.0	x	x	x	x	x	7.3	x	x	x	8.3	x	x	x		x		x	x	x			41	36	23
RV1-08	7	■	60.5	15.5	17.0	x	x			x	3.5	x	x		3.5		x	x		x		x	x	x			63	18	20
RV1-09	8	■	55.2	23.2	14.0	x	x			x	2.8	x	x	x	4.8		x		x			x	x	x			58	15	27
RV1-11	9	■	66.7	8.0	16.7	x	x	x		x	3.7	x	x		5.0	x	x	x	x	x	x	x	x	x	x		47	25	28
RV1-12	10	■	38.4	25.2	18.4	x	x			x	8.8	x	x		9.2	x	x	x		x	x	x		x		S	42	20	37
RSQ-09	11	●	33.6	25.6	17.6	x	x		x	x	10.8	x			8.3	x	x	x	x	x			x	x			38	20	42
FN1-07	12	◊	40.0	26.5	16.0	x	x			x	11.0	x		x	6.5					x	x	x	x	x			43	17	40
FN1-08	13	◊	66.4	20.4	10.4	x	x			x	2.0	x		x	0.8	x				x	x	x		x			67	10	23
FN1-09	14	◊	67.6	9.6	10.8	x				x	7.6	x	x		4.4	x				x		x	x	x			71	11	18
FN1-10	15	◊	44.0	34.0	9.6	x	x	x		x	7.6	x	x		4.8					x	x	x	x	x		S	46	10	44
FN3-17	16	◊	72.0	5.7	15.0	x	x		x	x	4.6	x	x		2.7					x			x	x	x		74	15	11
FN-111	17	◊	58.5	20.5	15.0	x	x			x	3.5	x			2.5					x			x	x			60	15	25
FN-112	18	◊	64.0	19.6	4.8	x	x			x	8.0	x	x	x	3.6					x			x	x			66	15	25
PP-37	19	▲	20.8	31.2	24.0	x	x			x	18.4	x	x		5.6	x	x	x		x		x	x	x			22	25	53
PP-39	20	▲	19.6	35.6	27.2	x	x			x	9.6	x	x	x	8.0	x		x		x			x	x	x		21	30	49

Table 3c Continued: Sandstone Xenolith Point Counting Results *

Sample			Quartz		Feldspar						Lithics				Accessory												Normalized**		
	Figure 3.4																												
	Number	Symbol	Qm	Qp	Total	Plagioclase	Microcline	Perthite	K-Feldspar	Untwinned	Total	Sedimentary	Igneous	Metamorphic	Total	Biotite	Muscovite	Chlorite	Epidote	Garnet	Rutile	Tourmaline	Zircon	Opaques	Hematite	Other***	Qm	F	Lt
KF1-55	21	⬟	40.0	28.8	8.8	x				x	16.8	x	x		5.6	x	x		x	x	x	x	x	x			42	9	48
M1-01	22	○	73.0	13.7	6.0	x	x	x		x	5.6	x	x		1.7	x	x	x				x		x		H	74	6	20
M2-04	23	○	57.5	14.0	17.0	x	x			x	3.0	x	x		8.5	x	x	x	x	x			x	x	x	A	63	19	19
M6-15	24	○	65.7	27.6	4.6	x	x	x	x	x	2.0	x	x		0.1	x				x	x		x	x	x		66	5	30
BH1-04	25	⬠	45.6	29.2	13.6	x	x	x	x	x	6.4	x			5.2	x	x			x				x		C,T	48	14	38
BH1-06	26	⬠	57.0	31.5	8.5	x	x	x		x	2.0	x			1.0	x	x						x	x	x		58	9	34
JG1-01	27	□	30.7	11.3	45.7	x	x	x	x	x	7.7	x	x		4.7	x				x	x		x	x		T	62	24	15
JG1-02	28	□	47.7	7.3	35.7	x	x	x	x	x	5.7	x	x		3.7	x	x			x				x		C	49	37	13
JG1-05	29	□	56.0	5.3	21.7	x	x			x	8.0	x			9.0	x	x	x		x		x	x	x			39	43	19
JG1-06	30	□	36.5	11.0	40.5	x	x		x	x	6.5	x			5.5		x	x		x		x		x			32	48	20
KV-106	31	+	38.0	17.0	30.0	x			x	x	9.5	x	x		5.5	x	x	x					x	x	x		40	32	28
KV-109	32	+	33.2	35.2	15.6	x				x	8.4	x	x		7.6	x	x	x				x	x	x			36	17	47
DB2-22	33	x	50.8	12.3	21.5	x	x			x	7.5	x		x	8.0	x		x		x		x	x	x			55	23	21
DB2-29	34	x	34.5	24.5	16.0	x				x	10.0	x			15	x	x		x	x	x		x			S	41	19	41
BF1-05	35	♦	45.5	6.5	25.5	x	x			x	3.5	x			19	x	x	x				x	x	x			56	31	12
BF2-12	36	♦	33.0	9.0	48.5	x				x	8.0	x			1.5	x		x	x				x	x			34	49	17
BF2-23	37	♦	65.0	23.0	6.0	x	x			x	4.0	x	x		2.0					x			x	x		C	66	6	28

* Values presented as percentages based on n = 300 for point counts

** Qm = monocrystalline quartz, F = total feldspar, Lt = total lithic fragments including polycrystalline quartz; values are normalized to 100% and free of accessory minerals*

*** Other: C = calcite; S = sphene; H = hornblende; T = titanite; A = apatite

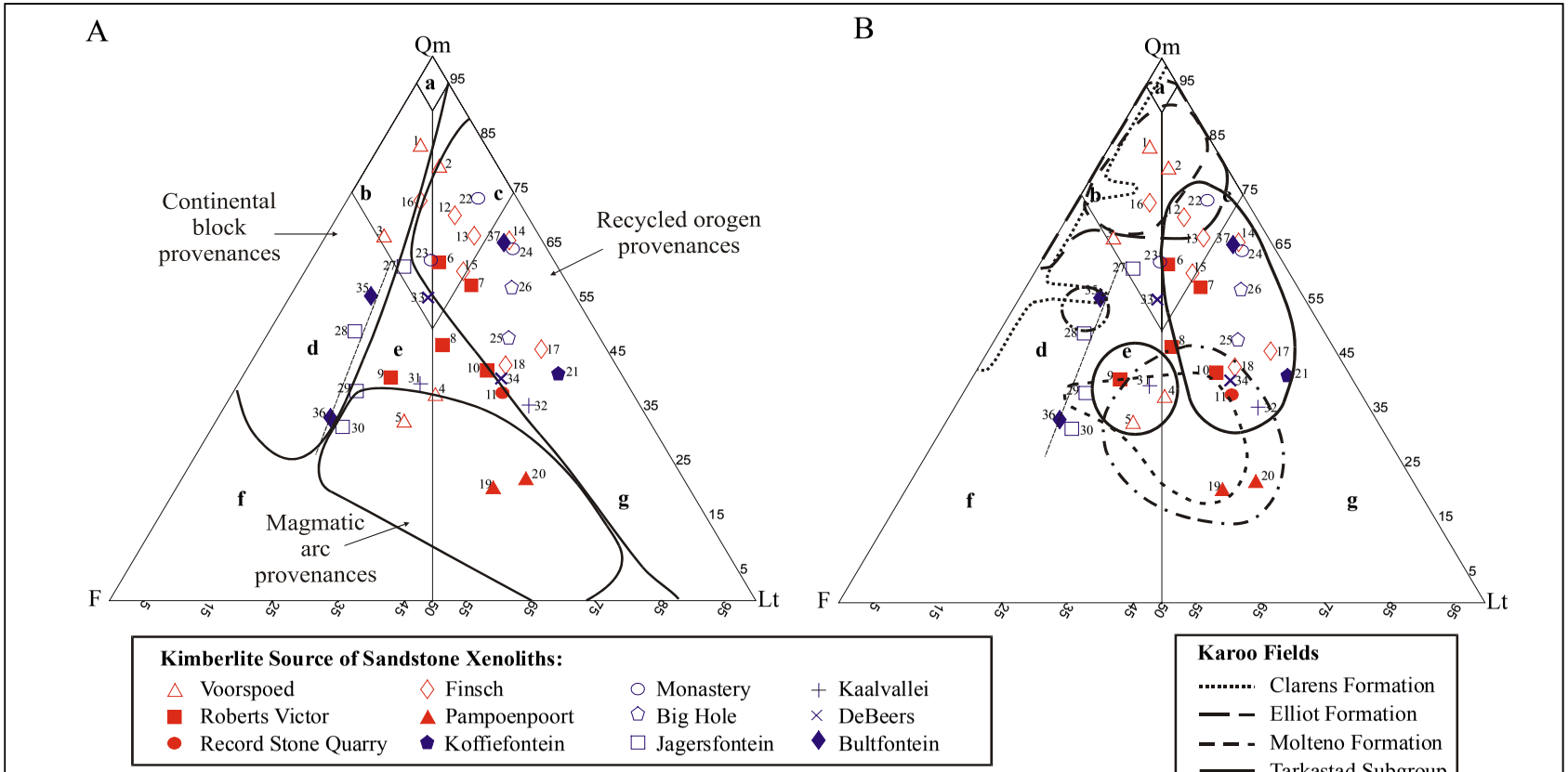

Figure 3.4: Ternary diagrams showing (A) point counting results, classification and provenance of the sandstone xenoliths; and (B) their relationship to Karoo Supergroup sandstones. Samples are listed in Table 7a and described in Appendix I. Samples numbered 2, 9, 11, 13, 21, 23, 25, 34 and 35 are classified as wackes, though are plotted here for comparison purposes. Qm:F:Lt (monocrystalline quartz : feldspar : total lithic fragments). Classification: a- quartz arenite, b- subarkose, c- sublitharenite, d- arkose, e- lithic arkose, f- arkosic arenite, g- litharenite, after Pettijohn *et al*. (1987). Provenance Fields after Dickinson *et al.* (1983). Point counting methods after Ingersoll *et al*. (1984). The classificiation fields of the Karoo sandstones are based on: Dwyka Group- Johnson (1991); Ecca Group- Kingsley (1985), Johnson (1991) and Fiedler and Adelmann (1998); Adelaide Subgroup- Johnson (1991), Haycock *et al.* (1997) and Fiedler and Adelmann (1998); Tarkastad Subgroup- Johnson (1991), Hancox (1998) and (left) Haycock *et al.* (1997); Molteno Formation- Eriksson (1984), Johnson (1991) and Hancox (1998); Elliot Formation- Eriksson (1984), Johnson (1991) and Bordy *et al*. (2004); and Clarens Formation- Eriksson (1984) and Johnson (1991).

3.3 CORRELATION OF THE SANDSTONE XENOLITHS WITH THE KAROO SUPERGROUP

3.3.1 Overview

The assignment of sandstones to any specific stratigraphic unit relies strongly on lithostratigraphic relationships and is supported by petrography and mineral composition. Because of the sample dimensions, in the case of the sandstone xenoliths samples, it is not possible to determine stratigraphic relationships; therefore the correlation of the xenoliths with the stratigraphic units of the Karoo Supergroup is based on point counting data (see in Table 3c, Appendix I: Table Ib and Figure 3.4), and the petrographic descriptions (see Appendix I: Table Ia).

It should be noted that while samples with greater than 15% matrix can be classified as wackes, this high matrix percentage might be a post-depositional feature, such as *in situ* weathering, which decreased the original feldspar content of the sandstones and ultimately altered the original composition of the sandstone. However, this study does not facilitate determination of whether the wackes are primary or secondary, and therefore it will be assumed that the matrix percentage, point-counting results, Qm:F:Lt ratios and petrography are representative of the primary sandstone.

3.3.2 Correlations

Samples plotting in the Clarens, Molteno and Elliot Formations fields

Six samples plot within, or proximal to the fields of the Molteno, Elliot and Clarens Formations (i.e., 'Stormberg' field) in the Qm-F-Lt diagram: V2-08, V4-13, V4-14, FN1-07, FN3-17 and M1-01. V2-08 and V4-13 both plot within the Molteno and Elliot Formation and close to the Clarens Formation fields, and V4-14 plots just below the fields. V2-08 and V4-14 are subarkoses and V4-13 is a lithic greywacke. V2-08 and V4-14 show an increase in grain roundedness with increased grain size, like the sandstones of the Molteno and Elliot Formations (Figure 3.5C), while V4-14 shows a decrease in roundedness with increased grain size. Polycrystalline quartz grains are dominantly <4 crystals and non-equigranular, though equigranular grains do occur. The heavy mineral suite includes garnet and hematite, which are found in the Molteno (Eriksson, 1984), Elliot (e.g. Eriksson, 1984) and Clarens Formations (Beukes, 1970). V4-13 also has epidote, which is only reported in Molteno Formation sandstones (Beukes, 1970), and V4-13 and V5-15 contain zircon, present in all of the Karoo sandstones.

Samples FN1-07 and M1-01 plot where the Elliot Formation and Adelaide Subgroup fields overlap. These samples are light grey (FN1-07) and pinkish-grey (M1-01) sublitharenites. In comparison, FN1-07 has finer, better-rounded grains than M1-01, both contain sedimentary lithic fragments and tourmaline. The polycrystalline quartz in FN1-07 has 2-4 crystals, with fewer crystals showing straighter contacts, and contains zircon, garnet and rutile, found in the Tarkastad Subgroup (Johnson, 1991). It is difficult to classify any of the Finsch sandstone xenoliths as 'Stormberg' rocks because the kimberlite is not proximal to the present outcrop (see discussion later). M1-01 can easily be correlated with the 'Stormberg' Group as it is the present country rock. Furthermore, the Monastery sample contains hornblende, only reported in the Clarens and Elliot Formations (Eriksson, 1984), as well as silica cement and quartz overgrowths, which are common in the 'Stormberg' Group sandstones.

FN3-17 is unique because the point counting results likely represent the secondary composition of the sandstone. In this sample, secondary silica cement is extremely abundant, to the point that it can be confused with primary quartz grains (Figs. 3.5A; 3.5B). It is therefore likely that quartz was overestimated during the point counting, and that FN3-17 is more compositionally similar to the Tarkastad Subgroup sandstones. This xenolith is a light grey subarkose, and the areas without silica cement, considered remnants of the primary sandstone, contain both very-fine to fine grains and better rounded coarse grains, and subangular to rounded quartz grains that have rutile and zircon inclusions and overgrowths. The polycrystalline quartz is dominantly 3-4 crystals with semi-sutured contacts and other lithics include chert, argillic sedimentary and igneous fragments, while the accessory minerals include zircon, garnet, hematite crystals and opaques. The areas with silica cement are dominated by sutured 'quartz' grains, or silica cement, with relict rounded quartz, feldspar and heavy mineral grains.

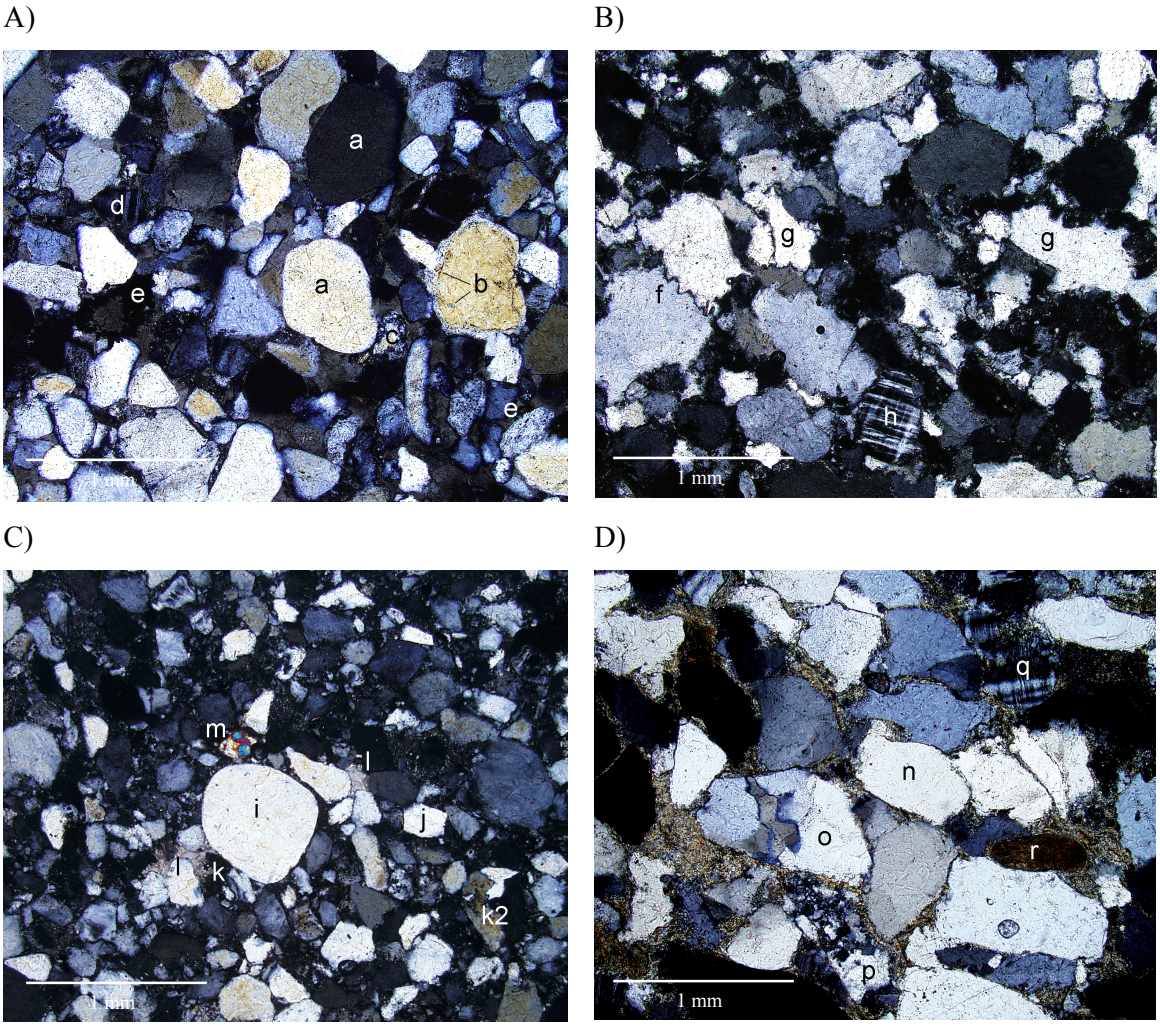

Figure 3.5: Photomicrographs of sandstone thin sections. Note several thin sections are thick giving the quartz grains a yellow colour. All at 10 x magnification and under crossed polars. (A) primary FN3-17 showing bimodal grain size distribution with better rounded coarser grains, a) rounded quartz grains, b) quartz with zircon inclusion and quartz overgrowth, c) fine grained chert, d) plagioclase feldspar with albite twinning, e) hematite blebs. (B) secondary FN3-17 showing f) sutured contacts likely caused by overgrowth of silica cement and difficulty in discerning between primary grains and g) secondary cement, h) relict primary, rounded microcline feldspar. (C) V2-08 showing bimodal distribution, i) well rounded quartz grain, j) finer, subangular quartz grain, k) polycrystalline quartz, 3 crystals with straight contacts, k2) polycrystalline quartz, 3 crystals with sutured contacts, l) patches of calcite cement, m) tourmaline. (D) BH1-06, note increased abundance in feldspar and lithics in comparison to V2-08, n) subrounded quartz grain with straight extinction, o) polycrystalline quartz, 3 crystals, sutured, p) chert q) moderately altered microcline feldspar, r) rounded, argillic sedimentary lithic fragment.

Samples plotting in the Tarkastad Subgroup field

Samples RV1-04, RV1-08, RV1-09, FN1-08, FN1-09, FN1-10, FN-111, KF1-55, M2-04, M6-15, BH1-04, BH1-06, JG1-01, DB2-22 and BF2-23 plot exclusively within or near the Tarkastad Subgroup field, and represent the largest number of samples that plot within any given field. This may be a result of sampling techniques or the relative size of the field. The samples are predominantly litharenites, followed by wackes, sublitharenites and subarkoses, with a recycled orogen or lesser mixed provenance.

The litharenites include RV1-08, RVI-09, FN1-09, FN-111, M6-15, BH1-06 and BF2-23, all of which have a recycled orogen provenance, except for RV1-09, which has a mixed provenance. Colours include different shades of grey and pale yellow (RV1-08, RV1-09). The samples are polymodal, except for RV1-08 and RV1-09, and like the Tarkastad Subgroup sandstones (Johnson, 1976; Haycock *et al*., 1997), the grain sizes range from very-fine to coarse-grained. According to Haycock *et al.* (1997), quartz overgrowths are common, though are only present in sample BH1-06 (Figure 3.5D). Calcite cement is also reported in some of the Tarkastad Subgroup sandstones (Johnson, 1991) and is present in FN1-09 and BF2-23. The accessory minerals found in previous studies of the Tarkastad Subgroup sandstones includes biotite, muscovite, chlorite, epidote, zoisite, zircon and rutile (Johnson, 1991). However, except for BH1-06, the xenoliths all contain garnet and or tourmaline as well as any or all of the above listed minerals, although no zoisite was observed.

RV1-04 and FN1-10 are classified as sublitharenites with recycled orogen provenances and JG1-01 and DB2-22 are subarkoses with mixed provenances. The sublitharenites are greenish-grey (RV1-04) and light grey (FN1-10) with 7-10% matrix and RV1-04 is coarser grained then FN1-10. FN1-10 has both quartz overgrowths and calcite cement, sedimentary and felsic igneous lithic fragments and does contain garnet and tourmaline. The subarkoses, JG1-01 and DB2-22, are slightly finer grained, both with 15% matrix, calcite cement, and contain garnet, zircon and mica as well as tourmaline (DB2-22) and titanite and rutile (JG1-10).

The wackes are classified as lithic greywackes, FN1-08, KF1-55 and BH1-04, and feldspathic greywackes, M2-04. All have a recycled orogen provenance, are light grey to medium-dark grey with 15-25 % matrix and very-fine to coarse grained; M2-04 being the finest and BH1-04 the coarsest. The feldspars are fresh to strongly altered to clay, sericite or calcite, while the quartz demonstrates straight and undulose extinction and, except for FN1-08, contains vacuoles. All of the wackes have sedimentary lithic fragments, and like the

Tarkastad Subgroup sandstones (Johnson, 1976), KF1-55 and M2-04 have felsic, quartz and feldspar igneous lithic fragments. The accessory minerals are variable, with biotite and garnet found in all, and muscovite, rutile, tourmaline, epidote, zircon in most of the wackes.

In summary, the petrography of the xenoliths that plot within the Tarkastad Subgroup field of the Qm:F:Lt diagram is variable. However, this may reflect the nature of the Tarkastad Subgroup as well as the wide distribution of the kimberlite pipes throughout the main Karoo Basin.

Samples plotting in the overlap of the Tarkastad and Adelaide Subgroups and Ecca Group fields

Several samples, including RV1-12, RSQ-09, FN-112, KV-109 and DB2-29, lie within the overlap of the Tarkastad Subgroup and the Adelaide Subgroup and Ecca Group fields; while samples V5-15, V5-17, RV1-11 and KV-106 lie within the overlap of the left sub-field of the Tarkastad Subgroup and the Adelaide Subgroup and Ecca Group fields. Differences between the Adelaide Subgroup and Ecca Group sandstones and the Tarkastad Subgroup are that Tarkastad Subgroup sandstones are slightly coarser grained (Johnson, 1976), the quartz is less well-rounded (Haycock *et al*., 1997; Fiedler and Adelmann, 1998), and they contain epidote, zoisite and chlorite (Johnson, 1991), as opposed to garnet, apatite, tourmaline and sphene reported in the Adelaide Subgroup and Ecca Group sandstones (Kingsley, 1977; Fiedler and Adelmann, 1998), while both reportedly have zircon and rutile. However, tourmaline and garnet were consistently found in the xenoliths that plot in the Tarkastad Subgroup field (see above). These features are semi-diagnostic at best, and can only be used to make indefinite conclusions about the source of each of the xenoliths that plot within the overlapping fields.

RV1-12, FN-112 and KV-109 are very fine- to medium-grained, olive grey (RV1-12 and KV-109) and light grey (FN-112) litharenites. When comparing the three, it is evident that RV1-12 and KV-109 are more similar and likely correlate with the Tarkastad Subgroup sandstones, whereas FN-112 is more likely from the Adelaide Subgroup or Ecca Group. For example, FN-112 has quartz that is better rounded than the other samples, calcite and silica cement and garnet. Furthermore, the point counting results of FN-112 may be skewed toward quartz as the sample has patches of secondary quartz, similar to FN3-17 though less abundant. If the quartz content is decreased by approximately 10%, FN-112 plots exclusively within the Adelaide / Ecca fields.

The left sub-field of the Tarkastad Subgroup, which was generated from sandstones collected in the southern Kwazulu-Natal and analyzed by Haycock *et al.* (1997), demonstrates the compositional variability of the sandstones found throughout the main Karoo Basin. The samples that plot within this field, V5-15, V5-17 and KV-106, are variable and the only common factors are the yellowish colour, hematite stains, and the occurrence of chlorite and zircon. V5-15 plots on the line that separates lithic arkoses and litharenites, and V5-17 and KV-106 are lithic arkoses. V5-15 is very fine- to medium-grained, where the coarser grains are better rounded, the yellowish colour, fine-grained nature. The presence of garnet and tourmaline and well rounded quartz grains are suggestive of a Adelaide Subgroup or Ecca Group origin, regardless of the chlorite, which is only found in the Tarkastad Subgroup sandstones, V5-15 is most likely Adelaide / Ecca. V5-17 is slightly coarser grained (v.f.g.-c.g.) and has more angular quartz grains with undulose and straight extinction, however the immaturity of the sample and feldspar abundance suggest that this sample is more likely from the Adelaide Subgroup or Ecca Group. Because KV-106 is coarser grained with less rounded quartz than sample KV-109 (Tarkastad) and contains sedimentary and felsic igneous lithic fragments as well as chlorite like KV-109, it is considered a Tarkastad Subgroup sandstone.

The remaining three samples are wackes and include RV1-11, a feldspathic greywacke with a mixed provenance, and RSQ-09 and DB2-29, lithic greywackes with recycled orogen provenances. They are all characterized by calcite cement, sedimentary fragments, garnet, epidote and zircon and are micaceous. RV1-11 is the coarsest of the samples, medium grained, has the highest matrix content (30%) of the wackes and it has sub-angular to sub-rounded quartz grains with rutile and zircon inclusions. RSQ-09 and DB2-29 are very fine- to medium-grained, with 20 to 25% matrix, two distinct quartz grain sizes, roundedness increasing with grain size, and are laminated with grains exhibiting preferred orientation. No attempt is made to correlate these samples any further because they are wackes.

Samples plotting in the overlap of the Adelaide Subgroup and Ecca Group fields

Because the Adelaide Subgroup and Ecca Group sandstones are essentially indistinguishable (Johnson, 1991; Fiedler and Adelmann, 1998) beyond a few diagnostic features such as differences in the feldspar and heavy mineral suites as described by Kingsley (1977), no methodical attempt was made to distinguish between the two. The Adelaide

Subgroup and Ecca Group fields encompass the litharenites and lithic arkose classification areas as well as the magmatic arc provenances field and border on the continental block provinces field. Samples PP-37, PP-39, JG1-05, JG1-06 and BF1-12 plot within this area, and are all petrographically similar to the Adelaide Subgroup and/or Ecca Group sandstones as described by Johnson (1976), Johnson (1991), Haycock *et al.* (1997), Fiedler and Adelmann (1998) and Van Lente *et al.* (2003). PP-37 and PP-39 are classified as litharenites with a magmatic arc provenance. Like the Ecca Group sandstones, the samples are grain-supported with 5-15% matrix, are poorly sorted and contain argillic sedimentary and felsic igneous lithic fragments, and the quartz in sample PP-37 shows dominantly straight extinction. They range from very fine- to fine-grained (PP-37) to medium-grained (PP-39) and contain tourmaline, garnet and zircon (PP-37 and PP-39) and rutile (PP-39) like the Adelaide Subgroup and Ecca Group sandstones. The samples also show preferred grain orientation (i.e, lamination).

JG1-05, JG1-06 and BF1-12 all plot on the lithic arkose side of these fields and have a mixed continental block and magmatic arc provenance. As with the litharenites discussed above, the Jagersfontein and Bultfontein sandstone xenoliths are very fine- to medium grained, with subangular to subrounded grains, 5-15% matrix and are mature to submature. The heavy mineral suite is variable in these samples, with zircon, tourmaline and garnet in JG1-05, tourmaline and garnet in JG1-06, and zircon and epidote in BF1-12. Again, except for epidote, which is only described in the Adelaide Subgroup sandstones (Kingsley, 1977), the observed heavy minerals are found in both Adelaide Subgroup and Ecca Group sandstones. The lithic arkoses are also laminated with grains in a preferred orientation.

Samples plotting in the Dwyka Group field

The Dwyka Group field hosts the smallest number of samples, namely JG1-02 and BF1-05. Emphasis must be placed on the fact that this field is based on a single sample analyzed by Johnson (1991) and it is therefore likely that a truly representative field would be much larger. When comparing the petrography of these samples to Dwyka Group sandstones, as described by Visser *et al*. (1976-77), except for the fact that the two samples are moderately sorted, have calcite cement, contain chert and quartzite-like polycrystalline quartz grains and are relatively micaceous, very few common characteristics are present.

Although Dwyka-like sandstones were only found in two of the kimberlite pipes, it is probable that each pipe contains Dwyka Group xenoliths. Because of the low proportion of

sandstones within the Dwyka Group, the chance of sampling them significantly decreases. Furthermore, the present distribution of the Dwyka Group encompasses the majority of the study area, indicating that the Group was present during the emplacement of all of the studied kimberlites, with the unlikely exception of Finsch and West End (Figure 3.6).

3.3.3 Summary of Sandstone Xenolith Correlations

Analyses of the sandstone xenoliths show that Tarkastad Subgroup sandstones are the most common xenoliths found in sampled kimberlites . The abundance of Tarkastad Subgroup xenoliths may be attributed to the wide-spread deposition of the Subgroup and to the fact that the Tarkastad Subgroup sandstones are coarser grained then the older stratigraphic units and thus more likely to be sampled as coarser grained sandstone xenoliths were preferably sampled over finer grained sandstones. The Adelaide Subgroup / Ecca Group xenoliths are also abundant, and are found in all of the pipes except for Voorspoed, Koffiefontein, Monastery and the Big Hole. The least represented stratigraphic unit in this study is the Dwyka Group and, as previously mentioned, it is likely a reflection of the lithological composition of the Dwyka Group (i.e., poor in sandstones). Finally, 'Stormberg' Group xenoliths are rare, and are confined to Voorspoed and Monastery, which are close the present day outcrop area of this Group. The correlations are presented in Table 3d and Appendix I: Table Ic.

Table 3d: Sandstone Xenoliths Found within the Studied Kimberlites

Kimberlite Pipe	Voorspoed	Roberts Victor	Record Stone Quarry	Finsch	Pampoenpoort	Koffiefontein	Monastery	Kimberley (BH)	Jagersfontein	Kaal Vallei	De Beers	Bultfontein
'Stormberg'	X						X					
Tarkastad		X		X		X	X	X	X	X	X	X
Beaufort / Ecca		X	X	X							X	
Adelaide / Ecca	X			X	X				X			X
Dwyka									X			X

Previous records of Beaufort Group xenoliths are consistent with the results of the present study, as sandstones that correlate with the Beaufort Group were found at Voorspoed, Roberts Victor, Finsch, Koffiefontein, Monastery, Jagersfontein and the KKC as reported by

Williams (1932), Visser (1972) and Clement (1982). Furthermore, some of the Beaufort Group xenoliths from Finsch (e.g. FN1-08, FN1-10, FN-111) have characteristics comparable to those described by Visser (1972) as they are predominantly massive, relatively fine grained and moderately sorted with moderately well to well-rounded quartz, feldspar and lithic fragments in a quartz-rich groundmass. Differences between the samples collected in this study and those described by Visser (1972) comprise of colour, light grey as opposed to white and cream, and the occurrence of subangular grains. Although Visser (1972) did not specify that the sandstones he described were Beaufort Group or not, Visser is adamant that they are from the Karoo Supergroup. The consistency between previous indications of Beaufort Group xenoliths and the results of the present study suggest that, without question, xenoliths correlating with the Beaufort Group occur in the Voorspoed, Roberts Victor, Finsch, Koffiefontein, Monastery, Jagersfontein and the KKC pipes.

Conversely, results of the sandstone analyses are not entirely consistent with earlier citations of 'Stormberg' sedimentary xenoliths. For example, Wagner (1914) reports that xenoliths from the "Red Beds" and "Cave Sandstones" of the 'Stormberg' Group occur in the KKC pipes. Similarly, Hawthorne (1975) incorporates the entire 'Stormberg' Group into his kimberlite model and erosion estimates. In contradiction to this, the geochemical results presented by Rambula (2005) show that the KKC sandstone xenoliths are limited to the Adelaide Subgroup. However, the above data suggest that the entire Beaufort Group succession once covered the Kimberley area, and that no 'Stormberg' Group sandstones were present when the KKC were emplaced. 'Stormberg' Group xenoliths were also documented from the Jagersfontein kimberlite (Wagner, 1914; Williams, 1932), though none were observed in this study.

3.3.4 Other Sedimentary Rock Xenoliths

Medium grey to black mudstones and shales, from small fragments to angular blocks less than 0.5 m in length, were found at all of the studied kimberlites. These fragments are likely derived from the Dwyka and Ecca Groups as they both contain grey, black and bluish mudstone and shale units (Johnson, 1976; Visser *et al.,* 1976-77). The presence of these xenoliths supports the results of the sandstone analyses as they provide further evidence that the Dwyka and Ecca Groups covered the study area at the time of kimberlite emplacement (140 – 75 Ma).

Green and purple fine sandstones, siltstones and mudstones were also collected and / or observed at several of the kimberlites, including Melton Wold, Roberts Victor, Record Stone Quarry, Finsch, Pampoenpoort, Uintjiesberg, Koffiefontein, Jagersfontein, and the KKC. It is probable that these xenoliths correlate with the Beaufort Group, which is typified by olive, dark green, greyish-red to reddish purple and red siltstones and mudstones (Johnson, 1976; Haycock *et al.,* 1997). All of the samples collected were too fine grained or altered to point count, therefore no analyses were conducted, and all correlations are based on previous accounts of xenoliths with similar macroscopic characteristics.

MW, FN, PP, UJ, KF and the KKC contain grey-green, light to dark green and mint green mudstone to fine sandstone xenoliths that are usually massive, less than 15 cm in size and sometimes rounded. Sample DB1-02 is an example of a typical grey-green, rounded siltstone xenolith found in the KKC. It has little to no internal structure, obvious weathering of the feldspar grains to white clay or calcite and calcite cement (Figure 3.6a). No xenoliths fitting this description are mentioned in earlier publications, instead the green xenoliths are described as olive green shale in the KKC (Wagner, 1914) and green mudstone and shale at Finsch (Visser, 1972; Clement, 1982), and are considered to originate from the Beaufort Group. The greenish xenoliths found at the other kimberlites are angular fragments of fine grained sandstone (FN, PP, UJ, KF), siltstone (PP, UJ) and mudstone (FN).

A)

B)

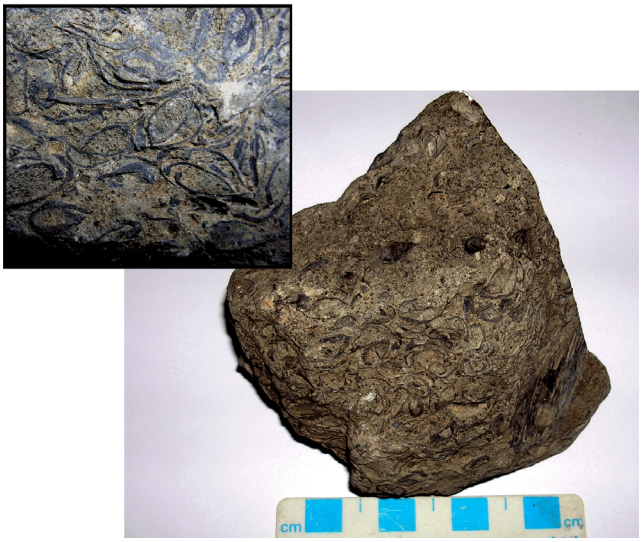

Figure 3.6: Other xenoliths found and collected at the KKC pipes. A) DB1-02. B) Sandstone xenolith with bivalve fossils collected from the Kimberley dumps.

The purple xenoliths tend to be finer grained then the green xenoliths and are predominantly massive mudstones ranging from purple to dark reddish-purple, and occur in the MW, RV, RSQ, FN and KKC pipes. Finsch contains unique mudstone xenoliths that are intermixed green and purple mudclasts in a darker purple muddy 'matrix'. An example was found in borehole core (65/283/5410). Previous accounts of similar xenoliths include purplish shale at KF (Wagner, 1914) and purple mudstone and shale at Finsch (Visser, 1972; Clement, 1982).

As previously mentioned, fossils are known to occur in the KKC pipes (e.g. Wagner, 1914). During this study, several trace fossils were found at the Kimberley dumps as well as a bone fragment, small fragments of fossilised wood, Permian glossopteroids (Prevec, pers. comm. 2006) and bivalves (Figure 3.6b). Further examination of these fossils may provide more concrete evidence as to the age of the xenoliths in which they are found and thus help to constrain the stratigraphic units that were present in Kimberley when the KKC was emplaced.

3.4 Implications for the Lateral Extent of the Main Karoo Basin During Kimberlite Emplacement

3.4.1 Introduction

Because the xenoliths collected represent a sub-sample of a population already sampled by each of the kimberlite pipes, examination of the sandstone xenoliths may not depict the complete stratigraphic package that was present during the time of kimberlite emplacement. As a result, assumptions ought to be made when commenting on the lateral extent of each of the stratigraphic units of the KSG during the emplacement of the kimberlites. The first assumption is related to the fact that the abundance of coarser grained rocks, sandstone as opposed to siltstone and mudstone, increases in the younger sedimentary units. For example, while the Ecca Group is dominated by shale and mudstone (Johnson, 1994), the younger Tarkastad Subgroup is dominantly sandstone (Haycock *et al.,* 1997). This overall coarsening upward trend designates that the sampling method used should allow for the collection of the youngest stratigraphic units represented in each kimberlite's xenolith suite. Therefore, it is assumed that the results of the sandstone analyses illustrate the youngest group that was present when each kimberlite was emplaced, and that older groups may not be represented.

Second, due to the foreland basin nature of the main Karoo Basin, it is assumed that the lateral extent of the depositional area progressively decreased from the start of Dwyka

times through Clarens times. It can therefore be assumed that in areas where sandstone xenoliths of a younger stratigraphic unit are found the older groups were also present. Regardless of these assumptions and short fallings of the sampling method, it is possible to comment on the lateral extent of the Dwyka, Ecca, Beaufort and 'Stormberg' Groups during the kimberlite emplacement based on the results of the sandstone xenolith analyses.

3.4.2 Lateral Extent of the Stratigraphic Units

Dwyka and Ecca Groups

None of the kimberlites outside of the present outcropping area of the Dwyka and Ecca Groups, namely Finsch and West End, contain xenoliths from these groups. According to Cole (1992), this is because original deposition of the Ecca Group occurred in a basin that was not much larger than the present outcrop area of the Ecca Group. However, Finsch does contain xenoliths that correlate with the Beaufort Group, so it can be assumed that the original depositional basin for the Dwyka and Ecca Groups extended at least as far northwest as Finch (Figure 3.7).

Beaufort Group

Beaufort Group sandstone xenoliths occur in all of the kimberlites from which sandstone xenoliths were analysed, although those from Voorspoed, Record Stone Quarry, Pampoenpoort, Jagersfontein and Kaal Vallei plot either in the overlap of the Beaufort and Ecca Group fields, or in the Ecca / Adelaide field. As previously discussed, RSQ, PP and JG do contain Beaufort-like mudstone and siltstone xenoliths. These results suggests that the Beaufort depositional basin was much more extensive than the modern remnant (i.e., it is likely that the basin was larger than inferred in Figure 3.7) and that like the Dwyka and Ecca Groups, it reached as far northwest as Finsch (Figure 3.7). In addition, if the mudstone xenoliths showing Beaufort-like characters (i.e., green and purple colour) are included, then it can be postulated that the Beaufort Group extended into the Uintjiesberg region (see Figure 3.7). The results of this study therefore agree with Smith's (1990) assumption that the original depositional area of the Beaufort Group extended over almost all of the present day outcrop areas of the Dwyka and Ecca Groups.

‘Stormberg’ Group

According to Cole (1992), it is unlikely that the original depositional environment of the ‘Stormberg’ Group extended much further than the modern outcrop area. However, based on this study, the northern extent of the ‘Stormberg’ Group during the kimberlite emplacement was further north the then present outcrop area to include Voorspoed, which contains several ‘Stormberg’-like sandstone xenoliths. It is difficult to comment on the westward extent of the ‘Stormberg’ Group because no kimberlites were studied close to the western outcrop boundary, however, in contrast to previous assumptions, it seems that ‘Stormberg’ Group sedimentary units were not deposited in the Kimberley area. Moreover, it is possible to conclude that the ‘Stormberg’ Group did not extend as far west as the present south-western outcrop margin of the Beaufort Group as no ‘Stormberg’-like sandstone xenoliths were found in the Melton Wold, Pampoenpoort or Jagersfontein kimberlites.

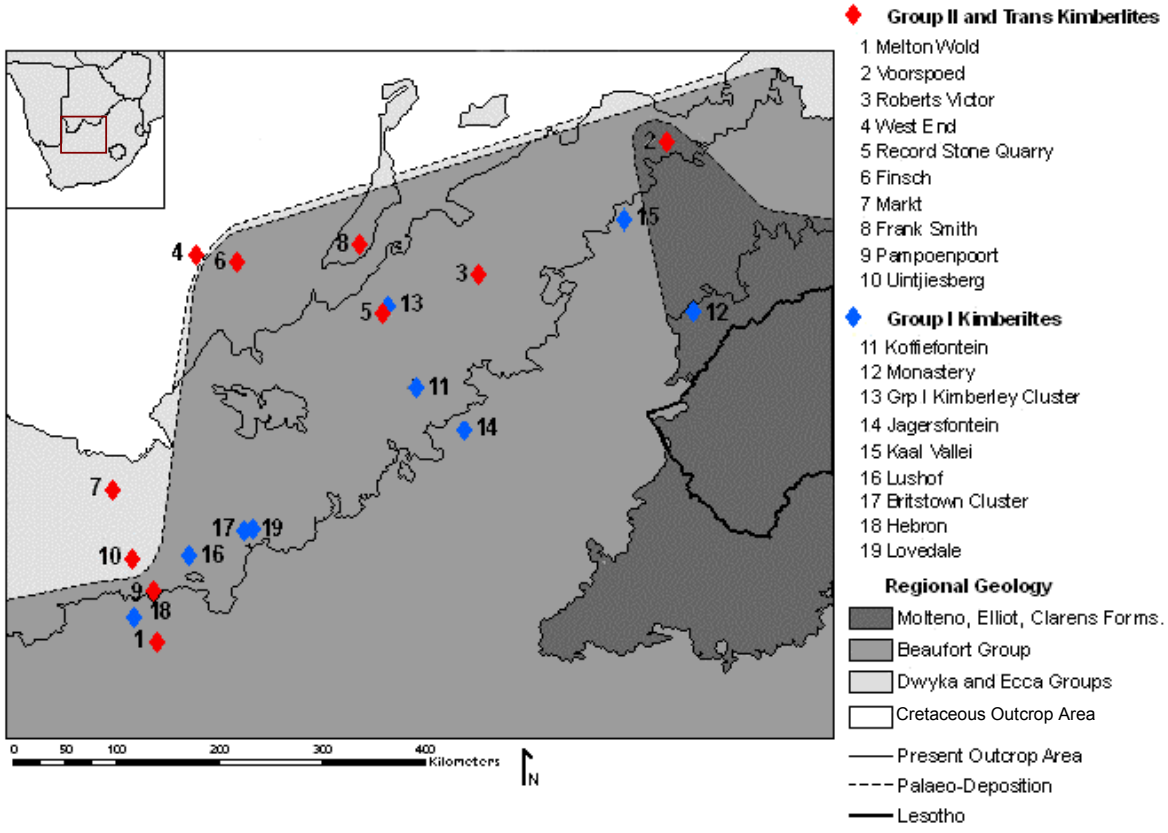

Figure 3.7: Lateral extent of the Dwyka, Ecca, Beaufort and ‘Stormberg’ Groups during the Cretaceous kimberlite emplacement based on the results of the sandstone xenolith analyses. Map constructed and modified from the De Beers database (unpubl.).

3.4.3 Conclusions

This study reveals that the present extent of the KSG sedimentary units is an eroded remnant of a once larger depositional basin. While the results of this study do not constrain precisely the lateral extent of each of the stratigraphic units of the KSG, these results do establish that the Beaufort and 'Stormberg' groups once covered an area larger than their present outcrop areas, that the extent of 'Stormberg' deposition is constrained to an area much smaller than the outline of the main Karoo Basin as defined by the Dwyka Group, and that the methods utilised in this study can be successfully applied to studies of the KSG sedimentary units, specifically to the nature of the stratigraphic units removed via erosion. Recommendations for further work include continued analyses of sandstone, siltstone and mudstone xenoliths from the studied kimberlites as well as in kimberlites outside the study area to achieve a better understanding of the extent of sedimentary fill of the main Karoo Basin.

4. KAROO SUPERGROUP BASALTS AND THE BASALT XENOLITHS

4.1 FORMATION AND GEOCHEMICAL STRATIGRAPHY OF THE KAROO BASALTS

4.1.1 Introduction

The formation of the Drakensberg Group in southern Africa, through the Karoo province continental flood basalt magmatism, occurred at 183 ± 1 Ma (Duncan *et al.,* 1997) and resulted in the cessation of Clarens sedimentation (Figures 3.1; 4.1; 4.2). The magmatism was related to a Gondwana-wide event that consisted of the intrusion of dykes and sills and continental-scale eruption of basaltic lavas associated with the break-up of southern Gondwana (Harris *et al.,* 1990; Riley *et al.,* 2006). Present day erosional remnants of the Karoo igneous province include outcrop areas in South Africa, Botswana, Zimbabwe, Namibia, Swaziland, Mozambique and Lesotho (Eales *et al.,* 1984; Marsh and Eales, 1984; Marsh *et al.,* 1997)(Figure 4.1).

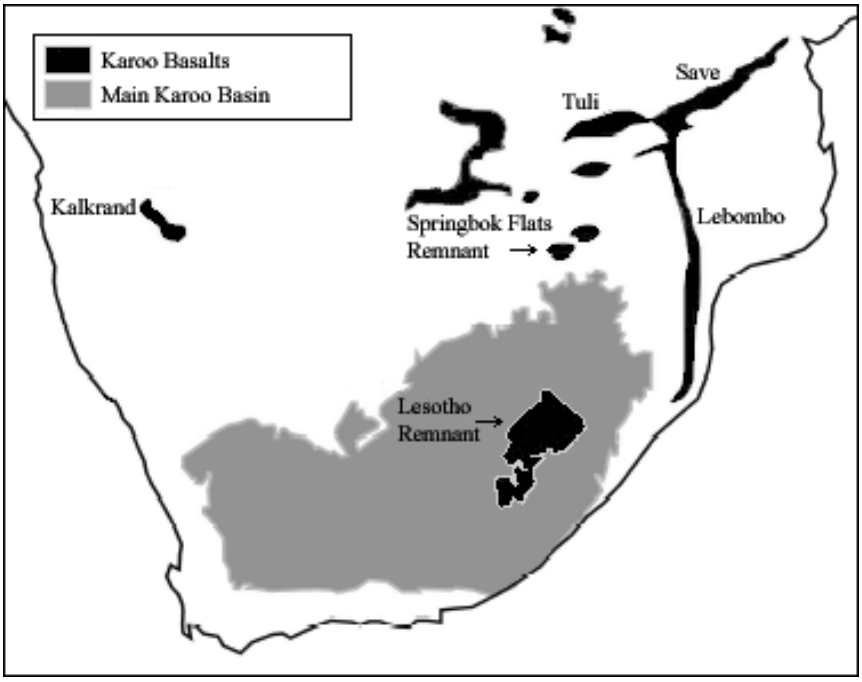

Figure 4.1: Map of the Karoo igneous province, distributions of the southern basalt remnant outcrops and location of the main Lesotho remnant in southern Africa. (after Marsh *et al.,* 1997; Catuneanu *et al.,* 1998).

Within South Africa and Lesotho, the Drakensberg Group consists of amygdaloidal, basaltic flows of the main Lesotho Remnant and associated intrusive suites (Marsh and Eales, 1984; Marsh, 1987; Marsh *et al.,* 1997); which erupted over a period of 0.5 myrs at 183 ± 1

Ma (Duncan *et al.,* 1997; Riley *et al.,* 2006). The Lesotho Remnant, subdivided into the Barkly East and Lesotho Formations, has a preserved thickness in excess of 1.5 km, though it is considered a small erosive remnant of a much thicker and more expansive lava pile (*e.g.* Eales *et al.*, 1984; Marsh, 1987; Marsh *et al.,* 1997) (Figure 4.2).

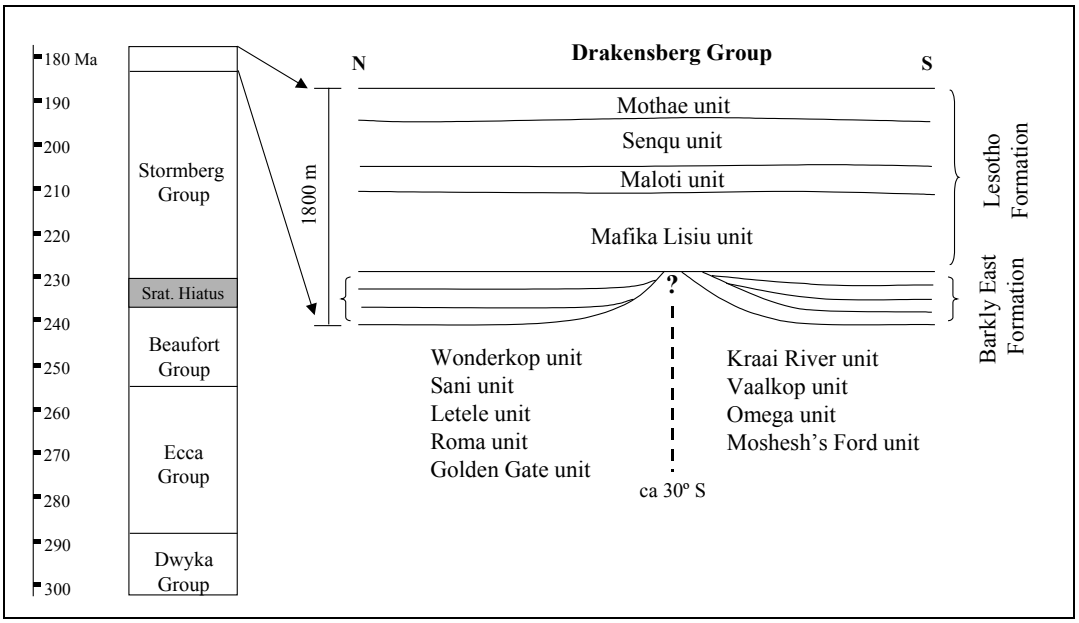

Figure 4.2: Stratigraphy of the Karoo Supergroup, with emphasis on the Drakensberg Group of the Lesotho Remnant. Drakensberg Group stratigraphy after Marsh *et al.* (1997), Karoo Supergroup ages and stratigraphy after Catuneanu *et al.* (1998); Catuneanu *et al.* (2002); Bordy *et al.* (2004); figure after Mitha (2006).

The basal Barkly East Formation is characterised by thin, spatially limited lava flows with sandstone intercalations, which indicate a gradual transition from a sedimentary into a magmatic phase (Lock *et al.,* 1974; Eales *et al.,* 1984). Overlying the Barkly East Formation is the Lesotho Formation, which is the main and volumetrically dominant part of the lava pile, predominantly composed of pahoehoe-type, amygdaloidal basaltic flows (Duncan *et al.,* 1984b; Eales *et al.,* 1984). These flows are relatively homogeneous in their horizontal disposition with uniform thickness, ranging from less than 0.5 m to greater than 50 m (Eales *et al.,* 1984), suggesting that the lava pile was erupted onto a planar surface by a series of widespread dykes (Marsh *et al.,* 1997).

4.1.2 Formation and Lateral Extent of the Karoo Basalts

Karoo magmatism was related to the early break-up-related rifting that occurred in southern Gondwana (Encarnación *et al.,* 1996). The timing of the main phases of magmatism

occurred prior to the break-up of Gondwana, suggesting that it was not a direct result of continental disintegration. Instead, it is likely that the processes that resulted in Karoo magmatism also contributed to the break-up of Gondwana and the opening of the Atlantic Ocean (Duncan *et al.,* 1984b). It has been attributed to deep-mantle plume processes that provided temperatures high enough to generate large volumes of basaltic magma; however the plume-lithosphere relationship remains debatable (Marsh *et al.,* 1997; Turner, 1999).

Regardless of this relationship, Karoo flood basalt lavas were likely erupted through fissures that were fed by the dykes now preserved throughout the main Karoo Basin (Marsh *et al.,* 1997). Potential feeders for some of the Barkly East Formation and all of the Lesotho Formation have been identified by Mitha (2006), suggesting that most of the Lesotho remnant was erupted from local fissures or vents.

4.1.3 Geochemical Stratigraphy of the Karoo Basalts

It has long been recognized that geochemical trends relating to different magma types occur throughout the basalts of the Drakensberg Group (*e.g.* Lock *et al.,* 1974). These geochemical trends and variations provide a qualitative means of subdividing the Drakensberg Group into distinct stratigraphic units (*e.g.,* Marsh and Eales, 1984; Marsh *et al.,* 1997), and values with which the geochemistry of the basalt xenoliths collected at each of the kimberlites can be compared and correlated.

Marsh *et al.* (1997) utilized variations in incompatible element ratios and element abundances to subdivide the Barkley East and Lesotho Formations into several stratigraphic units (Figure 4.2). These units are comprised of packages of geochemically similar lava flows, which define a magma type. The Barkley East Formation is identified as several thin, geochemically distinct units at the base of the Drakensberg Group. The stratigraphic units differ north and south of 30˚S, and the formation is thus divided into the 'northern' and 'southern' Barkley East Formations (Figure 4.2). Within the northern and southern formations, there are also localised variations in the stratigraphy. In contrast, units of the Lesotho Formation are much thicker and horizontally continuous across the Lesotho Remnant. The following descriptions are based on Marsh *et al.* (1997). Geochemical discrimination diagrams are presented in Figures 4.3 and 4.4 for the Barkly East and Lesotho Formations respectively.

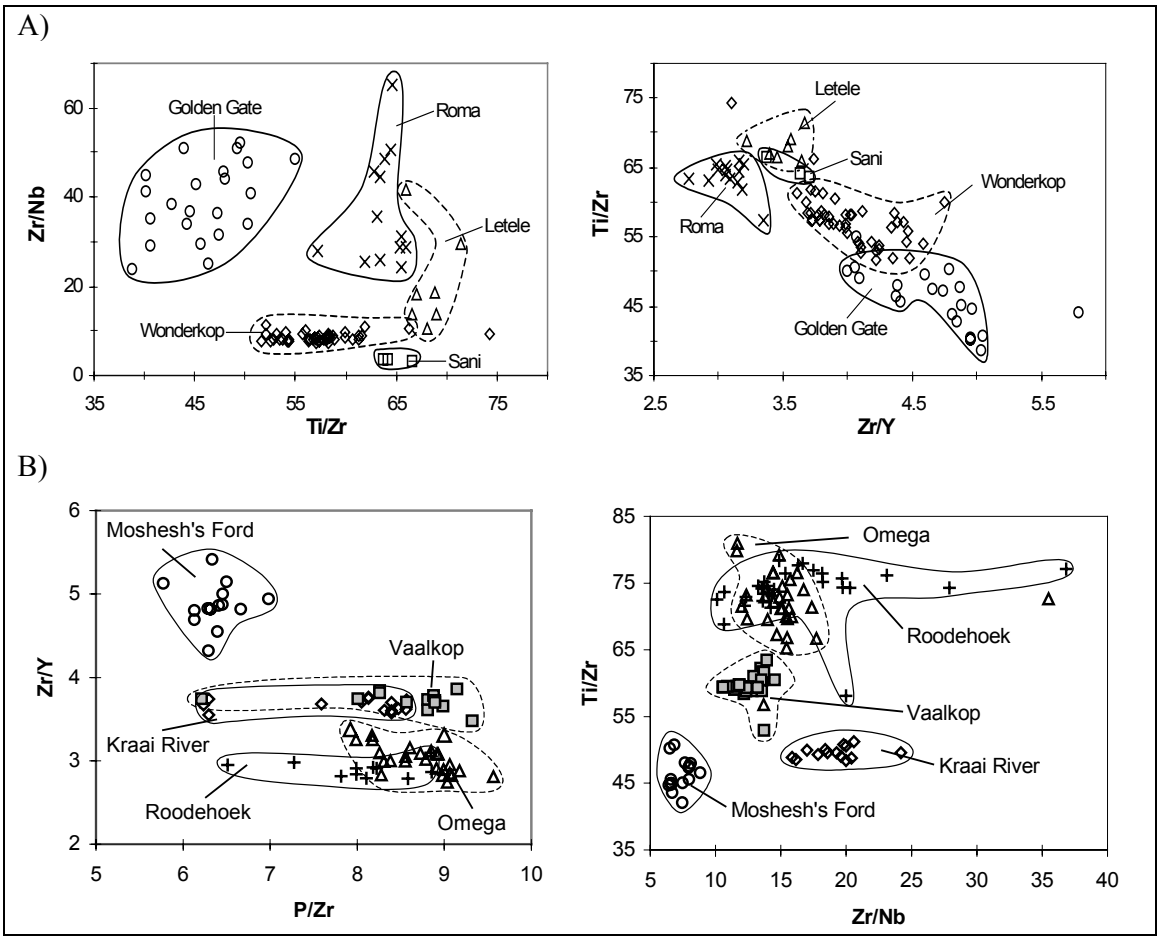

Figure 4.3: Geochemical discrimination diagrams of the northern (A) and southern (B) Barkly East Formation. Geochemical discrimination diagrams after Marsh *et al*. (1997); basalt data from Marsh *et al*. (1997) and Marsh (1998).

4.1.3a Northern Barkly East Formation

The Golden Gate, Roma, Letele, Sani and Wonderkop units occur north of 30˚S (Figure 4.2). The basal unit in the northern Barkly East Formation (nBEF), the Golden Gate unit, is characterised by low Ti/Zr and P/Zr as well as high Zr/Y and Zr/Nb ratios. Overlying the Golden Gate unit in the northern part of the nBEF is the Letele unit. Letele has similar incompatible element abundances as Golden Gate, but is distinguishable by low Zr/Y, moderate P/Zr and Zr/Nb and high Ti/Zr ratios. In the southern area of the nBEF, Golden Gate is overlain by the Roma and Sani units. Again, these are similar to Golden Gate, but Roma has low Zr/Y and P/Zr and distinctively high Ti/Zr; while Sani is characterised by high P/Zr and Ti/Zr. The uppermost unit in the nBEF, the Wonderkop unit, is readily recognized by low Zr/Nb and high Zr/Y ratios. In north and west basalt outliers, Wonderkop oversteps

the overlying units and directly overlies the sandstones of the Clarens Formation (Marsh, 1987).

4.1.3b Southern Barkly East Formation

The southern Barkly East Formation (sBEF) is comprised of the Moshesh's Ford, Roodehoek, Omega, Vaalkop and Kraai River units (Figure 4.2). The Moshesh's Ford unit is the basal unit for the entire sBEF. However, the overlying units are unique to the southwestern area (Roodehoek and Vaalkop units) and central portions (Omega and Kraai River units) of the sBEF. Moshesh's Ford is characterised by low Ti/Zr and Zr/Nb ratios, with high Zr/Y, Ba, Sr and Nb content. Roodehoek and Omega are stratigraphic equivalents that overlie Moshesh's Ford. Both are distinguished by low Rb, Zr, Nb, SiO_2, TiO_2, K_2O, P_2O_5 and Zr/Y, as well as high Cr, Ni, MgO, CaO, Al_2O_3 and Ti/Zr content. The upper Vaalkop and Kraai River units do show some similarities, such as Nb, Zr, Y, Cr and rare earth element abundances, but are easily distinguished from one another and from underlying units. Kraai River has low MgO, high SiO_2 and distinct Ti/P, Ti/Zr and Zr/Y ratios; while Vaalkop has high Rb, Sr, SiO_2, TiO_2, K_2O and P_2O_5 content.

4.1.3c Lesotho Formation

The Lesotho Formation accounts for most of the volume of the Drakensberg Group basalts. However, the geochemistry of the Lesotho Formation is more uniform than the underlying Barkly East Formation, although a broad upward trend in increasing differentiation is apparent (Marsh *et al.,* 1997). The low Ti-basalts of the Lesotho Formation are subdivided into the Mafika Lisiu, Maloti, Senqu and Mothae units (Figure 4.2). The basal Mafika Lisiu unit is ~400 m thick, making it the thickest of the Lesotho Formation units. Overall, the unit has variable P/Zr, Zr/Y and Zr/Nb ratios, and the highest Mg# and Ti/Zr values of the Lesotho Formation.

The overlying Maloti unit is markedly more evolved than Mafika Lisiu, with a sharp decrease in Ti/Zr, P/Zr and Zr/Nb ratios and increase in Zr/Y ratio at the base of the unit, which signifies a distinct compositional change in the upper Lesotho Formation basalts. It has a consistent thickness of approximately 100 m throughout the remnant, and has low Ti/Zr and P/Zr and high Zr/Y ratios relative to Mafika Lisiu. The upper flows of Maloti appear transitional towards the overlying, typical Senqu-type lavas, with overlaps in FeO, TiO_2 and P_2O_5 concentrations and Ti/Zr, P/Zr, Zr/Nb and Zr/Y ratios. Senqu is more evolved than the underlying units with lower Mg# and higher Zr content. However compositional variations

and overlaps with Maloti unit make discrimination between the two difficult without stratigraphic information.

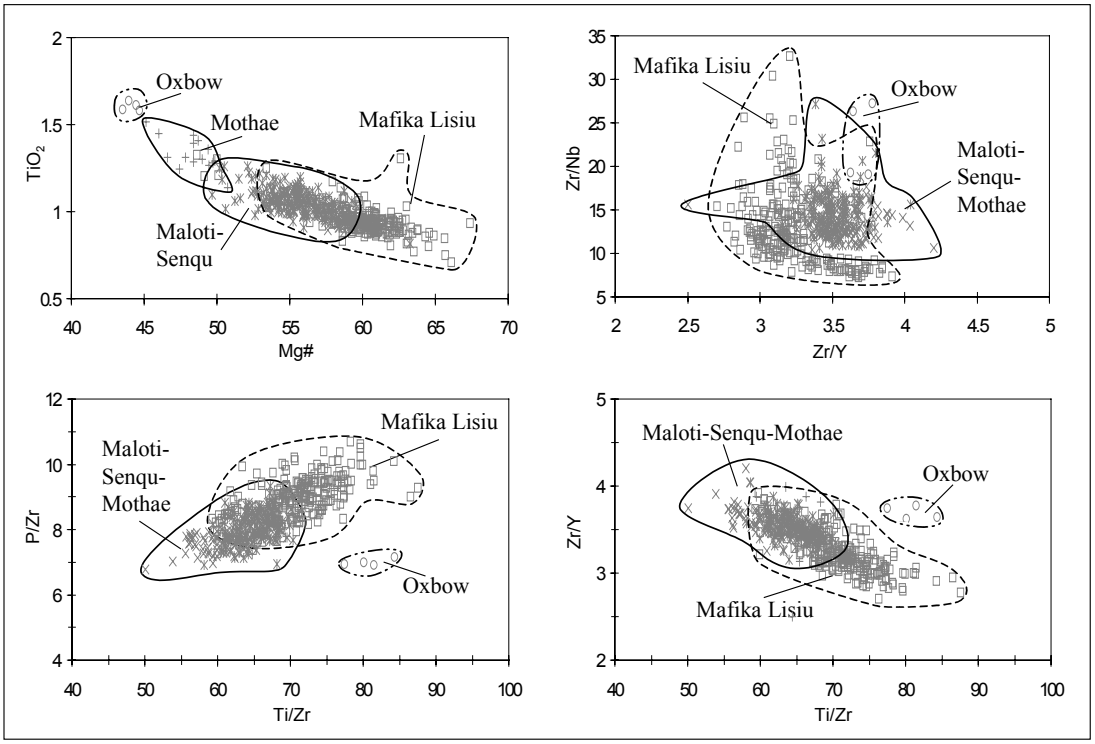

Figure 4.4: Geochemical discrimination diagrams of the Lesotho Formation. Diagrams after Marsh *et al*. (1997); basalt data from Marsh *et al*. (1997) and Marsh (1998). Mg# calculated with Fe as FeO.

The Mothae unit contains the upper and most evolved lava flows of the Lesotho Formation, and is distinguished from the underlying Maloti-Senqu units by a lower Mg# and higher TiO_2 content. It is also characterised by lower CaO, MgO, Al_2O_3 and Ni, and higher FeO, P_2O_5 and incompatible trace element contents than the other units of the Lesotho Formation. Because of overlaps on the geochemical discrimination diagrams, Mothae is also grouped with the underlying Maloti and Senqu units, and these units will be referred to as MSM for correlation purposes.

A series of chemically evolved dykes intrude the stratigraphy in northern Lesotho. These small intrusions have distinctly low Mg# content and high FeO, Ti/Zr and Zr/Nb rations that cannot be correlated with any of the known units in the Lesotho Remnant, and are therefore considered intrusive expressions of the now eroded upper portions of the Drakensberg Group lava pile (Marsh, pers. comm. 2006).

4.2 Analysis and Correlation of the Basalt Xenoliths

4.2.1 Sampling and Analytical Methods

A total of 74 (1 to 10 at each kimberlite) massive, vesicular or amygdaloidal basalt xenolith samples were collected from the coarse-material dumps, excavation pits, unmined surfaces, and/or borehole cores of each kimberlite (Figure 4.5). Although such samples were found and collected at the KKC, they are not Karoo-like basalts. No basalt xenoliths were found or collected at the Koffiefontein/Ebenheuyser, Hebron, Britstown cluster or Lovedale pipes. Vesicular and amygdaloidal xenoliths were preferentially sampled to avoid falsely identifying dolerites as basalts. Massive samples were only considered viable representations of Karoo basalts, as opposed to dolerites, if amygdaloidal or vesicular basalt xenoliths were not found at the sampling location.

The basalt samples were crushed to make fusion discs and powder pellets for X-Ray Fluorescence Spectrometry (XRF) analysis. Amygdales were removed from the amygdaloidal samples to avoid contamination. Fusion discs, prepared according to the methods outlined by Norrish and Hutton (1969), were used for major element determination. Trace element (Zn, Cu, Ni, Co, Cr, V, Nb, Z, Y, Sr, Rb, Ce, Nd and La) and Na_2O analyses were conducted on the fusion discs, which were prepared according to the method presented by Duncan *et al.* (1984a). The whole rock geochemical data were normalized to 100% free of volatiles for analytical and correlation purposes. The unnormalised major and trace element data are presented in Appendix II.

4.2.2 Analysis of XRF Data

The purpose of analysing the basalt xenoliths is to determine their whole-rock composition and to correlate their composition with the geochemical signatures of known lava-types present in the Karoo basalts, specifically those identified in the Barkley East and Lesotho Formations. Petrography was not considered because there are very few, if any, textural or mineralogical features that differ between, or are unique to, any of the magma types (Robey, 1976; Mitha, 2006).

The normalised trace, major and element ratio data were plotted on geochemical discrimination diagrams together with data from known units of the Karoo basalts to establish general correlations. Each xenolith is classified as Barkley East, Mafika Lisiu (ML), Maloti / Senqu / Mothae (MSM), or Oxbow depending with which of the pre-defined fields the xenolith geochemistry best correspond.

A)

B)

C)

D)

E)

F)

Figure 4.5: Representative samples of the variety of basalt xenoliths collected from each of the kimberlites. (A) Melton Wold - an *in situ* basalt xenolith found in an excavation pit. (B) RV1-22 (C) M4-10 (D) BF2-30 (E) FS1-11 (F) MK1-53.

4.3 Results and Correlation with the Karoo Basalts

4.3.1 XRF Analysis Results

The majority of the xenoliths can be classified as basalt and basaltic andesite in composition, with SiO_2 contents ranging from 45 - 53 wt%. In comparison to typical SiO_2 values for Karoo basalts (47-58 wt%, basalt to basaltic andesite) (Marsh *et al.,* 1997), samples MW1-03, MW1-05, V1-04, WE1-61, WE1-63, FN3-19, PP-32, PP-36, UJ1-24, UJ1-25, UJ1-26, M3-06, KV-105, BF2-28 and BF2-29 have relatively low SiO_2 content (41.59 – 45.66 wt%), but are still considered Karoo basalts. Sample PP-33 has anomalously low SiO_2 (35.92 wt%), and was therefore not considered in the correlation process.

Samples MW1-05, WE1-70 and UJ1-20 have high major element totals, ranging from 102.67 to 102.87 while BF2-28 has a low major element total of 97.15 (Appendix II). This may be due to sample preparation errors and the results of these samples therefore have high potential error.

4.3.2 Correlation Results

Like the sandstone xenoliths, correlation of the basalt xenoliths with the Karoo basalts is obscured by geochemical overlaps in the Drakensberg Group basalt units, particularly in the Lesotho Formation. However, the results demonstrate which xenoliths are indisputably derived from the Karoo basalts, as well as indicating whether they are from the basal Barkley East Formation or the overlying and more extensive Lesotho Formation. Furthermore, it is possible to determine, within reasonable doubt, whether the xenoliths that correlate with the Lesotho Formation were derived from the lower and less evolved (ML) or upper and more evolved (MSM) portion of the lava pile (Figure 4.7; Table 4.2). With the geochemical discrimination plots, it is also evident that the geochemical composition of some of the basalt xenoliths, such as those from the KKC and Markt kimberlites (Figure 4.7), diverges from the composition of typical Lesotho Formation basalts. These variations are discussed below. Refer to Figure 4.7 and Appendix II for analysis and correlation results.

Most of the samples also have notably high Na_2O, K_2O, Sr and Rb values in comparison to the Karoo basalts (Figure 4.6). This trend is attributed to interactions with the kimberlite magma and fluids at the time of kimberlite emplacement (e.g., Le Roex *et al.,* 2003). Several samples, such as MW1-03, MW1-05, V1-05, WE1-61, WE1-64, PP-32, PP-36, UJ1-26, M3-06 and M4-10 have variable P_2O_5, Zr, Nb content and immobile element ratios (Figure 4.7). It is likely that these variations are due to kimberlite contamination in the form of remnants external to the xenolith or intrusive veins or fracture fillings that were not

removed during the sample preparation process. Alternatively, these deviations from the typical geochemistry of the Lesotho Formation basalts may be due to flow or lateral variations that exist outside of the Lesotho Remnant that are therefore not recorded in the basalt types of the Lesotho Remnant.

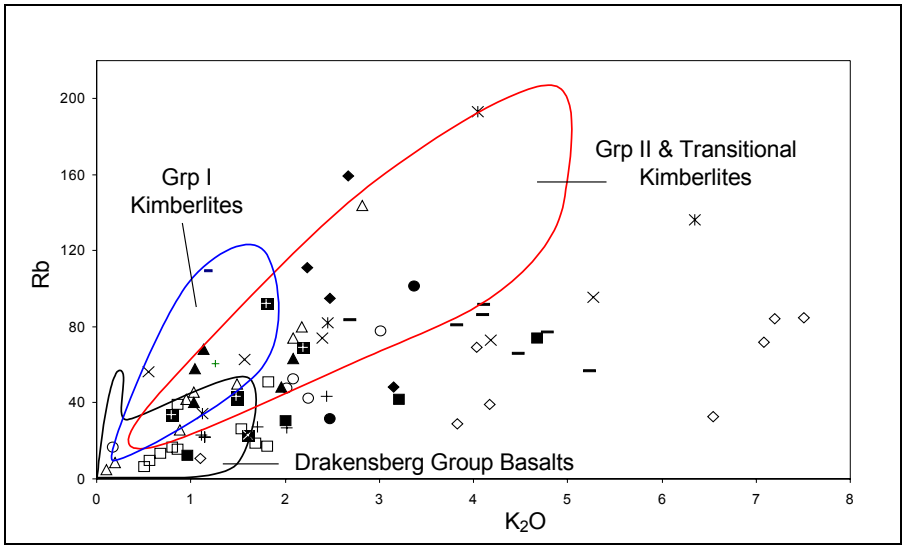

Figure 4.6: Geochemical discrimination diagram demonstrating the effects of kimberlite-xenolith interactions on mobile element compositions within the xenoliths. Symbols as follows: MW(♦), V(Δ), RV(■), WE(-), RSQ(•), FN(◊), MK (*), FS(⧓), PP(▲), UJ(▪), M(o), JG(□), KV(+), KKC (x). Geochemical discrimination diagrams after Marsh *et al*. (1997); basalt data from Marsh *et al*. (1997) and Marsh (1998); kimberlite data from Roberts (1997), Letsale (1998), Mambali (1998) and Le Roex *et al.* (2003).

Melton Wold

Two of the four basalt xenoliths, MW1-10 and MW1–11, collected from an excavation pit at Melton Wold correlate with the MSM units. Although MW1-10 has high Ti/Zr (72.9) ratio relative to MSM, the Mg# (49.9) and P/Zr (7.9) values are indicative of the MSM units. MW1-03 and MW1-05, have high Nb and low Zr/Nb values, 4.9 and 3.3. MW1-03 is also characterised by low Ti/Zr (38.7) and P/Zr (4.9) ratios due to a high Zr concentration, while MW1-05 has a high P/Zr (12.1) ratio. The Mg# (60.5 and 63.3) and TiO_2 concentrations of both of these samples are consistent with the ML unit.

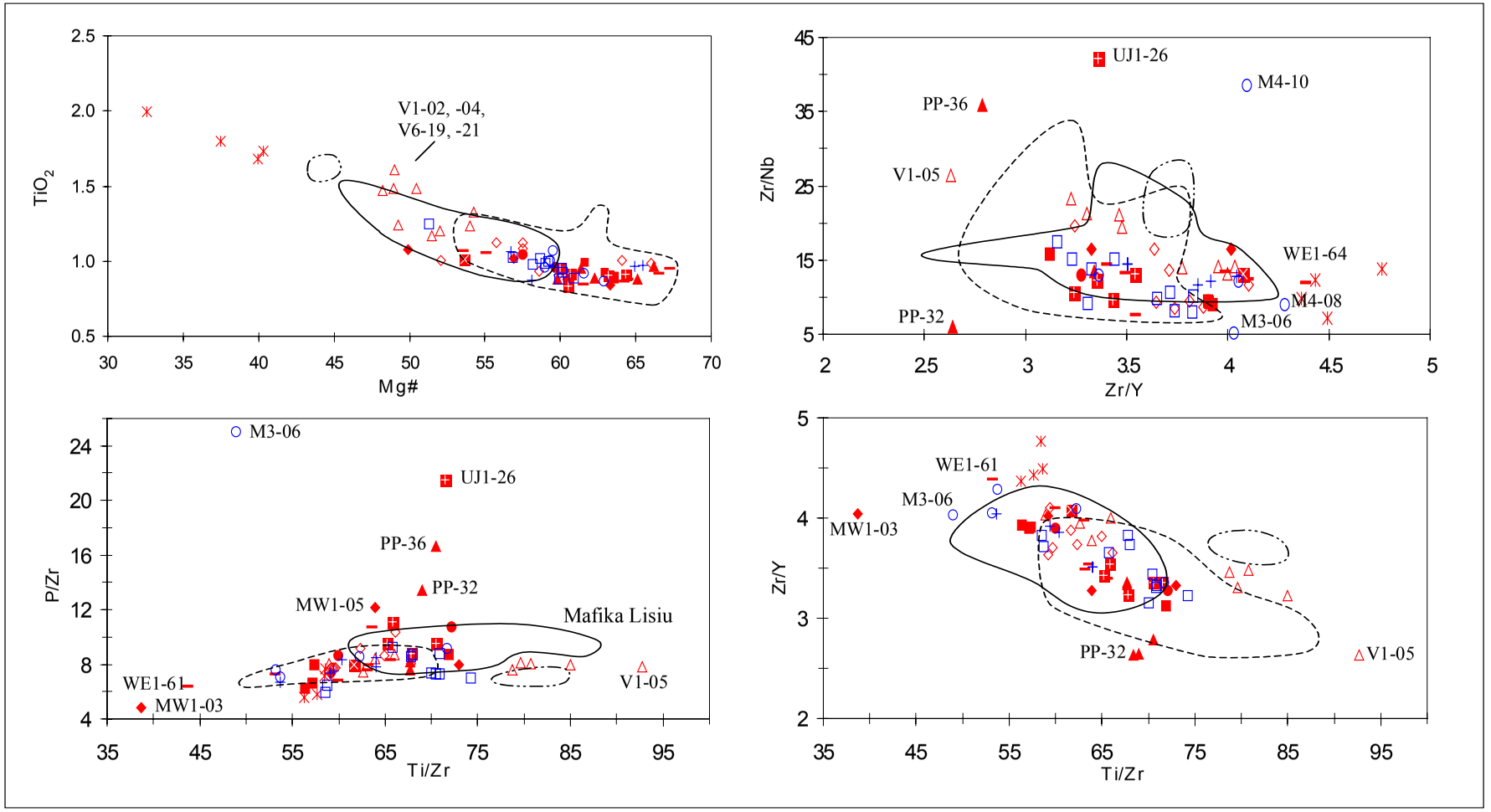

Figure 4.7: Results of the basalt xenolith analysis in comparison to Lesotho Formation basalts (Mafika Lisiu: --; MSM: —; Oxbow: -- —). Group II and transitional kimberlites in red, Group I kimberlites in blue. Symbols as follows: MW(♦), V(Δ), RV(■), WE(-), RSQ(•), FN(◊), MK (*), FS(▬), PP(▲), UJ(⊠), M(o), JG(□), KV(+). KKC results presented in Figure 4.10 Geochemical discrimination diagrams after Marsh *et al.* (1997); basalt data from Marsh *et al.* (1997) and Marsh (1998).

Voorspoed

All of the Voorspoed xenoliths are relatively evolved, with high or low TiO_2 concentrations and low Mg# values (48.2-54.4) that are similar to the Senqu and Mothae units. Samples V1-03, V1-04, V1-05 and V6-20 also have incompatible element ratios consistent to the MSM units and plot within the MSM units on the geochemical discrimination diagrams. V1-05 also has a notably high Ti/Zr ratio (92.73). The remaining samples have incompatible element ratios, with Ti/Zr, P/Zr and Zr/Y values comparable to the ML unit and Oxbow dykes, and a Zr/Nb value similar to ML and MSM but somewhat lower than the Oxbow dykes. Because of the low Mg#s (48.2-49.2) and affinity to the upper MSM units and Oxbow dykes, V1-02, V1-05, V2-10, V6-19 and V6–21 are considered MSM (specifically Senqu or Mothae). However, the similarities to the Oxbow dykes advocate the possibility that these samples are from fractionated flows that occurred above the Mothae unit and are now eroded from the Lesotho Remnant.

Roberts Victor

The four Roberts Victor basalt xenoliths show a strong correlation with the Lesotho Formation. RV1-22 is from the Mafika Lisiu unit, as it consistently plots within the ML fields (Figure 4.7). RV1-18, RV1-19 and RV1–21, have elevated Zr, Ti/Zr, moderately low Zr/Nb and low Ti/Zr values in comparison to RV1-22, and are more consistent with the upper MSM units or the Barkly East Formation values. Although the Mg#s are most similar to Mafika Lisiu (61.6-63.6), geochemical similarities with the MSM units are more prevalent and these samples are classified as MSM.

West End

Mafika Lisiu is the dominant lava-type represented by the West End basalt xenoliths. WE1-60, WE1-62 and WE1–64 consistently plot within the overlap of the ML and MSM fields. These samples have moderate Ti/Zr values (63.1-65.5) and high Mg#s (61.5-67.2), indicating a stronger affinity to the ML unit. WE1-70 and WE1–71 are more evolved than the other West End xenoliths, and are classified as MSM. WE1-61 has a high Zr concentration relative to TiO_2 resulting in a low Ti/Zr ratio of 43.6; while WE1-64 has a Zr/Y ratio of 4.4, which is similar to the Markt samples. Both samples have high Mg# content 66.5 and 64.4, and likely correlate with the ML basalts.

Record Stone Quarry

RSQ1-03 and RSQ1–10 correlate with the Mafika Lisiu unit of the Lesotho Formation.

Finsch

The Finsch xenoliths all correlate with the Lesotho Formation and show considerably elevated K_2O values as a result of kimberlite influences (Figure 4.4). FN1-03, FN1-04 and FN1–07 have Mg#s (52.1-57.5), TiO_2 and incompatible element ratios comparable to the MSM units. The remaining samples, FN1-05, FN3-15, FN3-18, FN3-19 and FN3–20 correlate with the ML unit as they have higher Mg#s (58.6-66.0) (except FN3-20, 57.5) and Ti/Zr (61.7-67.8 versus 59.2-59.7) and P/Zr (8.0-10.4 versus 7.7) and lower and Zr/Nb (8.6-9.5 versus 11.7-16.5) (except FN1-05, 19.5) relative to the other xenoliths, and consistently plot within the ML fields.

Markt

The basalt xenoliths from the Markt kimberlite are more evolved than the typical Lesotho Basalts as well as the Oxbow dykes. This geochemical trend indicates one of several possibilities: (1) the Markt xenoliths represent a localized equivalent of the Barkley East Formation and are thus from the bottom of the magma pile; (2) the xenoliths are from a younger, evolved magma type at the top of the lava pile, which is no longer preserved, or was never present in the Lesotho Remnant; or (3) the xenoliths originate from geochemically distinct lava flows preserved outside of the Lesotho Remnant (Figure 4.1).

It is unlikely that the Markt xenoliths correlate with the Barkly East Formation as Markt is far from the source and remnants of the BE units, which are considered localised flows with local feeders (Marsh *et al.,* 1997; Mitha, 2006). Furthermore, the geochemistry of the xenoliths is not compellingly similar to any of the sBEF units. The xenoliths are quite evolved and fractionated, with low Mg#s ranging from 37.5-40.3 and high TiO_2 and Zr/Y values, but moderate P/Zr and Ti/Zr. Geochemical discrimination plots of the xenoliths indicate that the MK basalts are highly fractionated or evolved Lesotho basalts and are most likely from a younger, more evolved lava-type that was eroded from the Lesotho Remnant (Figure 4.7).

A comparison of the Markt basalts with the Kalkrand[6] and Etendeka[7] basalts of Namibia, the Springbok Flats[8] remnant of northern South Africa and the Blaauwkrans and Hangnest sills[9] of western South Africa reveals that although there are several similarities, the Markt samples are still highly evolved or fractionated relative to the Karoo remnants (Figure 4.8). All of the above listed basalts have Mg#s and major element concentrations, including TiO_2, comparable to the Lesotho Formation except for the high-Ti flows of the Springbok Flats. Although the Mg#s of the Markt basalts are most consistent with the high-Ti Springbok Flats basalts, these xenoliths are still classified as low-Ti basalts.

While the element ratios of the Kalkrand, low-Ti Springbok Flats and Blaauwkrans are comparable to the Lesotho Formation, the Etendeka and Hangnest ratios are variable and have an affinity to the Markt ratios. For example, the low Ti/Zr and high Zr/Y ratios of two of the Etendeka samples (Tafelberg and Albin basalts) (Marsh, 1987) relative to the Lesotho Formation basalts trend with the Markt basalt ratios. The Hangnest dolerites are also characterised low Ti/Zr and high Zr/Y ratios, but the Zr/Nb values are high relative to the Mark samples.

The geochemistry of the Markt basalt xenoliths is inherently similar to the Drakensberg, Kalkrand, Etendeka and low-Ti Springbok Flats basalts and the Blaauwkrans and Hangnest dolerites. However, further work is required to characterize the evolved nature of these xenoliths and to deduce the relationship between the xenoliths and the Karoo remnants. Based on observations of the present study, the Mark xenoliths are considered samples of an evolved Lesotho-like magma now eroded from the Lesotho Remnant (Figure 4.7).

Frank Smith

FS1-11 correlates with the MSM units with a moderate Mg# (53.7) and Ti/Zr ratios and a high Zr/Y ratio. It is not possible to compare the result with other xenoliths because only one sample was found and analysed from the Frank Smith kimberlite.

---

[6] The Kalkrand basalts are of similar age and geochemistry to the Lesotho Formation basalts (Duncan *et al.,* 1984b; Fitch and Miller, 1984)

[7] The Etendeka remnant occur in north-western, coastal Namibia and is composed of tholeiitic basalts interbedded with silicic volcanics (Marsh, 1987). The remnant is early Cretaceous in age (120-135 Ma) (Erlank *et al.,* 1984)

[8] The Springbok Flats remnant is comprised of a basal, low-Ti zone that is similar to the Lesotho remnant, and an upper high-Ti zone (Marsh *et al.,* 1997).

[9] These sills are located in the Calvinia District, Western Cape Province, and are considered Karoo dolerite sills. Blaauwkrans is an olivine tholeiite and Hangnest a quartz tholeiite (Le Roex and Reid, 1978).

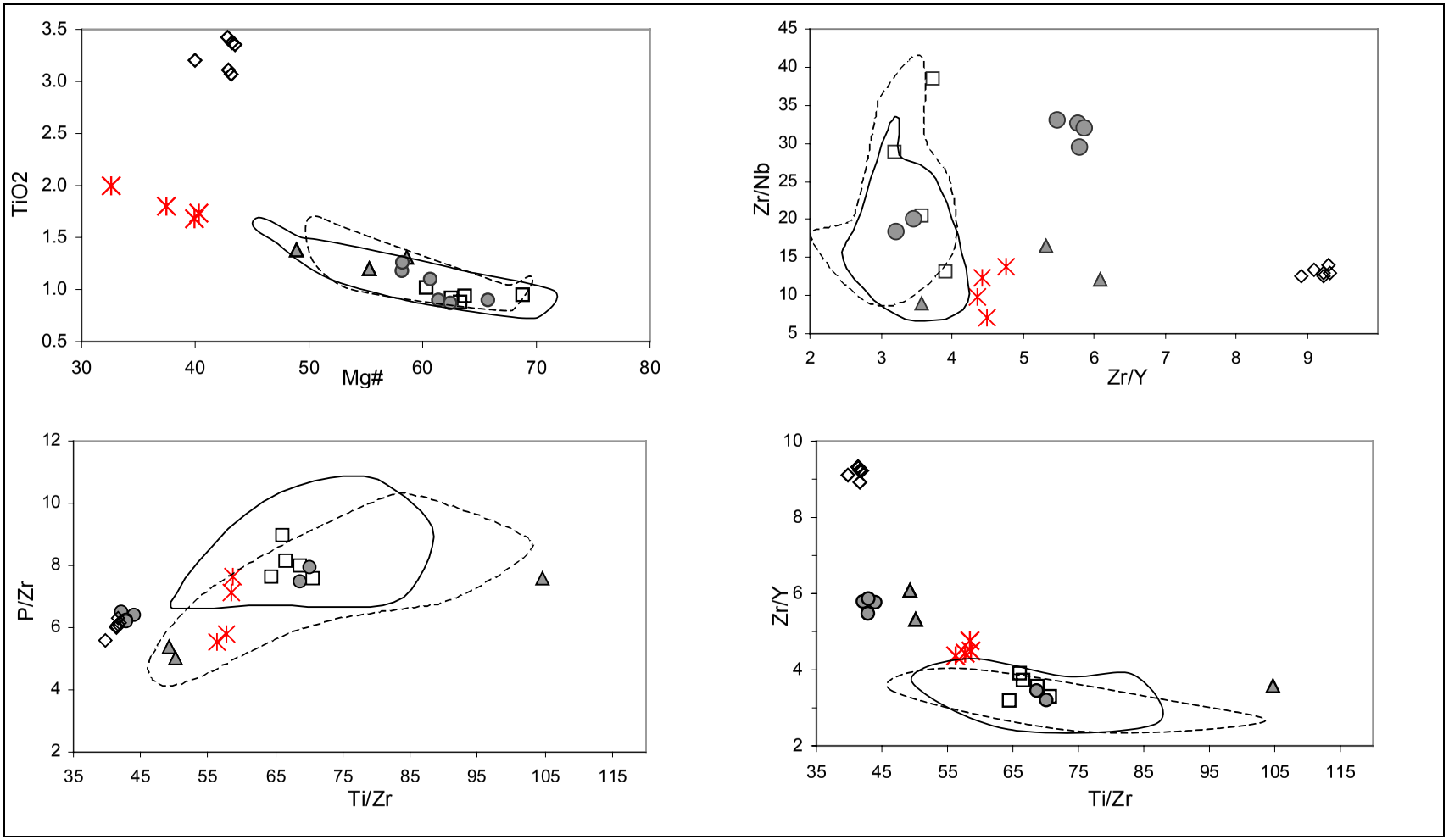

Figure 4.8: Geochemical discrimination diagrams comparing the geochemical composition of the Markt xenoliths with selected intrusive and extrusive Karoo remnants of southern Africa. Lesotho Formation (----), low-Ti Springbok Flats (——), high-Ti Springbok Flats (◊), Kalkrand ( ), Etendeka (▲), Blaauwkrans and Hangnest sills (●). Diagrams after Marsh *et al.,* (1997); data from Le Roex and Reid (1978), Duncan *et al.,* (1984a), Marsh (1987).

Pampoenpoort

PP-32 and PP–36 have variable SiO_2, P_2O_5 and Nb concentrations as well as Zr/Y and Zr/Nb ratios. These samples do have Mg# (59.8 and 62.3) and Ti/Zr (69.0 and 70.5) values indicative of ML basalts, and are therefore considered ML xenoliths. PP-30 and PP-31 show no variability and have a geochemical affinity to the ML units.

Uintjiesberg

Except for UJ1-26, all of the Uintjiesberg basalts consistently plot within the ML field on the geochemical discrimination diagrams. UJ1-26 is characterised by distinctive P_2O_5 and P/Zr as well as Zr/Nb and low Nb values, likely a result of kimberlite interactions or contamination. UJ1-26 most likely correlates with the ML unit as it has similarly high Mg# (64.4) and Ti/Zr (71.5) and moderate Zr/Y (3.4) values.

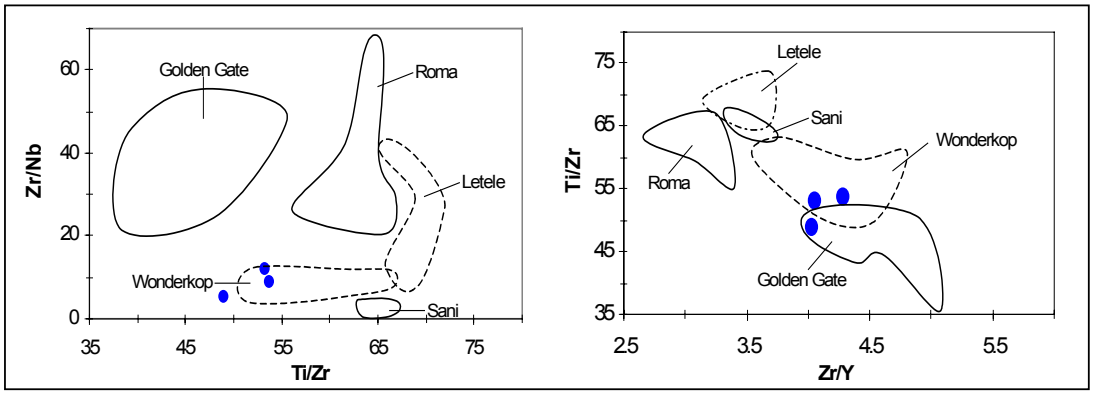

Figure 4.9 Comparison of the Monastery xenoliths (•) with the northern Barkly East Formation basalts. Diagrams after Marsh *et al*. (1997); basalt data from Marsh *et al*. (1997) and Marsh (1998).

Monastery

Xenoliths sampled from the Monastery kimberlite show the most geochemical variations of all of the basalt xenoliths suites. Because of its proximity to the Lesotho Remnant and thus the Barkly East Formation and its feeders, it is probable that the northern Barkly East Formation extended to the Monastery area. M3-05, M3-06 and M4-08 have compositions consistent with certain northern BE units (Wonderkop) as well as the MSM basalts (Figure 4.7; 4.9)

M4-09 is from the ML unit, as it consistently plots within the ML fields. M4-10 may also correlate with the ML unit, although the low Nb and high Zr/Nb and Ti/Zr, Zr/Y and

P/Zr values are more typical of the BE and MSM units respectively. Because of MSM-like incompatible element ratios, except Zr/Nb caused by a low Nb concentration, M4-10 is most likely related to the MSM units.

Jagersfontein

The Jagersfontein basalt xenoliths predominantly correlate with the Mafika Lisiu basalts, with similar Mg# (58.2-60.9), TiO_2, Ti/Zr, Zr/Nb and Zr/Y values. The P/Zr value is notably low in all of the samples except JG1-14, JG1-16, JG1-20 and JG1–21 (5.9-7.4 versus 8.6-9.3), presumably a result of lateral variations outside of the Lesotho Remnant. In comparison to the other xenoliths, JG1-15, JG1–21 and JG1-22 tend to plot more in the MSM fields and have TiO_2 and Ti/Zr ratios indicative of MSM basalts. JG1-21 also has a significantly lower Mg# (51.3) than the other JG xenoliths, suggesting it may be from the upper part of the MSM units, though incompatible element ratios are more similar to the lower MSM units.

Kaal Vallei

Geochemistry of KV-103 and KV-105 are most similar to ML, while KV-100 and –101 have lower Mg# than KV-103 and immobile element ratios similar to the more evolved MSM units. KV-102 also has a geochemical resemblance to the MSM units, but with anomalous Zr and Ti/Zr values, and an ML-like Mg# (65.5) content.

Kimberley Group I Kimberlites

Grey or brownish basalt xenoliths with white amygdales as opposed to the typically green and silicified Ventersdorp Group lavas, were collected from the De Beers (2) and Bultfontein (3) kimberlite dumps (Figure 4.5D). Analyses of the xenoliths will show that none of the basalt xenoliths from the Group I Kimberley pipes are geochemically similar to the Drakensberg Group basalts (Figure 4.7). In comparison to the Drakensberg Group, the xenoliths have very high Zr and Zr/Y, somewhat high SiO_2, Ca and La, low Ti/Zr, and Zr/Nb and P/Zr ratios similar to the Lesotho Formation. Unlike the other xenoliths with unique geochemistry, the deviations from the typical Drakensberg Group geochemistry cannot be explained by kimberlite-related alteration, contamination or flow variation. Furthermore, the basalt xenoliths found in the KKC consistently plot within fields for the Allanridge Formation of the Ventersdorp Supergroup on the geochemical variation diagrams (Figure

4.10). These factors confirm that the xenoliths collected at the Kimberley dumps are indisputably of Ventersdorp Supergroup origin.

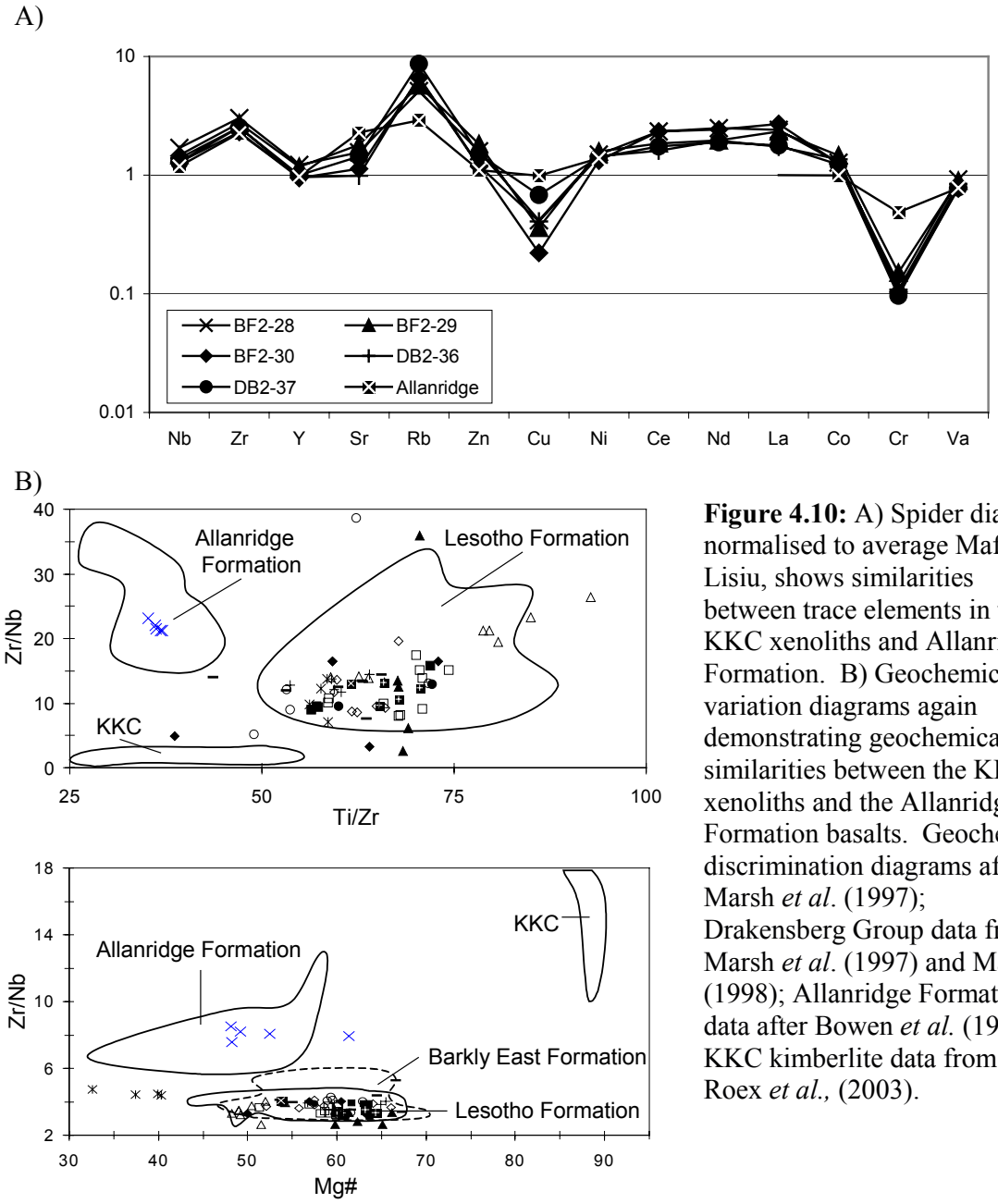

Figure 4.10: A) Spider diagram, normalised to average Mafika Lisiu, shows similarities between trace elements in the KKC xenoliths and Allanridge Formation. B) Geochemical variation diagrams again demonstrating geochemical similarities between the KKC xenoliths and the Allanridge Formation basalts. Geochemical discrimination diagrams after Marsh *et al*. (1997); Drakensberg Group data from Marsh *et al*. (1997) and Marsh (1998); Allanridge Formation data after Bowen *et al.* (1986); KKC kimberlite data from Le Roex *et al.,* (2003).

4.3.4 Summary of the Basalt Correlations

The geochemical discrimination plots of the major and trace element data for each of the xenoliths demonstrate that the Drakensberg Group basalts are found in all of the Group II

and transitional kimberlites, and only Group I kimberlites that lie closest to the Lesotho Remnant (Table 4a; Appendix II). Furthermore, the results suggest that most of the xenoliths were derived from the Lesotho Formation. This result is representative of the nature of the Drakensberg Group lavas, as the Lesotho Formation represents the thickest and most widely spread of the two formations within the Lesotho Remnant (Marsh *et al.,* 1997), and was thus the dominant basalt-type sampled by the kimberlites.

The occurrences of Karoo basalt xenoliths are also consistent with previous documentation of basalt xenoliths, except in the case of Koffiefontein and the KKC, which are discussed in section 4.4 below. As previously discussed, Karoo basalt xenoliths were documented in the Melton Wold (Mambali, 1998), Voorspoed (Roberts, 1997), Jagersfontein (Harger, 1913), Frank Smith (Du Toit, 1906), Markt and Untjiesberg (Letsale, 1998; Rogers and Du Toit, 1909), West End and Monastery (Harger, 1913) and Finsch (Clement, 1982) kimberlites. Geochemical analyses of the basalts previously collected from the Melton Wold, Voorspoed and Untjiesberg show that they correlate with the Mafika Lisiu unit of the Lesotho Formation (Roberts, 1997; Letsale, 1998; Mambali, 1998). Here, MSM basalt xenoliths were also found to occur at Melton Wold and Voorspoed.

Table 4a: Results of the Basalt Analyses and Correlations

KIMBERLITE	**Group I**	**GEOCHEMICAL CORRELATION**						
		Barkly East	ML	MSM	Oxbow	Other (Evolved)	Contaminated / Variable	Ventersdorp
Melton Wold			X	X			X	
Voorspoed			X	X	X?	X?	X	
Roberts Victor			X	X				
West End			X	X			X	
Record Stone Quarry			X					
Finsch			X	X				
Markt						X		
Frank Smith				X				
Pampoenpoort			X				X	
Uintjiesberg			X				X	
Monastery	X	X?	X	X			X	
Jagersfontein	X		X	X				
Kaal Vallei	X			X				
KKC	X							X

4.4 Kimberlites without Karoo Basalt Xenoliths

Karoo-like basalt xenoliths were not observed at several of the kimberlites sampled in this study, including Koffiefontein / Ebenheuyser, KKC, Lushof, Britstown cluster and Lovedale. These kimberlites did contain dolerites, presumably of Karoo affinity, but none of the crucial amygdaloidal or vesicular xenoliths to indicate the presence of basalts in each of the respective areas at the time of kimberlite emplacement.

4.4.1 LBH Kimberlites

No Karoo-like basalts were observed at the Lushof, the Britstown cluster and Hebron (LBH) kimberlites. Robey (1981) did cite the presence of amygdaloidal basalts at the Lovedale kimberlite, however, no basalts were observed during this study. The fact that all of these kimberlites are eroded down to their root zone may account for the absence of Karoo-like basalt xenoliths as it has been postulated that upper crustal xenoliths are only found in the diatreme facies (Dawson, 1971; Skinner, pers. comm. 2006). However, upper crustal xenoliths were collected from Record Stone Quarry, which is also eroded to the root, confirming that xenoliths can be down-rafted to this level. Therefore, the lack of basalt xenoliths in these kimberlites suggests that any of the Karoo basalts that were once in the greater Britstown area were removed by erosion by 78-74 Ma.

4.4.2 Koffiefontein and the KKC

The question still remains as to the occurrence of Karoo basalts in the Koffiefontein and KKC pipes. At Koffiefontein, basalts were noted by Harger (1913) and Wagner (1914). At the time, sampling opportunities were limited by mining operations and time available, so basalt xenoliths could easily have been overlooked. Nevertheless, there is by no means the same abundance of basalt xenoliths that is found at the other Group I kimberlites, indicating that if any basalts were present when Koffiefontein erupted, it was likely a very thin layer capping the Beaufort Group.

According to Williams (1932), Karoo basalts were present in the upper levels of several of the KKC pipes; however his documentation of these xenoliths contradicts other literature. A review of the literature presented in Chapter 2 reveals discrepancies in descriptions and classifications of the ‘basaltic’, doleritic and diabasic xenoliths observed in these kimberlites. Furthermore, basalts were not directly described by Hawthorne (1975) or Clement (1982), nor were they found by Rambula (2005). There is a possibility that kimberlite processes prevented the transport of fragments from the uppermost country rocks

down to significant depths, and that magma mixing and xenolith down-rafting mechanisms differ between Group II and Group I kimberlites (Skinner, pers. comm. 2006). If this is the case, no basalts would be preserved in the KKC as they would have to have fallen or subsided on the order of 1200 m (according to the Hawthorne model), or 850 m if the 'Stormberg' Group is removed from the model, to reach the depth equivalent to the present surface. Williams (1932) suggests that upper-crustal fragments were carried to a maximum of 800 m below their stratigraphic position. However, at Jagersfontein there is a plethora of basalt xenoliths. According to the Hawthorne model, the present surface at Jagersfontein is approximately 900 m below the base of the Karoo basalts, meaning that the xenoliths were down-rafted in excess of 900 m and likely more than 1200 m if the abundance of basalt xenoliths and the depth to which they occur in the preserved pipe is considered.

Because of the lack of any basalt xenoliths in the Koffiefontein and KKC kimberlites that are indisputably of Karoo origin, it is believed that either: (1) no Karoo basalts were present at the time of eruption; or (2) a thin veneer of Karoo basalt was present, but this cover was so minimal that basalts are poorly represented in the xenolith suites.

4.5 Implications for the Karoo Basalts

Analysis and correlation of the basalt xenoliths with the Drakensberg Group support the apparent lateral distributions of the Karoo basalt province and indicate that the Lesotho Formation was more extensive during the kimberlite emplacement than the present Lesotho Remnant. Furthermore, the spatial and temporal distribution of the basalt xenoliths imply that the basalts were eroded from the study area as an inland, southeast- or east-ward retreating escarpment during the Cretaceous.

It should also be noted that except for Voorspoed and Monastery, all of the kimberlites that do not contain 'Stormberg' Group sandstones do contain basalts. This further supports the observation that the Cretaceous lateral extent of the 'Stormberg' Group was confined to an area east of the Roberts Victor, Jagersfontein and Kaal Vallei kimberlites (Figure 3.7).

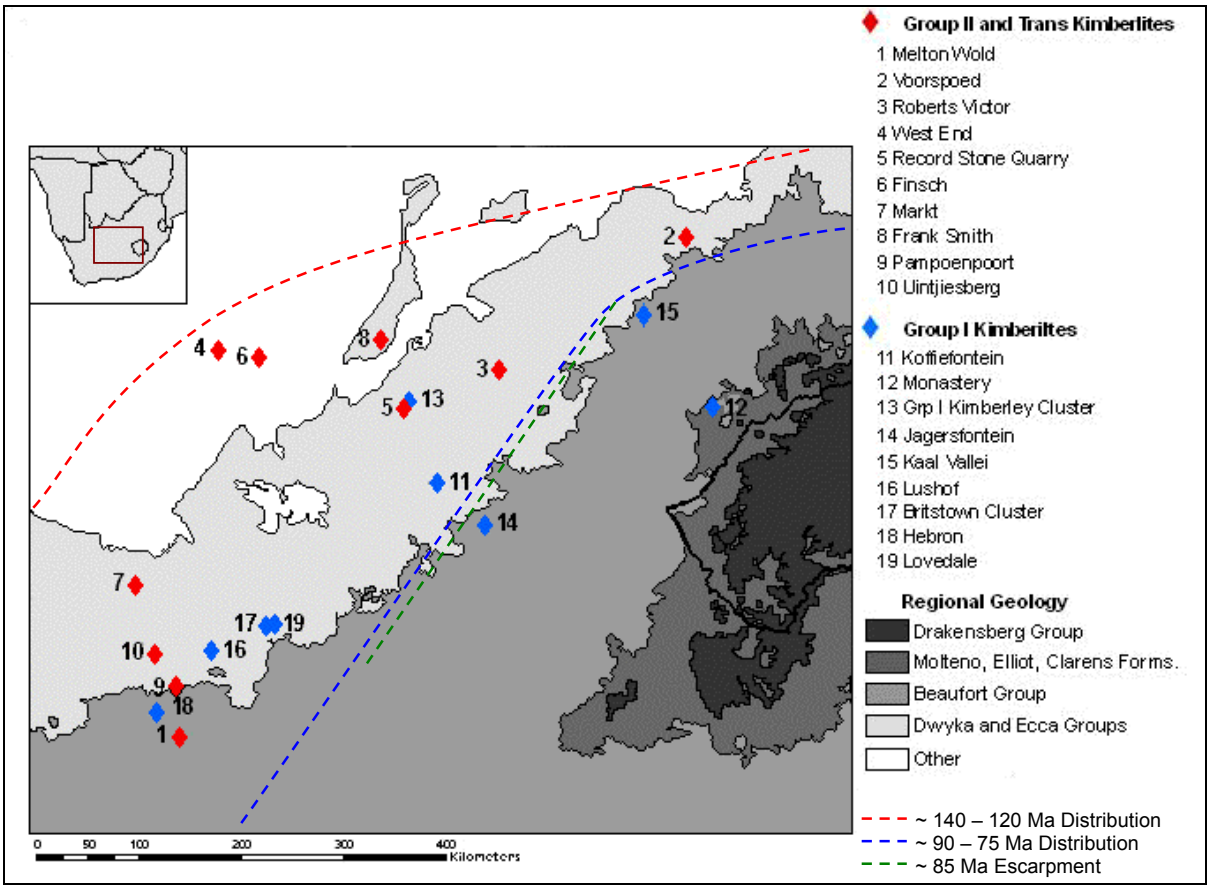

Figure 4.10 Study area map palaeo-distribution of the Karoo basalts based on the observations of this study and the results of the analysis of the basalt xenolith and position of the palaeo-escarpment. Map constructed from the De Beers database (unpubl.).

4.5.1 Lateral Extent of the Karoo Basalts during kimberlite emplacement

The vast network of intrusive sills, dykes and sheets located throughout the main Karoo Basin and further west in South Africa suggest that Karoo basalts once covered an area in excess of 10^6 km^2 (Eales *et al.,* 1984; Marsh, 1987; Marsh *et al.*, 1997). The question, however, still remains as to the palaeo-extent of the Drakensberg Group lavas. Examination of the basalt xenoliths suites found at each of the kimberlites shows that the Lesotho Formation did blanket the study area at the time of emplacement of the older, >100 Ma, kimberlites, with the exception of the Markt area, which was covered by Karoo lavas not necessarily from the Lesotho Formation. Therefore, the Lesotho Formation once extended at least as far southwest as Uintjiesberg and Melton Wold, and as far northwest as West End (Figure 4.10). Basalt or 'lava' fragments have also been reported in diatremes northwest of the study area, these include Prieska and Kolonkwanen (Du Toit, 1954; Hawthorne, 1975), indicating an even wider distribution of the Karoo basalts in South Africa. A geochemical

study of these 'lava' fragments is required to determine if they are related to the Drakensberg Group before any further suppositions are made about the full lateral extent of the Drakensberg Group lavas.

It is also probable that the upper lava flows of the Lesotho Remnant, perhaps fed by the Oxbow dykes, were lost to erosion (*e.g.,* Eales *et al.,* 1984; Marsh *et al.,* 1997). This study does not give an indication as to the extent of vertical erosion, yet some of the Voorspoed xenoliths and the highly evolved Markt xenoliths do indicate the possibility of a magma type that is not currently present in the Lesotho Remnant. The Letseng kimberlite also contains basalt xenoliths that are similar to, yet more evolved than the Drakensberg Group basalts. These xenoliths do not correlate with any of the units in the Lesotho Remnant and are therefore considered samples of now eroded magma types (Herbert, 2004).

4.5.2 Erosion of the Karoo Basalts

The presence of basalts in all of the Group II and transitional kimberlites demonstrate that basalts covered the study area from 143 Ma (time of Melton Wold kimberlite emplacement) through to 101 Ma (time of Uintjiesberg kimberlite emplacement). Between 101 and 90 Ma there was extensive erosion and a likely westward retreat of the inland erosion front of the basalt escarpment to a ~90 – 85 Ma position some 180-200 km from the present western outcrop margin of the Lesotho Remnant (Figure 4.10). This erosion pattern is evident by the presence of basalt xenoliths in the younger (< 100 Ma) Monastery, Jagersfontein and Kaal Vallei kimberlites, all of which lie within relatively close proximity to the Lesotho Remnant and west of the proposed ~85 Ma escarpment margin; and by the absence of basalt xenoliths in the Koffiefontein/Ebenheuyser, KKC Lushof, Britstown cluster or Lovedale kimberlites.

Between ~85 Ma and present day, the inland erosion front continued eastwards at just over 2 km / 1 myrs to its present position at the western margin of the Lesotho Remnant. This rate of erosion is an estimate and must be considered as a generalised suggestion based on the observations of this study and the proposed position of the ~85 Ma escarpment. Furthermore, beyond the location of the ~85 Ma erosion front between Jagersfontein and Koffiefontein, to the west of Kaal Vallei and east of the Britstown cluster, the delineation of the erosion front at ~85 Ma is pure supposition, based on the orientation of the present inland erosion front. Studies of kimberlites younger than 100 Ma, such as the Hanover cluster and those north of the study area, must be conducted to further constrain the ~85 Ma erosion front. Similarly, older kimberlites and melilitites west and northwest of the study area should be examined to more precisely determine the pre-85 Ma erosional patterns.

5. KIMBERLITE EROSION

5.1 PREVIOUS EROSION ESTIMATES

5.1.1 Kimberley Area Erosion Estimates

Current erosion level estimates for South African kimberlites, specifically the Group I Kimberley cluster (KKC), range from 500 (Edwards, 2005) to >1400 to 3500 m (Hawthorne, 1975; Brown *et al.,* 1998). Hawthorne (1975) estimated the depth of erosion in the Kimberley area based on an investigation of the depth of kimberlite sill formation (and thus the depth of formation of the sills that intrude the Kimberley area just below the surface) combined with geochemical and diagenetic studies of the sedimentary units of the country rock. According to Hawthorne (1975), the minimum depth of sill formation is 900 m (Mudge, 1968); while the degree of crystallinity of illite, bulk grain densities, residual carbon and total carbon in the Ecca Group shales and upper Dwyka Group tillites indicate a 1900 m depth of burial (by the overlying Ecca, Beaufort, 'Stormberg' and Drakensberg Groups). Therefore, 900 m and 1900 m are the lower and upper constraints of the depth of erosion, while 1400 m is the average and generally adopted value for the amount of rock that was removed post-KKC emplacement (Figure 5.1). This value, however, relies on the presence of Drakensberg Group basalt xenoliths within the KKC pipes, as it is unlikely that the Karoo Supergroup sedimentary units achieved such a thickness in the Kimberley area (e.g., Williams, 1932; Johnson, 1976; 1991).

As previously discussed, a specific pressure, and thus depth, is required for diatreme formation through crystallization-induced, juvenile, volatile exsolution. Based on observations from other kimberlites with preserved craters, such as Orapa, this depth is 2.1 to 2.3 km (Skinner, pers. comm. 2006). If the base of the diatreme of the KKC pipes is taken at 900 m below the present land surface (Clement, 1982), this means that 1200 to 1400 m of erosion had occurred in Kimberley, which is consistent with the Hawthorne model. Similarly, Dawson (1971) suggests 1600 m of erosion of sedimentary rocks since the time of kimberlite emplacement based on a depth of 2.4 km for diatreme initiation and expansion. It is notable that Dawson specifically refers to sedimentary rocks when discussing erosion levels.

However, Edwards (2005) suggests that the 'yellow ground' found at the surface of the Kimberley pipes is not in fact weathered 'blue ground' but crater remnants, and that the upwarped nature of the shale beds near the contact with the kimberlite bodies (e.g., Dunn, 1874)

indicates that little weight, and thus cover, overlaid the shales when the kimberlites erupted. Furthermore, Edwards (2005) emphasizes that the Karoo Supergroup succession was much thinner than previously believed in the Kimberley area at the time of KKC emplacement. Considering the above observations, Edwards (2005) concludes that erosion of the KKC is limited to a few hundred metres and that several of the Kimberley pipes "exhibited crater facies at the time of their first discovery". In contradiction to Edwards' (2005) small erosion estimate of a few hundred metres, fission track studies of the country rock imply an excess of 3.5 km of erosion at Kimberley, and over the Kaapvaal Craton as a whole (Brown *et al.*, 1998). However, this study does not establish a time period over which denudation of this cover occurred.

More recently, Rambula (2004) conducted a study of the KKC xenoliths, similar to the present study, and noted the absence of 'Stormberg' Group sandstones and Drakensberg Group basalts in the Kimberley pipes. By removing these stratigraphic units from the Hawthorne model, Rambula concluded that 800 m of erosion occurred post-KKC emplacement. This estimate is similar to early estimates of 900 m (Wagner, 1914), which are based on the presence of sandstones and fossils from the Beaufort Group. According to Wagner (1914), the Beaufort Group is ~900 m (3,000 ft) above the Dwyka Group, the present country rock in Kimberley, and assuming no thinning of the Ecca and Beaufort Groups occurred in the Kimberley area, "this is the thickness of strata (900 m) that has been removed by erosion since the pipes were formed" (p. 23).

5.1.2 Erosion Estimates Outside of the Kimberley Area

Erosion levels have also been estimated for the Melton Wold, Voorspoed and Finsch pipes based on the upper crustal xenoliths observed within the pipes. Geochemical analyses of basalt xenoliths found at Melton Wold and Voorspoed suggests that the samples best correlate with the Mafika Lisiu unit. Based on the thickness of the Ecca and Beaufort Groups and the Mafika Lisiu basalts, the correlation of the basalt xenoliths indicate approximately 1000 m of erosion at Melton Wold (Mambali, 1998) and as little as 300 m, but more likely 1.5 to 2 km erosion at Voorspoed (Roberts, 1997).

Similarly, earlier studies of mudstone xenoliths, collected from the upper levels of the open pit operation at Finch and associated with the Beaufort Group (Visser, 1972), indicate 1200 – 1700 m of erosion at Finsch (Robey, pers. comm. 2006). Based on isopachs presented by Ryan

(1968), the Ecca and Beaufort Groups reached maximum thicknesses of 600 m and 300 m respectively at Finsch, while the Dwyka Group was a very thin unit similar to that found in Kimberley today (Visser, 1972). Therefore, Visser (1972) estimated that the Beaufort Group xenoliths sank at least 600 m within the pipe, and approximately 900 m of Karoo Supergroup sedimentary units were removed by post-emplacement erosion. If the large basalt reef that occurs 500 – 600 m below the present surface is also considered, then an excess of 1000 m (Clement, 1982), and more likely 1300 – 1700 m of erosion occurred at Finsch based on the thickness of the Lesotho Remnant and the degree of lateral thinning of the units. Hawthorne (1975) also estimated 2200 m of total Karoo Supergroup thickness in the Koffiefontein area based on country rock diagenesis, and suggests that erosion levels at the Koffiefontein are slightly higher than at the Kimberley pipes.

5.2 KIMBERLITE EROSION ESTIMATES

5.2.1 Methods of Estimating Erosion

Post-emplacement erosion estimates are based simply on the xenoliths found at each kimberlite. These xenoliths, correlated with groups and formations of the KSG, broadly represent the stratigraphy through which each kimberlite was emplaced. As a result, there are multiple possible approaches to estimating erosion levels.

Method 1: The thickness of the eroded portion of the original stratigraphic succession found at each kimberlite pipe can be estimated by combining the documented thickness of each group or formation to generate maximum and minimum values bases on the maximum and minimum thickness of each stratigraphic unit (Appendix III, Table IIIa). For example, if the present country rock is at the Dwyka – Ecca Group contact and the youngest stratigraphic unit represented by the xenoliths is the Beaufort Group, then the amount of post-emplacement erosion is equivalent to the thickness of the Ecca + Beaufort Groups.

Method 2: The vertical difference between the present surface elevation and the elevation of the upper and lower contacts of the youngest stratigraphic unit represented by the xenoliths can be considered the maximum and minimum constraints on the possible extent of erosion for each individual kimberlite. Therefore, in the situation described above, the minimum and maximum estimates are equivalent to the vertical distance between the present surface elevation

and the average elevation of the Ecca – Beaufort Group contact, or the vertical distance to the average elevation of the base of the Drakensberg Group.

5.2.1a Kimberlites Containing Basalt Xenoliths

Palaeo-stratigraphy at the kimberlite pipes that contain basalt xenoliths, or at which basalt xenoliths were observed during this study, includes the Ecca, Beaufort and Drakensberg Groups, as well as the 'Stormberg' Group at Voorspoed and Kaal Vallei. Therefore, the thickness of each of these units is considered for method 1 (Appendix III, Tables IIIa; IIIb).

For method 2, the lower limit to the extent of erosion at each kimberlite is set as the thickness between present surface elevation at each location and the average elevation of the lower basalt contact on the western margin of the Lesotho Remnant, approximately 1900 m. Although this may be an overestimate for the minimum value, it is considered viable because each of these kimberlites has a significant volume of basalt xenoliths, which indicates that the kimberlites likely sampled a considerable amount of the basalt pile during emplacement. The upper limit is taken as the approximate elevation of the upper contact of the youngest lava unit represented by the xenoliths. The upper contact of the Mafika Lisiu unit is approximately 2300 m above sea level, based on an average Mafika Lisiu unit thickness of 400 m (Marsh *et al.,* 1997). However, the upper limit of the MSM units are difficult to determine because the original thickness of the Drakensberg Group is unknown; as a result it is taken to be the highest elevation in the Lesotho Remnant, approximately 3000 m (Appendix III, Table IIId).

5.2.1b Kimberlites with no Basalt Xenoliths

According to the results of this study, Koffiefontein and the KKC only intruded into the Dwyka, Ecca and Beaufort Groups, and the thickness of the Ecca and Beaufort Groups were therefore considered for method 1. Because no xenoliths were analyzed from the LBH kimberlites, it is not possible to determine a minimum value for erosion. Erosion levels for these pipes are thus presented as a maximum value based on the notion that the Beaufort Group was the youngest possible unit present when these kimberlites were emplaced (Appendix III, Table IIIa; IIIb).

In respect to method 2, the upper possible limit of erosion is based on the average elevation of upper contact of the sedimentary units with the Drakensberg Group basalts at the

western margin the Lesotho Remnant (averaging 1900 m). This value is used instead of the Beaufort – 'Stormberg' contact because the basalts presumably overstep the 'Stormberg' Group and lie directly on the Beaufort Group in the western part of the main Karoo Basin (see Chapter 4.5 for more explanation). The lower constraint for the Koffiefontein and KKC pipes is taken as the average elevation of the Ecca – Beaufort Group contact. The elevation of this contact is extremely variable, ranging from less than 1200 m at the southwestern margin of the basin up to 1500 m at the northwestern margin of the basin (De Beers database, unpublished), meaning it is necessary to use different values for each location. The elevation of the Ecca-Beaufort Group contact near Koffiefontein is 1300 m. Because Kimberley is approximately 70 km north of Koffiefontein, the elevation of this contact is approximated at 1350 m (Appendix III, Table IIId).

5.2.2 Comparison of the Results

5.2.2a Results Using Method 1

The results generated from method 1 most likely overestimate the degree of post-emplacement erosion because they do not consider thinning rates towards the main Karoo Basin margin, and are therefore not considered in the final estimates (Appendix III, Table IIIb). Instead, thinning rates of the upper Dwyka and Ecca Groups based on isopach studies presented by Ryan (1968) were used to approximate the total thickness of the upper Dwyka and Ecca Groups in the Melton Wold, Uintjiesberg, Pampoenpoort, Jagersfontein, Kaal Vallei and the LBH pipes; and to infer the palaeo-thickness in the remaining pipes (see Visser, 1972) (Appendix III, Table IIIa; IIIc).

Johnson (1976) also discusses southwest to northeast, or south to north, thinning rates within the preserved remnants of the basin (Appendix III, Table IIIa). The thinning rate presented for the Beaufort Group, approximately 26 m/km based on the rates presented for the Tarkastad and Adelaide Subgroups, is notably high and if applied in the east-west direction the Beaufort Group would not extend as far west as the kimberlites located on the western side of the study area. If the palaeo-thicknesses presented for the Beaufort Group at Finsch (maximum of 300 m; Visser, 1972), and the Kimberley area (approximately 550 m; Hawthorne, 1975) are considered, then the east-to-west thinning rate in the northwestern part of the basin is roughly 1.5 m/km. With this value, it is possible to extrapolate the palaeo-thickness of the Beaufort Group at the remaining kimberlites. For comparison purposes, the thickness of the Beaufort Group was

also determined using another thinning rate, 10 m/km east-to-west (just under half the rate presented by Johnson, 1976) at the Melton Wold, Pampoenpoort and Uintjiesberg pipes. The values obtained with this rate are much higher as they are calculated from the maximum thickness, 7000 m. At Voorspoed and Monastery, the thicknesses of the 'Stormberg' Group are based on Johnson (1976).

By incorporating thinning rates, the erosion estimates drop significantly, and realistic values are achieved. For example, the average value decreases from 5000 m to 1725 m at Melton Wold, indicating an erosion rate change from 35 m/myrs to 12 m/myrs. Similarly at the KKC, the estimated averages are 5800 m and just under 1100 m, resulting in denudation rates of 68 m/myrs and 13 m/myrs. The latter denudation rates for each of the kimberlites are more consistent with estimates of 10 to 15 m/myrs, which were achieved using other methods (Partridge and Maud, 1987; Brown *et al.,* 2002).

5.5.2b Results Using Method 2

The values calculated by using method 2 are lower than those obtained from method 1, and are adopted as the minimum erosion levels for each kimberlite (Appendix III, Table IIId). According to these estimates, denudation rates range from 4-5 m/myrs to 12 m/myrs, based on Koffiefontein and the KKC, and Markt and Frank Smith respectively. However, these results may be skewed due to post-emplacement uplift. According to Partridge and Maud (1987), significant post-Mesozoic uplift and consecutive erosion cycles occurred in southern Africa. This uplift was manifested along specific axes, where uplift in the eastern regions significantly exceeded that in the west, resulting in a westward tilt of southern Africa. Instead, the results of this study allow for uplift, but lead to the observations that no obvious manifestation of this uplift occurred on the flanks of the basin.

Kimberlite	Results using method 1			Results considering thinning rates			Results using method 2			Previous estimates	Estimate
	Min	Max	Avg	Min	Max	Avg	Min	Max	Avg		
Melton Wold	1500 m	8400 m	5000 m	1050 m	2400 m	1725 m	560 m	1660 m	1110 m	~1000 m[10]	1100 – 1700 m
Voorspoed	2150 m	11000 m	6575 m	930 m	2300 m	1615 m	490 m	1590 m	1040 m	1500 – 2000 m[11]	1050 – 1600 m
Roberts Victor	2400 m	11400 m	6900 m	1750 m	2450 m	2100 m	640 m	1740 m	1190 m		1200 – 2100 m
West End	2650 m	13300 m	7975 m	1600 m	2300 m	1950 m	570 m	1740 m	1155 m		1150 –1950 m
RSQ	1800 m	10400 m	6100 m	1050 m	1700 m	1375 m	680 m	1080 m	880 m		900 – 1400 m
Finsch	2650 m	13300 m	7975 m	1600 m	2300 m	1950 m	350 m	1450 m	900 m	1000 – 1700 m[12]	900 – 1950 m
Markt	2400 m	11400 m	6900 m	1825 m	3200 m	2510 m	870 m	1970 m	1420 m		1400 – 2500 m
Frank Smith	2400 m	11400 m	6900 m	1950 m	2950 m	2450 m	820 m	1920 m	1370 m		1400 – 2400 m
Pampoenpoort	1400 m	8900 m	5150 m	550 m	1400 m	975 m	630 m	1030 m	830 m		850 – 1000 m
Uintjiesberg	1500 m	8900 m	5200 m	900 m	1750 m	1325 m	590 m	990 m	790 m		1100 – 2300 m
Koffiefontein	1150 m	8500 m	4825 m			1350 m	70 m	670 m	370 m	>1400 m[13]	400 – 1350 m
Monastery	850 m	2200 m	1525 m	900 m	1700 m	1300 m	310 m	1410 m	860 m		850 – 1300 m
Jagersfontein	1500 m	8400 m	4950 m	1450 m	2150 m	1800 m	490 m	1590 m	1040 m		1050 –1800 m
Kaal Vallei	1500 m	8400 m	4950 m	1140 m	2100 m	1620 m	540 m	1640 m	1090 m		1100 – 1600 m
KKC	1600 m	10000 m	5800 m	850 m	1300 m	1075 m	120 m	670 m	395 m	300[14], 800-900[15], 1400[5], 3500[16] m	400 – 1100 m
Lushof					900 m			750 m[17]			< 825 m
Britstown					1125 m			780 m[8]			< 950 m
Hebron					1050 m			420 m[8]			< 750 m
Lovedale					1050 m			760 m[8]			<900 m

Table 5a: Erosion estimate summary based on results of methods 1 and 2 (Appendix III), values rounded to 50 m. Because of the difficulty encountered in correcting for thinning rates and the variable nature of the results, large estimate ranges are presented for all of the kimberlites based predominantly on the average results of method 2 (min) and method 1 considering thinning rates (max).

[10] Mambali, 1998
[11] Roberts, 1997
[12] Visser, 1972; Clement, 1982
[13] Hawthorne, 1975
[14] Edwards, 2005
[15] Rambula, 2004; Wagner, 1914
[16] Brown *et al.*, 1998
[17] It is difficult to put a lower constraint on the erosion estimates for the LBH pipes because no sandstone xenoliths were analyzed, thus only a maximum value is estimated

5.2.3 Erosion Estimates for the Group II and Transitional Kimberlites

Erosion levels for the older kimberlites range from 800 m at Uintjiesberg to 2500 m at Markt, with maximum levels occurring in the western region of the study area (Table 5a). The estimates for the Melton Wold, Voorspoed and Finch kimberlites are comparable to the results of previous studies. Mambali's (1998) estimate of approximately 1000 m is based on the occurrence of Mafika Lisiu-like basalts, while the present estimate of 1100 to 1700 m assumes that MSM-like basalts, and thus a thicker basalt cover, occurred. Previous estimates for Voorspoed are on the order of 900 to 1950 m (Roberts, 1997), which is very similar to 1000 to 1800 m estimate of erosion.

According to the basalt analyses, Record Stone Quarry only contains Mafika Lisiu basalt xenoliths. This means there has been little erosion at Record Stone Quarry relative to other kimberlites with similar ages. However, West End, Finsch and Frank Smith, which are of similar age and are located to the west of Record Stone Quarry, contain MSM-like basalts, suggesting that Record Stone Quarry should also contain MSM-like basalt xenoliths. This discrepancy may be attributed the fact that Record Stone Quarry is eroded to the root-diatreme zone interface such that diversity of the upper crustal xenoliths is limited, or may be due to limited sampling. If MSM basalts are accounted for, then the erosion estimate is closer to 1200 – 2100 m, which is more consistent with the Frank Smith estimates of 1400 – 2400 m.

Estimates for Finsch are variable as the present surface of the pipe is at a high elevation relative to other kimberlites on the margins of the main Karoo Basin. The higher elevation relative to the KSG units resulted in low values with method 2. If the maximum value instead of the average value determined by method 2 is considered, then erosion estimates increase to approximately 1550 – 19500 m. This is very similar to rates inferred from Visser (1972), 1300 – 1700 m, and is consistent with Clement's (1982) assumption that in excess of 1000 m of post-emplacement denudation occurred at Finsch.

5.2.4 Erosion Estimates for the Group I Kimberlites

Monastery, Jagersfontein, Kaal Vallei

In comparison to the kimberlites discussed above, the 'younger' Group I kimberlites experienced less erosion, as is expected (Table 5a). Except for Monastery, Jagersfontein and Kaal Vallei, which are closest to the western outcrop margin of the Lesotho Remnant and contain

basalt xenoliths, erosion estimates rarely exceed 1500 m. At Monastery, Jagersfontein and Kaal Vallei, erosion estimates range from 850 to 1800 m. The estimates for Monastery are significantly lower, 850 to 1300 m, because of its elevation, stratigraphic position and proximity to the Lesotho Remnant. Because Kaal Vallei is relatively close to and younger than Voorspoed, it likely experienced less post-emplacement erosion than Voorspoed. Therefore, the maximum value for erosion should be less then the maximum estimate for Voorspoed, and a range of 1100 to 1400 m erosion at Kaal Vallei is more likely.

Koffiefontein

According to Hawthorne (1975), erosion in the Koffiefontein area exceeded that in Kimberley by approximately 300 m. Although the results of this study indicate 400 – 1350 m of erosion as opposed to 1700 m (Hawthorne, 1975), the discrepancy between erosion levels in the Koffiefontein and Kimberley areas remains apparent.

Naidoo *et al.* (2004) report that a sequence of Karoo units greater than 250 to 300 m was present at the time of eruption. However the same authors concede that the thickness is unknown and cite Field and Scott Smith (1999b) to say that the full extent of the KSG was probably present. It is conceivable that basalt xenoliths occur at Koffiefontein (Harger, 1905; Wagner, 1914), but 'Stormberg' Group xenoliths are unfeasible as Koffiefontein is not located within the extent of the palaeo-basin. As discussed in Chapter 4, basalt xenoliths may have been overlooked due to limited sampling, but the fact that they were not readily noticeable suggests that very few, if any, basalt xenoliths occur within the kimberlite body. If basalts were present in this area at ~90 Ma, then they occurred as a layer no thicker than 500 m, and more likely 100 to 300 m. Incorporation of a basalt layer into the erosion model increases the erosion estimate to 500 - 1650 m.

Group I Kimberley Kimberlite Cluster

In contradiction to previous estimates, this study proposes that the kimberlites of the KKC do not contain Karoo basalt xenoliths and that the maximum extent of post-emplacement erosion was 850 m. If the 'Stormberg' and Drakensberg Groups are removed from the Hawthorne (1975) model, 850 m is also achieved (Figure 5.1). This is slightly higher than Rambula's (2004) estimate of 800 m because he also removed the upper Beaufort Group from

the Hawthorne model. These estimates are most comparable to the early hypothesis of 900 m (Wagner, 1914).

If previous accounts of basalt xenoliths in the upper levels of the KKC pipes are considered (Williams, 1932), the results are similar to those for Koffiefontein. Again, the rarity of the basalts is indicative of a thin layer of basalts during emplacement, on the order of 200 m (Hawthorne, 1975), resulting in 600 to 1300 m of erosion. Regardless of the presence or absence of basalts, 1400 m of erosion is improbable for the KKC as it requires a substantial thickness of both the 'Stormberg' Group and Karoo basalts to be present when it was emplaced. Similarly, to have as little as 300 m of erosion is unlikely because the thickness of both the Ecca and Beaufort Groups must be accounted for. Based on an observed lack of Karoo basalt xenoliths at Kimberley, a maximum of 850 m post-emplacement erosion is a realistic estimate for the Group I Kimberley kimberlite cluster.

LBH Kimberlites

As previously discussed, it is only possible to establish a maximum value for the erosion of the Lushof, Britstown Cluster, Hebron and Lovedale kimberlites. Because no basalts were observed at any of these locations, and based on their distance from the 'Stormberg' Group outcrops, the Beaufort Group is considered the youngest stratigraphic unit sampled by these kimberlites. With this in mind, post-emplacement erosion was less than 825 m at Lushof, 950 m at the Britstown cluster, 750 m at Hebron and 900 m at Lovedale.

5.3 Re-examination of the Hawthorne Model

The parameters that Hawthorne (1975) cited for his erosion estimates may be correct, though it is probable they were interpreted incorrectly. If the country rock studies are considered accurate, then at least 1900 m of cover was required to generate the degree of diagenesis and illite crystallinity observed in the Ecca and Dwyka Group country rocks. However, when Hawthorne generated his model of a kimberlite pipe, he overlooked the likelihood that erosion occurred in Kimberley prior to the emplacement of the KKC. Based on the difference between erosion estimates for Record Stone Quarry and the KKC, approximately 300 to 500 m were removed between 118 and 85 Ma.

The eroded remnants of these kimberlites can also be compared and utilized as another means to estimate erosion differences between Record Stone Quarry and the KKC. In comparison, Record Stone Quarry is eroded down to the root-diatreme interface, while this interface occurs at a depth of approximately 900 m below the present surface in the KKC (Clement, 1982). If Group I and Group II kimberlites are of similar size and shape, then Record Stone Quarry had to experience at least 900 m more erosion than the KKC to be eroded down to such levels. Based on this observation, post-emplacement erosion for Record Stone Quarry is closer to 1300 – 2000 m. These estimates are comparable to those obtained when MSM basalts are included in the calculations, as previously discussed (1200 – 2100 m). If these estimates are considered, then in excess of 2000 m was removed from the Kimberley area subsequent to the conclusion of Karoo province magmatism, and of which a total of 900 m between the time of Record Stone Quarry and KKC emplacement.

Hawthorne's (1975) quote for the depth of sill formation (minimum of 900 m) is also a reasonable estimate that supports the results of this study. The erosion estimate for the KKC based on the xenolith suite is approximately 850 m, which is just under Hawthorne's minimum depth requirement for sill formation. Assuming that Williams (1932) was correct in stating that Karoo basalt xenoliths occurred in the KKC, these values increase to approximately 800 to 1050 m. If, then, the new estimate of 850 m is accepted for the KKC, the kimberlite models that rely on a basalt capping rock (Field and Scott Smith, 1999b) must be reconsidered.

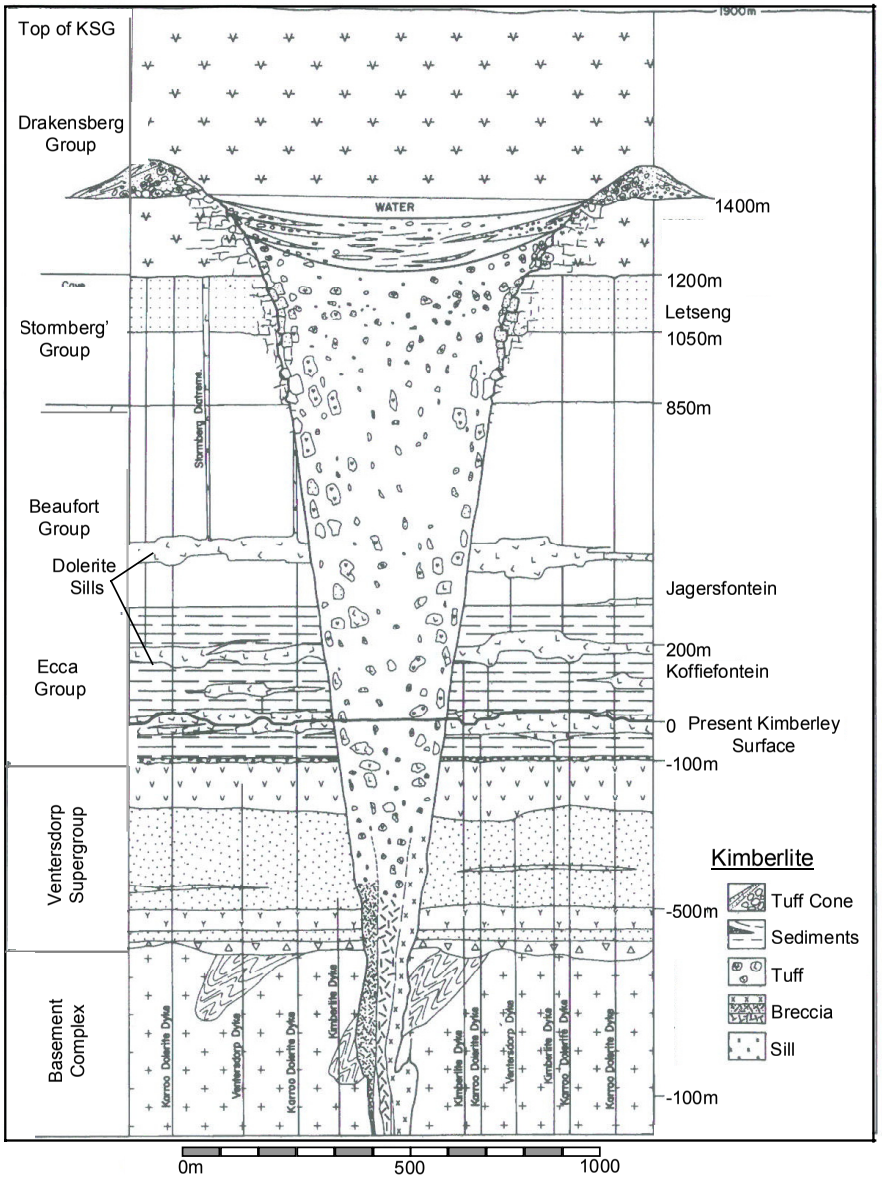

Figure 5.1 A) Hawthorne's model of a kimberlite showing the presence of Drakensberg Group basalts at the time of KKC emplacement. B) Possible model of the Group I Kimberley pipes based on the results of the current study and the removal of basalts and "Stormberg' Gorup sedimentary units from the Hawthorne model. This represents the maximum possible size of the KKC pipes based on the xenolith suites.

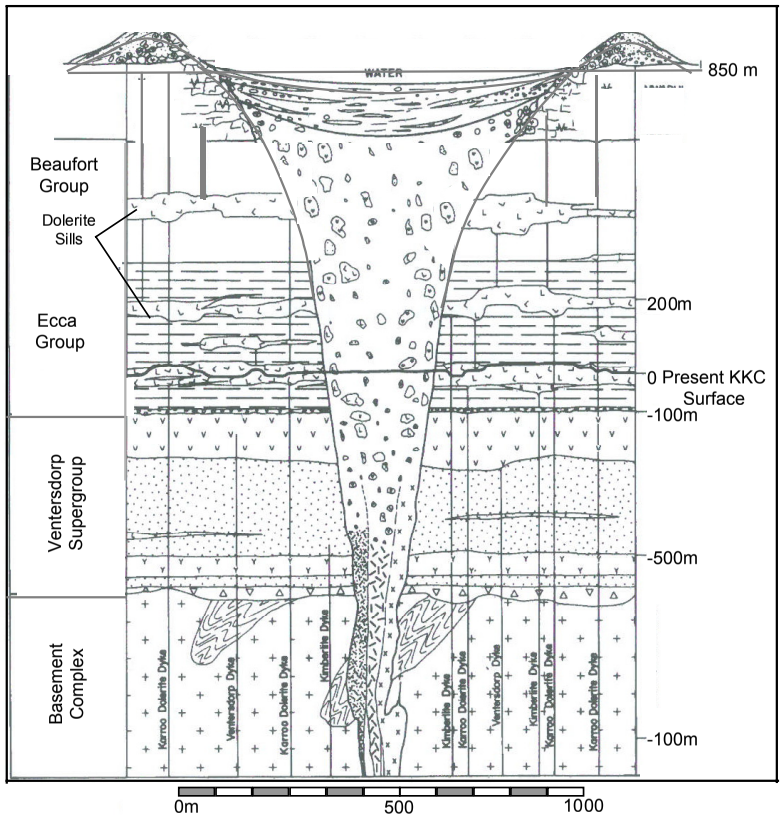

Chapter 5 – Erosion Estimates - 93

5.4 Implications for Landscape Development in South Africa

5.4.1 Kimberley Area

The Kimberley area experienced an excess of 2000 m post-Karoo erosion via westward flowing drainages coupled with African erosion cycles. At the time of the first kimberlite emplacement (~140 Ma), the area was covered by a thick succession of sedimentary units representing the Dwyka, Ecca and Beaufort Groups as well as Karoo basalts geochemically similar to the Mafika Lisiu unit. From 140 Ma to 85 Ma approximately 900 m of predominantly basalt was removed at a rate of 16 m/myrs. By ~85 Ma, Karoo basalts were removed from the Kimberley area. At this time, denudation rates slowed to an average of 10 m/myrs resulting in the erosion of 850 m of Beaufort and Ecca Group rocks and the development of the recent land surface.

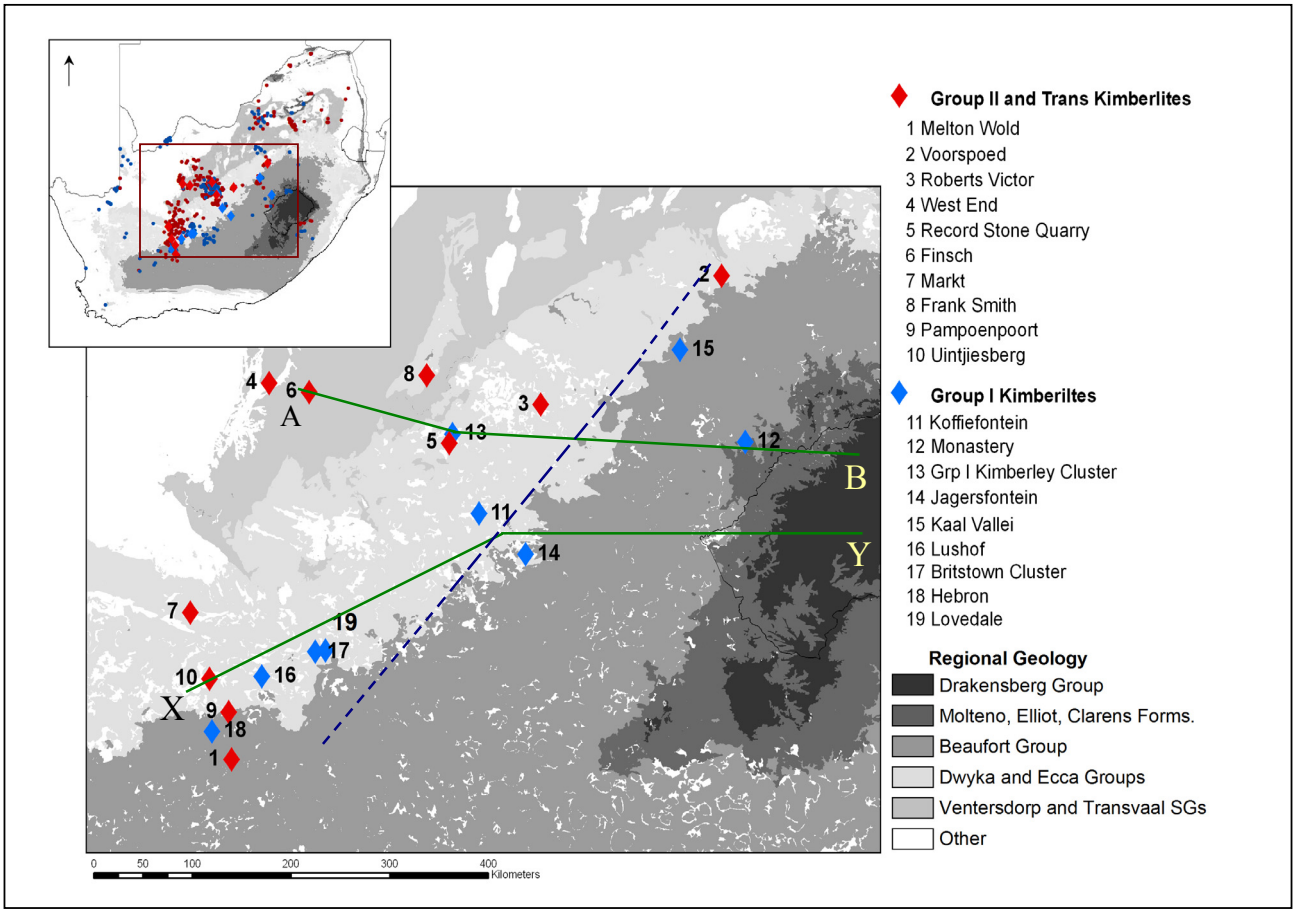

Figure 5.2: Study area map with x-section locations (green line) and the approximate position of the ~85 Ma escarpment (blue dashed line). Note that the position of the escarpment is based on the results of this study and assumes no basalts in KF and the KKC. Map compiled from the De Beers database (unpubl.).

A

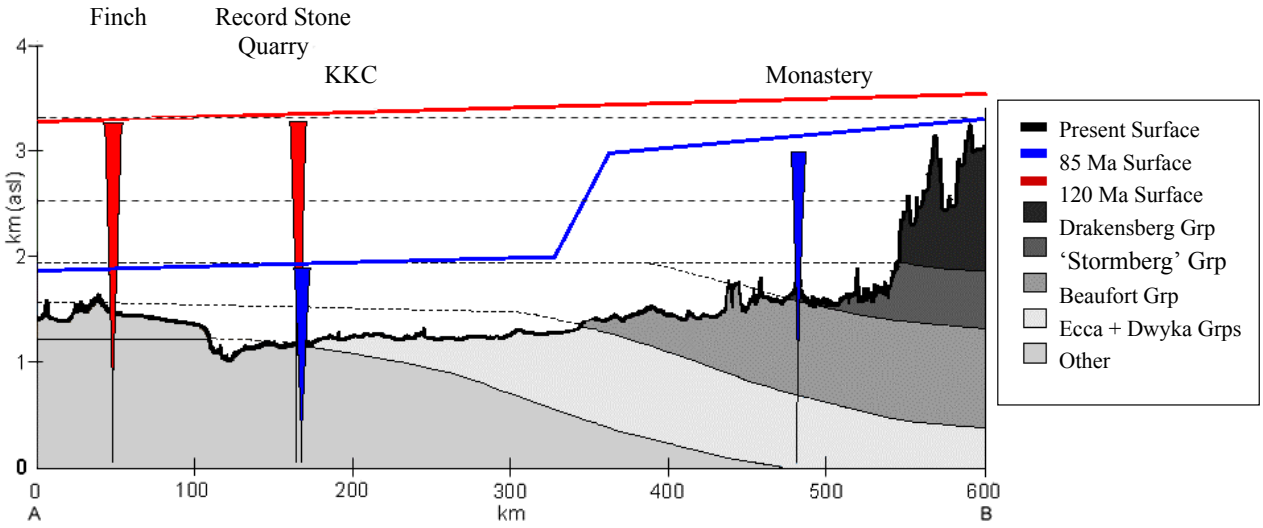

B

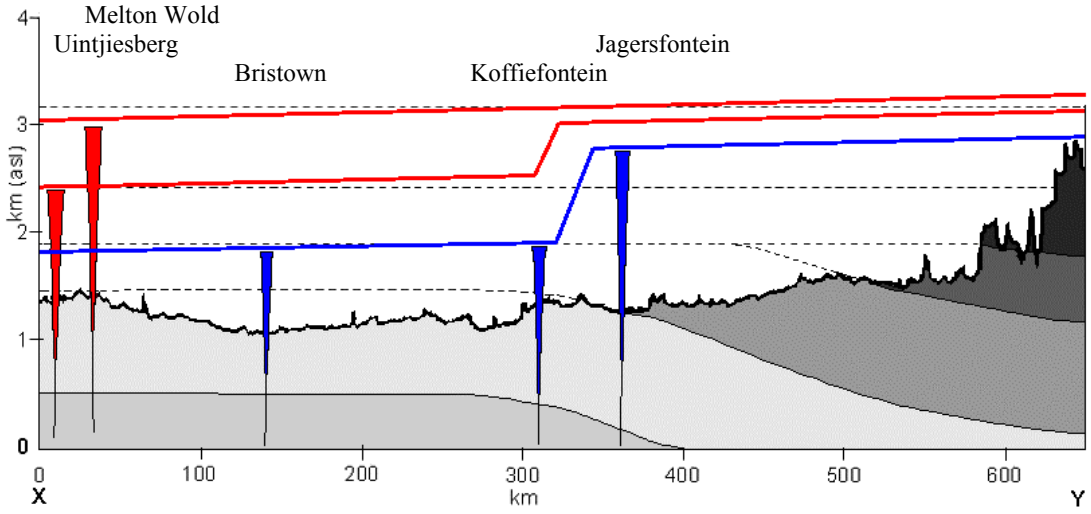

Figure 5.3: Generalized cross-sections showing approximated palaeo-topographies at ~120 Ma and ~85 Ma. Note that the position of the escarpment is based on the results of this study and assumes no basalts in KF and the KKC. Section locations present in Figure 5.2. Dashed lines represent inferred lateral extent and thickness of the KSG units at the time of kimberlite emplacements. The Drakensberg Group is subdivided into the Mafika Lisiu and Maloti-Senqu-Mothae units. Geology and topography based on De Beers database (unpubl.).

5.4.2 Regional Erosion Pattern

The modern landscape of South Africa is an artifact of the African erosion cycles (Partridge and Maud, 1987) and contemporaneous inland retreat of the Great Escarpment. The African erosion cycle dominated post-Gondwana landscape evolution, with denudation rates of up to 15 m/myrs and ensuing off-shore sedimentation peaking in the early stages, from Late Jurassic to Mid-Cretaceous, and slowing through the Late Cretaceous to minimum levels by Tertiary times as landscape planation was achieved. Inland, in the region of the Lesotho Remnant, peaks in erosion are also apparent in the Early (140-120 Ma) and mid-Cretaceous (100-80 Ma) (Brown *et al.,* 2002). Similarly, analysis of the upper crustal xenoliths show that from 140 – 100 Ma erosion rates (8 to upwards of 22 m/myrs) exceeded those from 90 Ma to present (10 to 12 m/myrs).

In summary, basalts covered the study area from 140 to 100 Ma. As opposed to predominant planation of the landscape (Partridge and Maud, 1987), it is likely that inland erosion was coupled with an east-ward retreat of an inland scarp front, similar to the erosion of the Great Escarpment. This scarp retreat accounts for the temporal distribution of basalt xenoliths, and is supported by the modern scarp-like nature of the Lesotho Remnant. By 90-85 Ma, the outcrop area of the basalts receded by means of this eastward-retreating inland escarpment to position approximately 200 km west of the present western outcrop margin (Figure 5.3); while Beaufort Group sandstones remained and covered the study area. In the period from ~85 Ma to present, the basalt escarpment continued its eastward movement at a rate of approximately 2.3 km/myrs and the underlying sedimentary units were subsequently eroded in a similar west to east pattern. This westward moving erosion front generated the inland outcrop patterns presently observed in the western and central part of the main Karoo Basin.

6. SUMMARY AND CONCLUSIONS

6.1 Summary

Upper crustal xenoliths from 17 Cretaceous-aged kimberlites were analyzed and correlated with the sedimentary groups and basalt units of the KSG, while 5 other kimberlites were visited to confirm the presence or absence of basalt xenoliths. In total, 37 sandstones from the Voorspoed, Roberts Victor, Record Stone Quarry, Finsch, Pampoenpoort, Koffiefontein, Monastery, Jagersfontein, Kaal Vallei and the KKC (Big Hole and De Beers) kimberlites as well as several mudstone and siltstone samples, and 74 basalts from the Melton Wold, Voorspoed, Roberts Victor, West End, , Record Stone Quarry, Finsch, Markt, Frank Smith, Pampoenpoort, Uintjiesberg, Monastery, Jagersfontein, Kaal Vallei and the KKC (Bultfontein and De Beers) kimberlites were analyzed.

Correlation of the sandstone xenoliths was primarily based on mineral composition as well as petrographic characteristics, which were compared with data previously collected from the KSG sedimentary units. Results of these analyses and correlations show that the Cretaceous lateral extent of the Dwyka, Ecca and Beaufort Groups was larger then the present outcrop area and encompassed the Finsch kimberlite pipe. The lateral extent of the 'Stormberg' Group appears to have been much smaller than the older Karoo units; however it extended approximately 120 km northwest of the present northern outcrop margin.

Geochemical discrimination diagrams from Marsh *et al.,* (1997) were used to correlate the basalt xenoliths with units of the Drakensberg Group on the basis of major and trace element composition. While the geochemical composition of some samples deviate from the typical compositions of the Lesotho Formation basalts, presumably due to secondary kimberlite influences or primary lateral variations outside of the Lesotho Remnant, most of the xenoliths have geochemical affinities with the Mafika Lisiu unit. Voorspoed and Markt kimberlites contain xenoliths that are more evolved than the Lesotho Formation basalts, and these xenoliths likely represent units that are no longer preserved, or were never present in, the Lesotho Remnant.

Most importantly, Karoo-like basalts were not found at the KKC. Instead, basaltic samples collected from the KKC pipes are most similar to the Allanridge Formation of the Ventersdorp Supergroup. Although the mere lack of basalt xenoliths in the kimberlite dumps does not justify the declaration that basalt xenoliths did not occur in the KKC pipes, careful review of the early literature on the Kimberley pipes coupled with the results of the present study as well as Rambula's (2005) study provide strong indications that the KKC pipes are

devoid of Karoo basalt xenoliths. Furthermore, the fact that the basalts were not found in the younger pipes to the southwest of Kimberley supports the supposition that basalts were eroded from the western part of the study area and the Kimberley area by the time the younger kimberlites were emplaced. Therefore, it is apparent that 1400 m of post-emplacement erosion is an overestimate in the KKC area, and that the erosion is more likely of the order of ~850 m.

The results of the basalt analyses and the observed distribution of basalts indicate that Karoo basalts covered the study area from approximately 140 to 100 Ma, as basalt xenoliths occur in all of the Group II and transitional kimberlites. By ~85 Ma, the outcrop area of the basalts receded eastward via inland scarp retreat. Because basalts were only found at Monastery, Jagersfontein and Kaal Vallei kimberlite, the position of the ~85 Ma escarpment was estimated to be approximately 200 km west of, and parallel to the western margin of the Lesotho Remnant. Denudation and westward retreat of the underlying strata followed after the basalts were removed and resulted in the modern configuration of the Dwyka, Ecca, Beaufort and 'Stormberg' Group remnants and the main Karoo Basin.

Based on the analyses of the upper-crustal xenoliths, it is evident that the removal of up to 1000 – 2700 m of Karoo cover occurred subsequent to the emplacement of the Group II and transitional kimberlites, 700 – 2000 m of which were removed subsequent to Group I kimberlite emplacement. Comparison of kimberlites from the same area, such as Record Stone Quarry and the KKC, indicates that earlier denudation rates from approximately 140 to 85 Ma exceeded those from 85 Ma to present, with estimates of 16 to 18 m/myrs and 10 m/myrs respectively.

6.2 Further Work

As previously mentioned, further work is required in order to construct a refined picture of post-emplacement erosion in South Africa, and to further constrain the lateral extent the Karoo Supergroup during the Cretaceous, the phases of scarp retreat and the temporal location of the inland erosion front of the Drakensberg Group basalts, as well as the depth of erosion for individual kimberlites. Suggestions for further work include:

- Further sampling and analyses of xenoliths from the kimberlites studied in this project to develop a more extensive database and a better understanding of the original size and post-depositional history of the main Karoo Basin.

- Examination of the other younger kimberlites in the Kimberley and Koffiefontein areas to further constrain the position of the ~85 Ma palaeo-escarpment and to strengthen the argument for or against the presence of basalt xenoliths in the KKC.
- Extension of this project outside of the study area to kimberlites such as Peiserton, Makanjane, Hanover cluster and Darleston to help confine the size of the depositional area of the main Karoo Basin during the Cretaceous as well as the extent and nature of the Karoo basalts.
- Emphasis should be placed on the examination of the Hanover Cluster as this group of kimberlites lies within the projected position of the ~85 Ma basalt escarpment.

The principles of this study can also be applied to areas out side of the main Karoo Basin to both estimate erosion levels and to develop a comprehensive database of stratigraphic units that are represented by xenoliths, but are no longer preserved in the vicinity of the kimberlite.

6.3 Conclusions

In conclusion, this study demonstrates that the examination of upper crustal xenoliths can provide an indication as to the amount, or thickness, of kimberlite that has been lost to post-emplacement erosion. Furthermore, this study shows that post-Cretaceous erosion in the Kimberley area is likely to be closer to 850 m, as opposed to 1400 m (Hawthorne, 1975) as previously assumed. This new estimate has several implications for kimberlites and their diamonds. First, the discrepancies between the amount of erosion experienced at Record Stone Quarry versus that at the KKC, as well as between the other older and younger kimberlites, indicates that the Group II kimberlites were much larger bodies than their younger counterparts. Second, because less erosion occurred at the KKC, less diamondiferous material was available from the sources for the westward flowing drainages. As a result, fewer diamonds were transported to the west coast via these drainages. Finally, the magmatic fluidization model requires a basalt cap and the model should therefore be reconsidered.

APPENDIX I: SANDSTONE XENOLITHS

Table Ia: Sandstone Xenolith Descriptions

Sample	**V2-08 (1)**	**V4-13 (2)**	**V4-14 (3)**	**V5-15 (4)**
Classification	Subarkose	Lithic greywacke	Subarkose	Litharenite
Provenance	Continental Block	Recycled Orogen	Continental Block	Magmatic Arc
Colour*	Pinkish-Grey and Greyish-blue (5YR 8/1) (5PB 5/2)	Pale yellow (5Y 8/3)	Greyish Yellow (5Y 8/4)	White (N9) to Pale Yellow (5Y 8/4)
Supported by:	Grain	Grain	Grain	Grain
% Matrix	12	15-20	10	10-15
Cement	Calcite, minor	Silica		
Grain Boundaries	Point and concavo-convex	Point	Concavo-convex and sutured	Point
Grain Size**	v.f.g-f.g. / m.g.	v.f.g.-f.g. / f.g.-m.g. / m.g.	m.g.–v.c.g.	v.f.g. / m.g.-c.g
Grain Roundedness***	SA-SR / R-WR	SA / WR / SR-R	SA	SA-SR / SR - R
Sortedness	Moderate	Poor	Poor	Moderate
Maturity	Submature	Immature	Immature	Submature
Quartz	Coarse grains, R-WR, straight > undulose extinction, occur in clusters, lenses and discrete grains	Dominate the coarser fraction, SR>R, straight > undulose extinction	0.3-0.5 mm grains are R with straight extinction	0.4-0.6 mm, R-WR, zircon and rutile inclusions, vacuoles (quartz is the only mineral present in the coarser fraction)
	Finer more abundant, SA-SR, dominantly straight extinction	Finer grains more angular (SA)	finer and coarser grains are SA with straight and undulose extinction	Finer, 0.06-0.2 SA-SR
Quartz P	2-4 crystals, straight and sutured contacts, irregular crystal shapes; FG chert	2-3 crystals, sutured > straight contacts, irregular crystal shapes; chert	3->5 crystals, sutured contacts; 2 grains, straight contacts; FG and CG chert	2-3 crystals, sutured contacts, non-equigranular; FG chert
Feldspar	Untwinned > microcline > plagioclase > perthite	Untwinned > plagioclase > microcline	Microcline > untwinned > plagioclase	Untwinned > plagioclase > microcline
	All fresh to minor clay alteration, dominantly finer grained, microcline shows typical cross-hatch twinning, plagioclase albite twinned	Fresh, few moderate to strongly clay or sericite altered, plagioclase dominantly albite twinned, microcline cross hatched	All fresh to strong clay or sericite altered, microcline is often perthitic and rarely encloses biotite, plagioclase has polysynthetic and albite twinning	Plagioclase occurs as laths with albite twinning and is fresh, microcline is SA and fresh, untwinned moderately clay or sericite altered
Lithics	Sedimentary	Sedimentary = 0.2-0.3 mm	Igneous = quartz + feldspar Metamorphic = schistose	Sedimentary = 0.1 and 4mm grains, SR
Accessory Minerals	Zircon, garnet, tourmaline, opaques, calcite, hematite blebs	Garnet, hematite crystals, epidote muscovite, opaques	Biotite, muscovite, hematite blebs and crystals, garnet, zircon, opaques	Zircon, garnet, chlorite, rutile, tourmaline, opaques, hematite coatings
Other				

Table Ia Continued:

Sample	V5-17 (5)	RV1-04 (6)	RV1-08 (7)	RV1-09 (8)
Classification	Lithic arkose	Sublitharenite	Litharenite	Litharenite
Provenance	Magmatic Arc	Recycled Orogen	Recycled Orogen	Mixed
Colour*	Pale Yellowish Orange (10YR 8/6)	Greenish Grey (5GY 6/1)	Pale Yellow (5Y 8/3)	Pale Yellow (5Y 8/3)
Supported by:	Grain	Grain	Grain	Grain
% Matrix	10	7	10	10
Cement			silica	
Grain Boundaries	Point and concavo-convex	Concavo-convex to sutured	Point, tightly packed	Point and Concavo-convex
Grain Size**	v.g.f.-f.g. / m.g.-c.g.	m.g. / m.g.-c.g.	v.f.g.-f.g.	v.f.g.-f.g.
Grain Roundedness***	A-SA / SA-SR	SA / SR	SA-SR	SA-SR
Sortedness	Poor	Poor-Moderate	Well	Moderate
Maturity	Immature	Submature	Mature	Submature
Quartz	Coarser, SA-SR, undulose = straight extinction, common Conchoidal surfaces	0.4-0.6 mm, SR, straight extinction, semi-sutured contacts, vacuoles	SA-SR with few R grains, dominantly straight extinction	SA-SR, dominantly straight extinctions
	Finer, SA-SR, straight > undulose extinction,	0.2-0.3 mm, SA-SR, straight and undulose extinction		
Quartz P	2-4 grains, straight contacts; >5 grains, sutured contacts; FG chert	2-3 grains, straight contacts; 3->5 grains, sutured contacts; abundant FG chert	2 grains, straight to sutured contacts; minor chert	2 grains, straight contacts; >2 grains, sutured contacts; FG chert
Feldspar	Untwinned > microcline > plagioclase > perthite	Untwinned > microcline > plagioclase > perthite > K-feldspar	Untwinned > plagioclase > microcline	Untwinned > plagioclase > microcline
	All are fresh to strongly altered alteration	Plagioclase occurs as laths with albite twinning or SA-SR grains and has minor to moderate alteration; Microcline is fresh and larger grains are more rounded; K-feldspar is fresh with simple twinning	Plagioclase fresh to strong clay alteration with albite twinning; Microcline fresher, all feldspar predominantly SA	Untwinned is moderately to completely clay or calcite altered, Plagioclase fresh to strongly altered, occurs in laths and SA grains with albite twinning, Microcline is fresher and more well rounded
Lithics	Igneous = quartz + feldspar Sedimentary	Sedimentary = conform to surrounding grains Metamorphic= schistose Igneous = granitic	Igneous = granitic; Sedimentary	Metamorphic = muscovite-schist Sedimentary Igneous = quartz + altered feldspar
Accessory Minerals	Biotite, muscovite, opaques, zircon, hematite coatings and diffuse stain	Biotite, chlorite, muscovite, garnet, tourmaline, zircon, opaques	Muscovite, tourmaline, zircon, chlorite, garnet, opaques	Tourmaline, zircon, muscovite, epidote, opaques
Other	Sample is very 'dirty' with abundant hematite staining, some grains appear fragmented		Very similar to RV1-09	Very similar to RV1-08, abundant pore space

Table Ia Continued:

Sample	RV1-11 (9)	RV1-12 (10)	RSQ-09 (11)	FN1-07 (12)
Classification	Feldspathic greywacke	Litharenite	Lithic greywacke	Sublitharenite
Provenance	Mixed	Recycled Orogen	Recycled Orogen	Recycled Orogen
Colour*	Light Grey (5Y 7/1)	Grey Olive (5Y 3/2)	Grey (5Y 5/1)	Light Grey (5Y 7/1)
Supported by:	Grain	Grain	Matrix	Grain
% Matrix	30	10	20	10-15
Cement	Calcite, variable		Calcite	
Grain Boundaries	Concavo-convex > point	Point	Point (where contacts occur)	Point and concavo-convex
Grain Size**	m.g.	f.g.-m.g.	v.f.g.-f.g.	v.f.g. / f.g. / m.g.
Grain Roundedness***	SA	A-SR	SA-R	SA / R-WR / SA-SR
Sortedness	Moderate	Poor	Moderate	Poor
Maturity	Immature	Immature	Immature	Submature
Quartz	0.25-0.5 mm, SA-SR, undulose extinction common, few zircon and rutile inclusions	0.3 mm, R, straight extinction; very few 0.4 mm, elongated rectangular grains	0.15-0.2 mm, A-SA, elongated rectangular and wedge-shaped, straight extinction	0.3-0.4 mm, SA-SR, undulose and straight extinction, vacuoles, inclusions
	Several grains with zircon inclusions	0.15-0.3 mm, SA-SR, some 'wedge' shapes, dominantly straight extinction	0.06-0.1 mm, SA-R, more spherical and wedge shaped, straight extinction	0.15-0.2 mm, R-WR, straight extinction
				0.1 mm, SA, rectangular
Quartz P	Crystal number variable, straight contacts dominant, uniform crystal size within grains; CG chert	2-3 crystals, sutured contacts, non-equigranular crystals, grains 0.2-0.3 mm and SR; FG chert; Chalcedony	0.15-0.2 mm, 2-3 crystals, straight contacts, non-equigranular; Minor chert	4 crystals, semi-sutured contacts; 2-4 crystals, straight contacts; All non-equigranular CG and FG chert
Feldspar	Plagioclase > microcline > untwinned > perthite	Plagioclase > untwinned > microcline	Plagioclase > untwinned > microcline > K-feldspar	Untwinned > plagioclase > microcline
	Plagioclase grains occur as SA grains and broken laths with albite and polysynthetic twinning; all are fresh to moderately sericite, clay or calcite altered	Plagioclase is A-SA grains or broken laths with albite twinning, microcline is SA-SR; all are fresh to moderate clay and lesser calcite alteration	Plagioclase albite and polysynthetic twinned; Microcline and feldspar 0.1-2 mm, SA-SR; K-feldspar broken laths with simple twinning; All fresh to strong clay, sericite or calcite alteration	Plagioclase is 0.1-0.2 mm, SA-SR, albite twinning; Microcline is 0.05-0.3 mm, SA-SR, All fresh to moderate clay or sericite alteration
Lithics	Igneous = quartz + feldspar Sedimentary = irregular grain shape	Sedimentary = irregular grain shapes, conform to surrounding grains Igneous = quartz + feldspar	Lithics are rare, other than Qp, and occur as 0.05-0.1 mm, SR sedimentary grains	Metamorphic = schistose, 0.2-0.3 mm, SA Sedimentary = 0.1 mm, SR
Accessory Minerals	Muscovite, garnet, chlorite, biotite, rutile, epidote, zircon, tourmaline, opaques, hematite blebs	Biotite (very abundant), muscovite, tourmaline, garnet, chlorite, sphene, rutile, opaques	Biotite (abundant), muscovite, zircon, garnet, epidote, chlorite, opaques	Zircon, Garnet, Rutile, Tourmaline, opaques
Other		Grains elongated with preferred orientation	Preferred orientation; wavy laminations	

Table Ia Continued:

Sample	FN1-08 (13)	FN1-09 (14)	FN1-10 (15)	FN3-17 (16)
Classification	Lithic greywacke	Litharenite	Sublitharenite	Subarkose
Provenance	Recycled Orogen	Recycled Orogen	Recycled Orogen	Recycled Orogen / Continental Block
Colour*	Light Grey (N7)	Light Grey (N7)	Light Grey (N7)	Light Grey (5Y 7/2)
Supported by:	Grain	Grain	Grain	Grain
% Matrix	25	5-10	10	7
Cement	Calcite	Calcite	Calcite and Silica	Silica
Grain Boundaries	Point	Point	Point and concavo-convex	Point and sutured[18]
Grain Size**	f.g.-m.g.	v.f.g / m.g. / c.g.	f.g.-m.g.	v.f.g.-f.g. / c.g.
Grain Roundedness***	SA-SR	SA / SA-SR / A	SA – R	SA-R / SR-WR
Sortedness	Moderate	Poor	Moderate	Moderate
Maturity	Submature	Immature	Submature	Submature
Quartz	0.15-0.3 mm, SA-SR, elongate-rectangular and semi-spherical grains, straight >> undulose extinction	0.2-0.4 mm, SA-SR, undulose = straight extinction, overgrowths present	0.3-0.4 mm, R-WR, straight extinction, overgrowths present but uncommon	0.5-0.6 mm, SR-R, straight and undulose extinction, zircon and rutile inclusions, overgrowths common (in sutured area)
	0.2 mm, R, straight extinction	0.06-0.1 mm, A-SA, straight extinction	Coarser and finer SA-SR, wedge, rectangular and semi-spherical, straight and undulose extinction	0.06-0.2 mm, SA-R, straight and undulose extinction
Quartz P	> 5 crystals, sutured contacts, crystals elongated in a fabric; 3-5 crystals, straight contacts, non-equigranular, rare; FG chert abundant	>5, crystals, sutured contacts, non-equigranular, uncommon; Chert minor	3-5 crystals, sutured contacts; 2 crystals, straight contacts; All non-equigranular; FG and CG chert	3-4 crystals, semi-sutured contacts, non-equigranular, found in the coarser size fraction; CG and FG chert
Feldspar	Untwinned > plagioclase > microcline	Untwinned > plagioclase	Untwinned > plagioclase > microcline > perthite	Untwinned > microcline > plagioclase > K-feldspar
	All 0.1-0.3 mm, SA-SR, fresh to strongly sericite or clay altered and rimming or pervasive calcite replacement common	Plagioclase 0.1-0.2 mm, SA-SR, albite twinning, fresh to minor alteration; Untwinned minor to strong sericite, clay or calcite alteration	Plagioclase 0.1-0.3 mm, SA-SR grains > laths; Microcline 0.2-0.4 mm, more rounded, All fresh to strong clay or sericite altered	Plagioclase albite twinned; K-feldspar simple twinned; All 0.4-0.6 mm > 0.05-0.2, more WR than quartz, fresh to moderately altered
Lithics	Sedimentary = relatively abundant, 0.1-0.2 mm, SA-R; Metamorphic = (>5 crystal Qp above)	Sedimentary = 0.1-0.3 and 0.6-1.2 mm, SR and A, fragments / mud clasts; Igneous = granitic	Sedimentary = tend to conform to surrounding grains Igneous = felsic quartz + feldspar	Sedimentary = 0.2-0.4 mm, SR-R; Igneous = quartz + moderately altered feldspar
Accessory Minerals	Biotite, garnet, tourmaline, rutile, opaques	Biotite, garnet, tourmaline, zircon, opaques	Tourmaline, garnet, rutile, sphene, zircon, opaques	Zircon, opaques, garnet, Hematite (crystals and blebs, abundant)
Other		Abundant pore space		

[18] FN3-17 sutured contacts likely caused by overgrowth of the silica cement, therefore grain size and shape descriptions are based on the areas with point contacts and no silica cement

Table Ia Continued:

Sample	FN-111 (17)	FN-112 (18)	PP-37 (19)
Classification	Litharenite	Litharenite	Litharenite
Provenance	Recycled Orogen	Recycled Orogen	Magmatic Arc
Colour*	Light Grey (N7)	Very Light Grey (N8)	Light Grey (2.5Y 7/2)
Supported by:	Grain	Grain	Grain
% Matrix	10	15	5-10
Cement		Minor calcite, silica	
Grain Boundaries	Concavo-convex	Point	Concavo-convex
Grain Size**	v.f.g. / m.g.	f.g. / m.g.	v.f.g.-m.g.
Grain Roundedness***	SA-SR / SR-WR	SA-SR / SR-R	SA-SR
Sortedness	Moderate	Moderate	Poor
Maturity	Submature	Submature	Immature
Quartz	Dominates larger size fraction (0.25-0.4 mm), R-WR, dominantly straight extinction	0.3-0.5 mm, R-WR, straight >> undulose extinction, vacuoles	0.06-0.2, dominantly SA, though some 0.1 mm grains R, grains are elongated, rectangular and show straight extinction
	0.06-0.1 mm, SA>SR, rectangular and semi-spherical grains, straight extinction	0.15-0.25 mm, SA-SR, dominantly straight extinction	
Quartz P	2 crystals, straight contacts, non-equigranular; 3 crystals, sutured contacts, more equigranular	2 crystals, straight contact; 3 crystals, semi-sutured contacts; >5 crystals elongated in a fabric; All non-equigranular; Chert	2 crystals, straight contact; 3 crystals, sutured contact; All non-equigranular; FG Chert
Feldspar	Untwinned > plagioclase > microcline	Untwinned > plagioclase > microcline	Plagioclase > untwinned > microcline
	Plagioclase 0.05-Microcline 0.1-.03 mm, microcline and untwinned coarser grains more WR; All show minor to strong clay or sericite alteration	Plagioclase albite and polysynthetic twinned; Plagioclase and microcline 0.1-0.3 mm, SA-SR; All are fresh to moderately clay or sericite altered,	Plagioclase 0.05-0.15 mm, SA-SR with albite and polysynthetic twinning; Microcline is uncommon; All have minor to strong clay or sericite alteration
Lithics	Sedimentary = 0.1-0.2 mm	Igneous = felsic, quartz + feldspar; Sedimentary Metamorphic = (see >5 crystal Qp above)	Igneous = felsic quartz + moderately altered feldspar; Sedimentary = conform to surrounding grains
Accessory Minerals	Garnet, zircon, opaques	Zircon, opaques, garnet	Muscovite, biotite, chlorite, tourmaline, garnet, zircon, opaques
Other	Matrix is quartz rich and some areas show Fe staining, abundant pore space	1-2 mm, irregularly shaped patches of secondary quartz throughout sample	Preferred orientation; laminated; organic rich; widely dispersed circular Fe-rich patches

Table Ia Continued:

Sample	PP-39 (20)	KF1-55 (21)	M1-01 (22)
Classification	Litharenite	Lithic greywacke	Sublitharenite
Provenance	Magmatic Arc	Recycled Orogen	Recycled Orogen
Colour*	Light Brownish Grey (10Y 6/2)	Light Grey (N7)	Pinkish Grey (5YR 8/1)
Supported by:	Grain	Matrix	Grain
% Matrix	15	25	5
Cement		Silica, minor	silica
Grain Boundaries	Point and concavo-convex	Point	Semi-sutured
Grain Size**	v.f.g.-m.g.	v.f.g. / m.g.	m.g. / minor c.g.
Grain Roundedness***	SA-SR	SA / SA-SR	SA-SR / SR
Sortedness	Poor	Moderate	Moderate
Maturity	Immature	Immature	Submature
Quartz	0.13-0.3 mm, SA-SR, elongated, rectangular grains, straight > undulose extinction, minor conchoidal surfaces	0.25-0.4 mm, SA-SR, undulose and straight extinction, vacuoles common	0.25-0.4 mm, SA-SR, straight > undulose extinction, vacuoles common, zircon inclusion, quartz overgrowths
	2nd generation is 0.1-0.15 mm, R-WR, spherical, straight extinction	0.06-0.1 mm, SA-WR with elongated rectangular and spherical grains, straight extinction	0.25 mm, R-WR, undulose > straight extinction
Quartz P	3->5 crystals, sutured contacts, non-equigranular; 2 crystals, straight contacts, semi-equigranular; Chert	Dominantly FG chert; > 5 crystals, sutured contacts, non-equigranular; Chalcedony uncommon	3-5 crystals, sutured contacts, non-equigranular; >5 crystals, straight but rounded contacts, non-equigranular; FG chert
Feldspar	Plagioclase > untwinned > microcline	Untwinned > plagioclase	Untwinned > plagioclase > microcline > perthite
	Plagioclase is dominantly 0.1-0.2 mm, SR-SR with albite and polysynthetic twinning; Microcline is uncommon; All are moderately to strongly clay or sericite altered	Plagioclase is dominantly 0.2-0.4 mm, broken laths and SA-SR grains, albite extinction, some grains with strained extinction; All show fresh to moderate clay or sericite alteration	Plagioclase and microcline 0.2-0.4 mm, SA>SR, Plagioclase dominantly albite twinned; All with minor to strong clay or sericite alteration
Lithics	Igneous = felsic quartz + moderately altered feldspar; Sedimentary = conform to surrounding grains Metamorphic = schistose	Sedimentary = 1-10 mm mud clasts and finer grains; Igneous = felsic quartz + moderately altered feldspar	Sedimentary = 0.2-0.6 mm, SR, mud to VFG sandstone Igneous = quartz + altered feldspar
Accessory Minerals	Biotite, garnet, zircon, chlorite, hematite, opaques	Muscovite, biotite, tourmaline, garnet (abundant), zircon, epidote, rutile, opaques	Chlorite, biotite, muscovite, tourmaline, hornblende, opaques
Other	Weak preferred orientation, elongate grains; sample very similar to PP-37	Abundant poor space; muddy, organic-rich matrix	Abundant poor space

Table Ia Continued:

Sample	M2-04 (23)	M6-15 (24)	BH1-04 (25)
Classification	Feldspathic greywacke	Litharenite	Lithic greywacke
Provenance	Recycled Orogen	Recycled Orogen	Recycled Orogen
Colour*			Medium Dark Gray (N3)
Supported by:	Grain	Grain	Grain
% Matrix	20-25	5-10	15-20
Cement			Calcite
Grain Boundaries	Concavo-convex	Point	Concavo-convex
Grain Size**	v.f.g.-f.g.	v.f.g. / f.g.-m.g. / c.g.	f.g. / m.g.-c.g.
Grain Roundedness***	SA-SR	A / SA / SA-SR	SR
Sortedness	Moderate	Poor	Moderate
Maturity	Immature	Submature	Submature
Quartz	0.06-0.2 mm, SA<SR, elongated rectangular and spherical grains, straight > undulose extinction, vacuoles	0.4-0.8 mm, SR-R, undulose and straight extinction, vacuoles common, zircon and needle-like rutile inclusions	0.4-0.6 mm, SA-SR, larger grains more elongated, dominantly straight extinction, vacuoles common
		Finer grains more angular with less vacuoles	0.25-0.4 mm, R-WR, straight > undulose extinction
Quartz P	2 crystals, straight contacts, non-equigranular; >3 crystals, sutured contacts, non-equigranular; Chert	2-5 crystals, straight contacts, semi-equigranular; 4- >5 crystals, sutured contacts, non-equigranular; Chert	3 crystals, straight contacts, non-equigranular; 3- >5 crystals, sutured contacts, non-equigranular; All dominantly 03-0.5 mm and SA-SR; FG chert common
Feldspar	Untwinned > plagioclase > microcline	Untwinned > plagioclase > microcline = perthite > K-feldspar	Plagioclase > untwinned > microcline > perthite > K-feldspar
	Plagioclase 0.06-0.1 mm > 0.2 mm, SA, albite twinning, All fresh to very strong calcite, sericite or clay alteration	Plagioclase is albite twinned and K-feldspar has simple twinning; All increase roundedness with increased grain size and show minor to strong clay or sericite alteration, microcline is fresher	Plagioclase and Microcline 0.4-0.5 mm > 0.15-0.2, SR, Plagioclase albite twinned; K-feldspar dominantly 0.2-0.3 mm broken laths and simple twinned; All fresh to strongly altered to clay, sericite or calcite
Lithic	Igneous = quartz + feldspar; Sedimentary	Igneous = microcline + quartz Sedimentary	Sedimentary =, dominantly 0.2-0.4 mm, irregular grain shapes
Accessory Minerals	Chlorite, biotite, garnet, epidote, zircon, muscovite, apatite (?), opaques, hematite blebs	Muscovite, garnet, zircon, rutile, opaques, hematite staining	Muscovite, biotite, calcite, titatnite (?), garnet, opaques
Other	Semi-preferred orientation, x-laminations of finer and coarser grains	Muscovite, garnet, zircon, rutile, opaques, hematite staining	Matrix is Fe-rich

Table Ia Continued:

Sample	BH1-06 (26)	JG1-01 (27)	JG1-02 (28)
Classification	Litharenite	Subarkose	Arkose
Provenance	Recycled Orogen	Continental Block / Recycled Orogen	Continental Block
Colour*			Yellowish Grey (5GY 8/1)
Supported by:	Grain	Grain	Grain
% Matrix	5	15	7
Cement	Silica	Calcite and Silica	Calcite
Grain Boundaries	Concavo-convex, few sutured	Point	Concavo-convex and semi-sutured
Grain Size**	m.g. / c.g.	f.g. / m.g.	m.g. / c.g. / minor v.c.g.
Grain Roundedness***	SA / SR-R	A-SA / SA-R	SA / R-WR
Sortedness	Poor	Poor	Moderate
Maturity	Submature	Immature	Submature
Quartz	0.5-0.8 mm, SA>SR-R, dominantly straight extinction, vacuoles abundant, minor quartz overgrowths	0.4-0.5 mm SR-WR, straight and undulose extinction, vacuoles,	0.5-0.8 mm, SA-SR, straight > undulose extinction, vacuoles, semi-sutured contacts dominant
	0.3-0.4 mm, SA-SR, rectangular, spherical and wedge shaped, straight and undulose extinction	0.15-0.25 mm and few 1.5-2 mm, A-SA, straight > undulose extinction	0.4-0.5 mm, R-WR, straight extinction, rutile and zircon inclusions
Quartz P	2 crystals, semi-sutured, non-equigranular, 0.6 mm, SR; 3- >5 crystals, sutured contacts, non-equigranular, 0.4-0.7 mm and 2-2.5 mm, SA-SR; Chert	2-5 crystals, straight contacts, equi- and non-equigranular; 2-3 crystals, sutured contacts, rare; FG and CG chert	3-5 crystals (4 dominant), straight contacts, non-equigranular>4 crystals, sutured-contacts, non-equigranular; Minor chert
Feldspar	Plagioclase > untwinned > microcline > perthite	Untwinned > plagioclase > microcline > perthite > K-feldspar	Untwinned > microcline > plagioclase > K-feldspar > perthite
	Plagioclase 0.2-0.8 mm, coarser is more well rounded, albite and polysynthetic twinning; Microcline dominantly 0.3-0.6 mm, SR; All fresh to moderately clay or sericite altered, or strongly calcite altered	Plagioclase occurs as laths to SA fragments; Microcline and K-feldspar are SA; All are fresh to moderately clay or sericite altered, or strongly calcite altered	Plagioclase occurs as SA grains and laths, fresh to strongly altered; Microcline 0.4-0.8 mm and few 1.2 mm grains, no to minor alteration; K-feldspar is moderately to strongly altered
Lithics	Sedimentary =, 0.3-0.9 mm, SA-WR	Sedimentary Igneous = quartz + feldspar	Sedimentary = irregular shapes; Igneous = quartz + feldspar
Accessory Minerals	Muscovite, biotite, zircon, opaques, hematite blebs	Garnet, biotite, rutile, zircon, titanite, opaques	Muscovite, biotite, calcite, garnet (abundant, very angular), opaques
Other	X-bedding	In areas with calcite cement Qm and Qp are rimmed by matrix remnants	Layers of organic-rich matrix

Table Ia Continued:

Sample	JG1-05 (29)	JG1-06 (30)	KV-106 (31)
Classification	Lithic arkose	Lithic arkose	Lithic arkose
Provenance	Continental Block / Magmatic Arc	Continental Block / Magmatic Arc	Mixed
Colour*		Medium Bluish Grey (5B 5/1)	Yellowish Grey (5GY 8/1)
Grain / Matrix Supported	Grain	Grain	Grain
% Matrix	10-15	5	10
Cement			Calcite
Grain Boundaries	Concavo-convex	Point	Concavo-convex
Grain Size**	v.f.g.-f.g.	v.f.g. / f.g.	f.g.-m.g.
Grain Roundedness***	SA-SR	SA / SR	A-SA
Sortedness	Poor	Well	Well
Maturity	Submature	Mature	Submature
Quartz	0.06-0.2 mm, SA-R with coarser grains more rounded, straight extinction; tend to be coarser grained than other minerals	0.15-0.25 mm, SR-R, straight extinction 0.06-0.1 mm, elongated rectangular grains, straight extinction	0.25-0.3 mm, A-SA wedge-shaped and elongated grains, vacuoles low abundance, straight and undulose extinction 0.125-0.2 mm, SR, spherical grains, straight extinction dominant
Quartz P	3-4 crystals, straight contacts, semi-equigranular, low abundance; Chert very abundant	2 crystals, sutured contacts, semi-equigranular; Chert	2-3 crystals, straight contacts, semi-equi and equigranular; >4 crystals, semi-sutured contacts, non-equigranular
Feldspar	Untwinned > plagioclase > microcline	Untwinned > plagioclase = microcline > K-feldspar	Untwinned > plagioclase > K-feldspar
	Plagioclase 0.06-0.2 mm broken laths and SA-SR grains, fresh to strong alteration; Microcline and untwinned are moderately to strongly sericite or clay altered	Plagioclase occurs as laths and SA grains with albite twinning, low to moderate alteration; K-feldspar is broken laths with simple twinning and moderate to strong alteration; untwinned has moderate to strong clay or sericite alteration	Plagioclase 0.15-0.25 > 0.3mm, SA grains and broken laths with albite and polysynthetic twinning; K-feldspar shows simple twinning and has a low abundance, both are fresh to moderately altered; Untwinned grains show moderate to strong clay and calcite alteration
Lithics	Sedimentary = conform to surrounding grains	Sedimentary = mudstone clasts, irregular shape and size	Igneous = feldspar + quartz; Sedimentary = 0.15-0.3 mm grains with irregular shapes
Accessory Minerals	Biotite, muscovite, zircon, chlorite, tourmaline, garnet, opaques	Muscovite, chlorite, garnet, tourmaline, opaques	Muscovite, chlorite, biotite, zircon, hematite, opaques
Other	Weakly preferred orientation, sample shows strong clay alteration	preferred orientation, elongated grains	Hematite occurs as 'blebs' and circular Fe-rich patches in the matrix

Table Ia Continued:

Sample	KV-109 (32)	DB2-22 (33)	DB2-29 (34)
Classification	Litharenite	Subarkose	Lithic greywacke
Provenance	Recycled Orogen	Recycled Orogen	Recycled Orogen
Colour*	Light Olive Grey (5Y 6/2)		Light Olive Grey (5Y 6/2)
Grain / Matrix Supported	Matrix	Grain	Grain
% Matrix	15	15	25
Cement		Calcite	Calcite
Grain Boundaries	Point	Pont	
Grain Size**	v.f.g.-f.g.	v.f.g.-f.g. / minor m.g.	v.f.g. / f.g.-m.g.
Grain Roundedness***	A-SA	SA	SA-R / A-SR
Sortedness	Well	Moderate	Moderate
Maturity	Submature	Immature	Immature
Quartz	0.1-0.2 mm, A-SA, elongated rectangular grains, straight extinction dominant	0.1-0.2 mm, SA, elongated rectangular grains, straight and undulose extinction	0.15-0.3 mm, SA-SR, elongated grains with dominantly straight extinction, show preferred orientation
	0.06-0.1 mm, SR straight extinction, low abundance	0.06-0.15 mm and very few 0.3 mm, SR-R, straight and undulose extinction, relatively low abundance, vacuoles present in some of the larger grains	0.06-0.1 mm, SR-R, straight extinction
Quartz P	3-4 crystals, semi-sutured contacts, non-equigranular, 0.2 mm, SA; FG chert abundant	Dominantly chert; 2 crystals, straight to sutured contacts, non-equigranular, low abundance	3 crystals, straight contacts; >4 crystals, sutured contacts; both non-equigranular; FG chert
Feldspar	Plagioclase > untwinned	Untwinned > plagioclase > microcline	Untwinned > plagioclase
	Plagioclase 0.1-0.2 mm, A-SA, albite > polysynthetic twinning, fresh to minor alteration; Untwinned moderately to strongly clay or sericite altered	Plagioclase is albite twinned; All are 0.06-0.2 mm, SA and are fresh to strongly clay or sericite altered; Moderate to complete calcite replacement of the calcic-feldspars replacement	Plagioclase 0.06-0.2 mm, SA, albite twinned; All show Moderate to very strong clay, sericite or calcite alteration
Lithics	Sedimentary = conform to surrounding grains, most abundant lithic type Igneous = feldspar + quartz	Sedimentary = some R-WR fragments occur Metamorphic = micaceous and schistose, low abundance	Sedimentary
Accessory Minerals	Biotite (abundant), muscovite, chlorite, tourmaline, zircon, opaques	Biotite, opaques, muscovite, garnet, tourmaline, zircon	Biotite (very abundant), muscovite, zircon, rutile, epidote, garnet, sphene
Other	Grains show preferred orientation, wavy laminations, Fe-rich matrix more abundant in some laminations	Slight laminations of coarser (0.1-0.2 mm) and finer (0.05-0.15 mm) grains	Preferred grain orientation, matrix is organic-rich

Table Ia Continued:

Sample	BF1-05 (35)	BF1-12 (36)	BF2-23 (37)
Classification	Feldspathic greywacke	Lithic arkose	Litharenite
Provenance	Continental Block	Continental Block	Recycled Orogen
Colour*		Medium Grey (N5)	
Supported by:	Grain	Grain	Grain
% Matrix	15-20	10	<5
Cement	Calcite	Calcite	Calcite and silica
Grain Boundaries	Point	Concavo-convex and sutured	Concavo-convex to semi-sutured
Grain Size**	v.f.g.	v.f.g. / m.g.	f.g. / m.g.-c.g.
Grain Roundedness***	SA	R / SA-SR	SA-SR / SR-R
Sortedness	Moderate	Moderate	Moderate
Maturity	Submature	Submature	Mature
Quartz	0.06-0.1 mm, SA to SR, elongated rectangular and lesser spherical grains, straight extinction	0.25-0.4 mm, SA-SR, straight and undulose extinction	Dominantly 0.5-0.6 mm, SR-R and few WR, straight and undulose extinction, vacuoles, zircon inclusions (low abundance)
		0.1 mm, R-WWR, straight extinction	0.125-0.2 mm, SA-R, straight extinction dominant, less abundant that coarser grained
Quartz P	2 crystals, straight contacts, non-equigranular; 3-5 crystals, semi-sutured, non equigranular; FG chert	2-5 crystals, moderately sutured to sutured, non-equigranular, low abundance	Chert dominant; 2-3 crystals, straight contacts, equigranular; 2- >4 grains, sutured contacts, equigranular; Chalcedony
Feldspar	Untwinned > plagioclase > microcline	Untwinned > plagioclase	Untwinned > plagioclase > microcline
	All 0.06-0.1 mm, SA and moderate to strongly altered to clay, sericite or less commonly calcite	Untwinned feldspar very abundant with moderate clay or sericite alteration; Plagioclase albite twinned with minor to moderate alteration	All are dominantly 0.4-0.6 mm, SR and fresh to strongly altered to calcite, clay or sericite. Plagioclase is albite and polysynthetic twinned
Lithics	Sedimentary	Sedimentary = some conform to surrounding grains	Igneous = feldspar + quartz Sedimentary = dominantly 0.3-0.6 mm, SR-R
Accessory Minerals	Biotite, muscovite, tourmaline, zircon, chlorite, opaques	Biotite, zircon, chlorite, epidote, opaques	Garnet, zircon, opaques, calcite
Other	Strongly altered, finely laminated	laminated	Grains are tightly packed

*Colours based on Goddard *et al*. (1970) and Munsell (1971)

** Grain Size based on Udden-Wentworth Scale:

Size (mm)	< 0.0625	0.0625-0.125	0.125-0.25	0.25-0.5	0.5-1	1-2	> 2
Size Class	Clay to Silt	Very Fine Sand	Fine Sand	Medium Sand	Coarse Sand	Very Coarse Sand	Granule to Pebble
Abbreviation		v.f.g.	f.g.	m.g.	c.g.	v.c.g.	

*** Grain Roundedness as Follows:

Roundedness	Angular	Subangular	Subrounded	Rounded	Well Rounded
Abbreviation	A	SA	SR	R	WR

Table Ib: Point Counting Results of the Sandstone Xenoliths*

	Raw Data as %:													Combined Data as %:				
Sample	**Qm**	**Qp**	**Ls**	**Li**	**Lm**	**F-Plag**	**F-Perthite**	**F-Microcline**	**F-untwinned**	**K-Feldspar**	**Acc**	**Total**		**Qm**	**Qp**	**F**	**Lt**	**Acc**
V2-08	63.0	6.0	2.0	0.0	0.0	5.5	0.0	2.5	14.5	0.0	6.5	100		63.0	6.0	22.5	2.0	6.5
V4-13	78.5	9.0	1.5	0.0	0.0	0.0	0.0	1.0	8.0	0.0	2.0	100		78.5	9.0	9.0	1.5	2.0
V4-14	37.0	30.0	0.0	1.0	0.0	7.0	0.0	8.0	11.0	4.0	2.0	100		37.0	30.0	30.0	1.0	2.0
V5-15	79.0	3.3	2.7	0.0	0.0	1.7	0.0	0.7	7.3	0.0	5.3	100		79.0	3.3	9.7	2.7	5.3
V5-17	32.3	24.0	1.3	2.7	0.0	7.3	3.3	12.7	14.0	0.0	2.3	100		32.3	24.0	37.3	4.0	2.3
RV1-04	38.0	13.3	6.0	0.7	0.7	6.7	2.0	12.0	11.0	1.3	8.3	100		38.0	13.3	33.0	7.3	8.3
RV1-08	60.5	15.5	2.5	1.0	0.0	5.5	0.0	3.0	8.5	0.0	3.5	100		60.5	15.5	17.0	3.5	3.5
RV1-09	55.2	23.2	2.0	0.4	0.4	7.6	0.0	0.0	6.4	0.0	4.8	100		55.2	23.2	14.0	2.8	4.8
RV1-11	66.7	8.0	3.7	0.0	0.0	4.3	0.0	5.7	6.7	0.0	5.0	100		66.7	8.0	16.7	3.7	5.0
RV1-12	38.4	25.2	5.2	3.6	0.0	8.4	0.0	1.6	8.4	0.0	9.2	100		38.4	25.2	18.4	8.8	9.2
RSQ-09	33.6	25.6	7.6	2.0	1.2	12.0	0.0	0.4	5.2	0.0	12.4	100		33.6	25.6	17.6	10.8	12.4
FN1-07	40.0	26.5	8.5	2.5	0.0	3.5	0.0	0.0	12.5	0.0	6.5	100		40.0	26.5	16.0	11.0	6.5
FN1-08	66.4	20.4	1.2	0.8	0.0	4.0	0.0	0.8	5.6	0.0	0.8	100		66.4	20.4	10.4	2.0	0.8
FN1-09	67.6	9.6	6.8	0.8	0.0	4.0	0.0	0.0	6.8	0.0	4.4	100		67.6	9.6	10.8	7.6	4.4
FN1-10	44.0	34.0	4.4	3.2	0.0	3.2	0.4	1.6	4.4	0.0	4.8	100		44.0	34.0	9.6	7.6	4.8
FN3-17	72.0	5.7	4.0	0.7	0.0	2.3	0.0	3.3	8.7	0.7	2.7	100		72.0	5.7	15.0	4.7	2.7
FN-111	58.5	20.5	3.5	0.0	0.0	4.0	0.0	0.5	10.5	0.0	2.5	100		58.5	20.5	15.0	3.5	2.5
FN-112	64.0	19.6	6.4	1.6	0.0	0.4	0.0	2.4	2.0	0.0	3.6	100		64.0	19.6	4.8	8.0	3.6
PP1-37	20.8	31.2	13.6	4.8	0.0	8.0	0.0	0.4	15.6	0.0	5.6	100		20.8	31.2	24.0	18.4	5.6
PP1-39	19.6	35.6	6.8	2.4	0.4	8.8	0.0	1.2	17.2	0.0	8.0	100		19.6	35.6	27.2	9.6	8.0
KF1-55	40.0	28.8	12.8	4.0	0.0	2.0	0.0	0.0	6.8	0.0	5.6	100		40.0	28.8	8.8	16.8	5.6

Table Ib: Continued: Point Counting Results of the Sandstone Xenoliths*

	Raw Data as %:													Combined Data as %:				
Sample	**Qm**	**Qp**	**Ls**	**Li**	**Lm**	**F-Plag**	**F-Perthite**	**F-Microcline**	**F-untwinned**	**K-Feldspar**	**Acc**	**Total**		**Qm**	**Qp**	**F**	**Lt**	**Acc**
M1-01	73.0	13.7	5.0	0.7	0.0	1.3	0.3	0.3	4.0	0.0	1.7	100		73.0	13.7	6.0	5.7	1.7
M2-04	57.5	14.0	2.0	1.0	0.0	4.5	0.0	1.5	11.0	0.0	8.5	100		57.5	14.0	17.0	3.0	8.5
M6-15	65.7	27.7	1.3	0.7	0.0	0.0	0.3	0.0	4.3	0.0	0.0	100		65.7	27.7	4.7	2.0	0.0
BH1-04	45.6	29.2	3.6	2.4	0.4	7.2	0.4	2.0	4.0	0.0	5.2	100		45.6	29.2	13.6	6.4	5.2
BH1-06	57.0	31.5	2.0	0.0	0.0	3.0	0.5	2.5	2.5	0.0	1.0	100		57.0	31.5	8.5	2.0	1.0
JG1-01	56.0	5.3	7.7	0.3	0.0	6.3	0.7	1.3	13.3	0.3	9.0	100		56.0	5.3	21.7	8.0	9.0
JG1-02	47.7	7.3	5.0	0.7	0.0	4.7	0.0	12.7	18.3	0.0	3.7	100		47.7	7.3	35.7	5.7	3.7
JG1-05	36.5	11.0	6.5	0.0	0.0	4.5	0.0	1.0	35.0	0.0	5.5	100		36.5	11.0	40.5	6.5	5.5
JG-06	30.7	11.3	7.3	0.3	0.0	5.0	0.0	3.7	36.7	0.3	4.7	100		30.7	11.3	45.7	7.7	4.7
KV-106	38.0	17.0	8.0	1.5	0.0	13.0	0.0	0.0	17.0	0.0	5.5	100		38.0	17.0	30.0	9.5	5.5
KV-109	33.2	35.2	7.2	1.2	0.0	11.6	0.0	0.0	4.0	0.0	7.6	100		33.2	35.2	15.6	8.4	7.6
DB-22	50.8	12.3	7.0	0.0	0.5	2.8	0.0	0.5	15.8	2.5	8.0	100		50.8	12.3	21.5	7.5	8.0
DB2-29	34.5	24.5	10.0	0.0	0.0	4.0	0.0	0.0	12.0	0.0	15.0	100		34.5	24.5	16.0	10.0	15.0
BF1-05	45.5	6.5	3.5	0.0	0.0	5.0	0.0	2.5	18.0	0.0	19.0	100		45.5	6.5	25.5	3.5	19.0
BF1-12	33.0	9.0	8.0	0.0	0.0	1.0	0.0	0.0	47.5	0.0	1.5	100		33.0	9.0	48.5	8.0	1.5
BF2-23	65.0	23.0	3.0	1.0	0.0	2.0	1.0	1.0	2.0	0.0	2.0	100		65.0	23.0	6.0	4.0	2.0

*percentages based on n = 300 point counts

Table Ic: Correlation of the Sandstone Xenoliths

	Sample	Qm:F:Lt Field*	Correlation**
1	**V2-08**	'Stormberg' Group	Stormberg
2	**V4-13**	'Stormberg' Group	Stormberg
3	**V4-14**	'Stormberg' Group	Stormberg
4	**V5-15**	Tarkastad / Adelaide Subgroups / Ecca Group	Adelaide / Ecca
5	**V5-17**	Tarkastad / Adelaide Subgroups / Ecca Group	Adelaide / Ecca
6	**RV1-04**	Tarkastad Subgroup	Tarkastad
7	**RV1-08**	Tarkastad Subgroup	Tarkastad
8	**RV1-09**	Tarkastad Subgroup	Tarkastad
9	**RV1-11**	Tarkastad / Adelaide Subgroups / Ecca Group	Beaufort / Ecca
10	**RV1-12**	Tarkastad / Adelaide Subgroups / Ecca Group	Tarkastad
11	**RSQ-09**	Tarkastad / Adelaide Subgroups / Ecca Group	Beaufort / Ecca
12	**FN1-07**	'Stormberg' Group	Tarkastad
13	**FN1-08**	Tarkastad Subgroup	Tarkastad
14	**FN1-09**	Tarkastad Subgroup	Tarkastad
15	**FN1-10**	Tarkastad Subgroup	Tarkastad
16	**FN3-17**	'Stormberg' Group	Tarkastad
17	**FN-111**	Tarkastad Subgroup	Tarkastad
18	**FN-112**	Tarkastad / Adelaide Subgroups / Ecca Group	Adelaide / Ecca
19	**PP1-37**	Adelaide Subgroup / Ecca Group	Adelaide / Ecca
20	**PP1-39**	Adelaide Subgroup / Ecca Group	Adelaide / Ecca
21	**KF1-55**	Tarkastad Subgroup	Tarkastad
22	**M1-01**	'Stormberg' Group	Stormberg
23	**M2-04**	Tarkastad Subgroup	Tarkastad
24	**M6-15**	Tarkastad Subgroup	Tarkastad
25	**BH1-04**	Tarkastad Subgroup	Tarkastad
26	**BH1-06**	Tarkastad Subgroup	Tarkastad
27	**JG1-01**	Tarkastad Subgroup	Tarkastad
28	**JG1-02**	Dwyka Group	Dwyka
29	**JG1-05**	Adelaide Subgroup / Ecca Group	Adelaide / Ecca
30	**JG-06**	Adelaide Subgroup / Ecca Group	Adelaide / Ecca
31	**KV-106**	Tarkastad / Adelaide Subgroups / Ecca Group	Tarkastad
32	**KV-109**	Tarkastad / Adelaide Subgroups / Ecca Group	Tarkastad
33	**DB-22**	Tarkastad Subgroup	Tarkastad
34	**DB2-29**	Tarkastad / Adelaide Subgroups / Ecca Group	Beaufort / Ecca
35	**BF1-05**	Dwyka Group	Dwyka
36	**BF1-12**	Adelaide Subgroup / Ecca Group	Adelaide / Ecca
37	**BF2-23**	Tarkastad Subgroup	Tarkastad

*based on point counting data and where sample plots on the Qm:F:Lt diagram in relation to the Karoo Supergroup fields

**based on point counting and petrographic data, as discussed in section 7.3

Table IIa: Raw major and trace element XRF data for the Basalt Xenoliths

Sample		MW1-03	MW1-05	MW1-10	MW1-11	V1-02	V1-03	V1-04
Major Elements								
(wt%)	**SiO2**	48.71	46.76	46.74	47.43	49.05	46.34	44.74
	TiO2	0.85	0.82	1.02	0.97	1.25	1.50	1.36
	Al2O3	14.72	13.71	14.00	13.73	14.08	13.16	14.27
	FeO*	9.42	8.95	10.62	10.05	10.58	12.92	11.84
	MnO	0.15	0.15	0.18	0.15	0.19	0.18	0.19
	MgO	7.412	7.95	5.45	6.82	6.45	6.39	6.20
	CaO	9.47	14.96	10.34	10.59	7.92	8.16	8.23
	Na2O	3.74	0.35	4.18	2.72	2.68	4.38	4.28
	K2O	2.17	3.06	2.35	2.54	2.05	0.18	0.09
	P2O5	0.15	0.21	0.15	0.16	0.20	0.20	0.25
	LOI	4.79	5.6-	5.52	4.97	4.69	6.19	7.49
	H2O	0.35	0.35	0.21	0.19	0.77	0.78	0.59
	total**	101.94	102.87	100.78	100.32	99.92	100.37	99.53
Trace Elements								
(ppm)	**Zn**	109	80	92	92	82	101	81
	Cu	146	87	125	91	99	174	125
	Ni	41	70	58	60	50	64	46
	Co	37	40	44	42	38	48	42
	Cr	102	298	127	245	152	139	129
	V	313	262	288	267	284	363	301
	Nb	27	23	5	6	8	5	9
	Z	132	77	84	98	120	114	129
	Y	33	23	25	24	30	33	34
	Sr	1280	1527	648	1026	493	595	474
	Rb	108	47	90	151	76	8	4
	Ce	34	33	14	24	25	20	29
	Nd	19	18	10	14	17	14	17
	La	18	19	8	11	11	8	13
Colour		Grey	Grey	Grey	Grey	Grey	Grey	Dk Grey
Amygdales			White	White	White	White		White
Other							Vesicular	

Table IIa Continued:

Sample		**V1-05**	**V2-10**	**V6-19**	**V6-20**	**V6-21**	**RV1-18**	**RV1-19**
Major Elements (wt%)	**SiO2**	48.53	47.08	47.83	48.39	48.53	46.55	48.61
	TiO2	1.13	1.17	1.39	1.16	1.39	0.90	0.82
	Al2O3	14.03	13.30	13.69	14.79	13.37	12.85	15.32
	FeO*	12.38	12.07	12.57	10.81	12.58	8.51	8.49
	MnO	0.21	0.12	0.16	0.20	0.17	0.24	0.13
	MgO	6.76	6.02	6.20	6.53	6.03	7.03	7.64
	CaO	10.11	8.97	9.10	8.28	9.29	7.11	7.15
	Na2O	2.38	2.67	1.77	2.16	1.85	2.79	4.15
	K2O	0.92	2.65	0.97	1.97	0.84	4.22	0.90
	P2O5	0.13	0.15	0.19	0.21	0.19	0.14	0.13
	LOI	2.95	5.04	4.35	3.97	3.33	7.35	4.48
	H2O	0.71	0.82	1.3	1.27	1.38	1.25	1.91
	total**	100.23	100.07	99.53	99.74	98.96	98.95	99.75
Trace Elements (ppm)	**Zn**	91	97	105	84	103	73	78
	Cu	172	131	179	122	154	85	79
	Ni	69	69	67	50	64	81	109
	Co	51	49	50	44	50	36	39
	Cr	94	197	147	128	143	310	362
	V	327	324	342	237	352	245	239
	Nb	3	4	5	9	5	11	9
	Z	74	84	105	118	106	95	87
	Y	27	26	30	29	32	24	22
	Sr	328	1288	225	460	224	415	697
	Rb	41	137	44	78	25	67	12
	Ce	15	13	19	28	17	23	18
	Nd	12	12	14	17	13	15	11
	La	6	6	18	12	7	12	14
Colour		Dk Grey	Red	Red	Grey	Red	Grey	Dk Grey
Amygdales		White			White		Pink	
Other								

Table IIa Continued:

Sample		**RV1-21**	**RV1-22**	**WE1-60**	**WE1-61**	**WE1-62**	**WE1-63**	**WE1-64**
Major Elements								
(wt%)	**SiO2**	47.74	48.14	47.91	45.66	46.87	42.87	47.75
	TiO2	0.86	0.84	0.81	0.84	0.82	0.87	0.84
	Al2O3	14.52	15.26	14.74	14.95	15.04	13.40	16.21
	FeO*	8.90	8.88	9.03	8.73	9.35	9.46	9.08
	MnO	0.17	0.14	0.15	0.17	0.15	0.19	0.20
	MgO	7.79	8.00	7.43	8.93	8.63	10.00	8.47
	CaO	5.83	7.67	9.72	7.00	7.38	9.38	7.38
	Na2O	3.85	2.26	1.61	1.41	1.05	2.16	0.58
	K2O	2.97	1.87	3.64	3.76	4.49	2.44	4.25
	P2O5	0.16	0.14	0.19	0.17	0.14	0.15	0.16
	LOI	4.50	3.08	4.54	7.95	5.81	10.07	6.05
	H2O	1.23	3.34	0.4	1.3	0.82	0.29	0.77
	total**	98.53	99.62	100.16	100.89	100.55	101.30	101.74
Trace Elements								
(ppm)	**Zn**	78	71	79	81	81	84	83
	Cu	92	65	85	83	82	83	81
	Ni	66	92	87	86	86	88	89
	Co	40	44	42	43	41	44	42
	Cr	223	263	233	217	256	228	192
	V	236	226	279	240	239	231	235
	Nb	10	4	10	8	6	5	8
	Z	91	71	76	116	77	79	95
	Y	23	23	22	22	22	23	22
	Sr	297	482	997	407	547	406	771
	Rb	39	29	77	84	73	76	63
	Ce	19	19	15	21	15	15	25
	Nd	12	14	11	12	9	9	14
	La	10	9	8	10	9	7	11
Colour		Grey	Grey	Grey	Grey	Grey	Grey	
Amygdales		White	White	White	White	White	White	
Other								

Table IIa Continued:

Sample		**WE1-70**	**WE1-71**	**RSQ-03**	**RSQ-10**	**FN1-03**	**FN1-04**	**FN1-05**
Major Elements								
(wt%)	**SiO2**	48.94	49.45	47.19	49.34	49.31	48.91	49.63
	TiO2	1.02	1.01	0.90	0.98	1.06	1.04	0.84
	Al2O3	13.88	14.22	13.94	14.67	12.26	14.30	13.63
	FeO*	10.50	10.37	9.25	9.43	11.14	9.58	8.90
	MnO	0.16	0.11	0.15	0.14	0.20	0.13	0.13
	MgO	6.61	6.14	7.05	6.57	7.23	6.68	6.83
	CaO	8.93	6.06	8.92	9.25	6.39	5.12	4.86
	Na2O	1.87	1.64	2.61	1.58	2.86	3.02	1.21
	K2O	3.94	4.92	3.15	2.34	3.95	3.74	6.58
	P2O5	0.17	0.16	0.18	0.19	0.19	0.19	0.14
	LOI	6.35	6.64	5.75	3.27	5.09	5.66	6.25
	H2O	0.44	1.34	0.89	2.16	1.3	2.08	2.58
	total**	102.80	102.07	99.98	99.92	100.99	100.43	101.58
Trace Elements								
(ppm)	**Zn**	89	88	83	85	105	91	80
	Cu	101	45	86	96	69	85	111
	Ni	111	61	81	56	104	55	72
	Co	45	39	41	41	50	43	41
	Cr	157	174	342	171	372	148	307
	V	278	245	253	236	287	276	279
	Nb	7	8	6	10	6	9	4
	Z	97	101	75	99	107	105	74
	Y	24	25	23	25	29	26	23
	Sr	422	348	412	283	82	238	641
	Rb	83	54	96	30	37	64	67
	Ce	23	20	15	26	20	21	16
	Nd	14	13	11	15	14	13	10
	La	10	11	8	12	11	10	6
Colour		Grey	Red	Grey	Grey	Red	Dk Grey	Purple
Amygdales		White	White	White	White	White	White	Green
Other								

Table IIa Continued:

Sample		**FN1-07**	**FN3-15**	**FN3-18**	**FN3-19**	**FN3-20**	**MK1-50**	**MK1-53**
Major Elements								
(wt%)	**SiO2**	49.14	47.82	46.64	43.13	49.61	50.04	50.03
	TiO2	0.94	0.93	0.86	0.88	1.03	1.56	1.67
	Al2O3	14.32	14.86	14.07	12.85	14.07	11.55	12.24
	FeO*	9.83	8.74	8.39	8.44	9.14	11.21	12.82
	MnO	0.08	0.13	0.14	0.20	0.15	0.13	0.15
	MgO	5.50	8.02	6.11	8.45	6.37	3.83	3.95
	CaO	5.17	9.69	10.33	7.29	5.58	5.19	4.69
	Na2O	1.13	1.40	2.05	1.13	2.32	3.01	4.92
	K2O	6.70	1.02	3.54	6.70	6.20	5.88	2.27
	P2O5	0.17	0.17	0.17	0.19	0.19	0.28	0.23
	LOI	5.23	5.44	7.57	10.10	5.16	6.74	5.61
	H2O	2.84	2.55	0.63	0.97	0.6	0.7	0.63
	total**	101.06	100.79	100.52	100.34	100.41	100.13	99.23
Trace Elements								
(ppm)	**Zn**	77	75	62	72	86	105	117
	Cu	71	76	78	87	79	157	197
	Ni	60	96	65	57	54	25	45
	Co	40	43	39	35	40	38	41
	Cr	150	292	231	265	286	25	8
	V	235	235	220	238	233	405	494
	Nb	7	10	10	9	10	22	14
	Z	94	91	83	80	95	159	174
	Y	25	23	22	22	25	35	39
	Sr	141	219	321	323	205	390	698
	Rb	78	10	27	76	31	126	76
	Ce	18	26	21	21	21	41	38
	Nd	11	14	12	13	12	23	24
	La	9	12	9	10	10	17	21
Colour		Grey	Grey	Grey	Grey	Grey	Grey	Grey
Amygdales		White				White	White	White
Other			Vesicular Core Smpl	Core Smpl	Calcite vein Core Smpl	Core Smpl		

Table IIa Continued:

Sample		MK1-54	MK1-55	FS1-11	PP-30	PP-31	PP-32	PP-33*
Major Elements								
(wt%)	**SiO2**	47.52	52.14	47.57	46.78	46.28	45.09	35.92
	TiO2	1.58	1.87	0.94	0.89	0.91	0.83	0.77
	Al2O3	11.58	11.86	15.63	14.45	15.11	13.68	11.52
	FeO*	12.60	12.54	9.94	9.26	9.66	9.05	8.07
	MnO	0.19	0.13	0.14	0.14	0.18	0.16	0.16
	MgO	4.38	3.12	5.93	7.56	9.74	6.93	7.75
	CaO	7.46	3.19	7.16	9.29	7.26	12.06	17.81
	Na2O	4.66	4.61	4.38	3.07	4.09	4.28	3.62
	K2O	1.02	3.78	1.50	1.95	0.98	1.84	0.99
	P2O5	0.21	0.31	0.17	0.15	0.14	0.22	0.52
	LOI	7.51	4.79	6.14	6.13	7.06	5.94	12.09
	H2O	0.26	0.4	1.11	0.36	0.4	0.2	0.34
	total**	98.99	98.74	100.61	100.02	101.82	100.29	99.57
Trace Elements								
(ppm)	**Zn**	106	113	87	62	91	82	80
	Cu	160	98	55	91	89	77	79
	Ni	28	22	60	76	81	69	72
	Co	41	38	45	41	45	42	41
	Cr	9	39	155	305	276	308	285
	V	467	442	263	237	218	242	331
	Nb	17	14	7	6	6	12	26
	Z	168	191	94	79	81	72	67
	Y	39	40	23	23	24	27	25
	Sr	583	5363	281	632	600	1185	4299
	Rb	31	180	22	59	55	46	59
	Ce	38	53	21	16	20	109	132
	Nd	25	31	12	11	14	41	49
	La	19	25	9	8	8	71	87
Colour		Grey	Grey	Red	Grey	Grey	Grey	
Amygdales		White	White	White / Green	White	White		
Other								

*Low SiO2 value, sample not correlated with Karoo Basalts

Table IIa Continued:

Sample		PP-36	UJ1-20	UJ1-22	UJ1-24	UJ1-25	UJ1-26	M3-05
Major Elements (wt%)	**SiO2**	41.59	46.26	46.31	45.66	44.25	41.14	48.08
	TiO2	0.80	0.80	0.86	0.89	0.82	0.80	0.89
	Al2O3	13.58	16.75	14.12	15.11	13.66	11.58	14.28
	FeO*	8.45	8.76	9.28	9.32	9.03	8.50	9.75
	MnO	0.16	0.15	0.15	0.15	0.16	0.16	0.19
	MgO	7.18	6.92	7.36	7.19	7.97	7.90	7.20
	CaO	12.23	10.47	9.55	9.14	9.30	13.65	8.93
	Na2O	5.47	3.98	4.21	4.10	3.83	3.42	1.87
	K2O	0.93	1.42	1.38	1.68	2.00	0.70	1.88
	P2O5	0.26	0.14	0.16	0.18	0.19	0.33	0.18
	LOI	9.41	6.63	6.27	7.46	8.44	10.41	4.58
	H2O	0.42	0.38	0.48	0.48	0.59	0.22	1.09
	Total**	100.49	102.67	100.12	101.36	100.25	98.82	98.92
Trace Elements (ppm)	**Zn**	83	75	85	85	87	86	82
	Cu	84	76	85	102	78	81	88
	Ni	82	80	93	70	90	78	72
	Co	41	43	45	42	43	41	42
	Cr	292	238	296	227	289	268	258
	V	238	210	215	225	216	294	217
	Nb	2	7	6	8	6	2	8
	Z	68	71	73	82	75	67	102
	Y	24	22	22	24	21	20	25
	Sr	5844	1303	862	581	823	7069	1003
	Rb	36	41	41	86	63	30	45
	Ce	50	21	17	22	17	26	25
	Nd	21	12	11	13	10	17	19
	La	37	11	11	14	11	21	11
Colour		Grey	Grey	Grey	Grey	Grey	Grey	Dk Grey
Amygdales		White		White	White	White	White	
Other								

Table IIa Continued:

Sample		**M3-06**	**M4-08**	**M4-09**	**M4-10**	**JG1-14**	**JG1-15**	**JG1-16**
Major Elements (wt%)	**SiO2**	42.55	48.07	49.86	48.03	49.53	49.76	46.75
	TiO2	0.80	0.93	0.88	1.01	0.94	0.90	0.91
	Al2O3	12.31	14.80	14.82	15.58	14.67	15.52	13.83
	FeO*	8.80	8.73	9.52	9.64	8.83	8.86	9.08
	MnO	0.15	0.12	0.17	0.18	0.16	0.16	0.14
	MgO	7.68	6.54	7.84	7.29	6.54	6.90	6.50
	CaO	16.83	7.96	8.78	9.23	10.46	10.54	10.16
	Na2O	1.92	2.24	2.29	1.67	2.32	2.74	3.91
	K2O	0.16	2.78	2.01	2.13	1.61	0.83	1.69
	P2O5	0.56	0.17	0.16	0.19	0.17	0.12	0.15
	LOI	8.28	4.69	3.59	3.69	3.42	2.76	7.35
	H2O	0.5	1.27	0.44	0.82	1.01	0.94	0.4
	total**	100.54	98.29	100.38	99.48	99.66	100.01	100.89
Trace Elements (ppm)	**Zn**	93	64	81	83	80	75	72
	Cu	86	88	96	98	75	98	71
	Ni	77	76	84	97	72	96	70
	Co	39	38	47	44	37	38	38
	Cr	220	247	343	321	242	317	293
	V	350	230	236	233	212	237	234
	Nb	19	12	5	3	10	9	8
	Z	97	104	72	100	83	91	77
	Y	24	24	21	24	22	24	23
	Sr	4205	690	1390	2692	298	290	305
	Rb	15	73	49	41	18	15	48
	Ce	50	26	18	22	23	25	18
	Nd	22	14	12	15	13	14	11
	La	37	12	9	10	11	11	21
Colour		Dk Grey	Grey	Grey	Grey	Dk brown-grey	Dk brown-grey	Dk grey
Amygdales		White	White					White
Other						Strong weathering		

Table IIa Continued:

Sample		JG1-17	JG1-18	JG1-19	JG1-20	JG1-21	JG1-22
Major Elements (wt%)	**SiO2**	49.32	49.22	49.42	49.03	47.62	49.94
	TiO2	0.97	0.85	0.84	0.98	1.19	0.92
	Al2O3	15.89	14.58	14.72	15.28	13.36	15.37
	FeO*	9.58	9.25	8.86	9.53	10.80	9.01
	MnO	0.16	0.15	0.17	0.14	0.17	0.15
	MgO	7.16	7.41	6.82	6.47	5.86	6.99
	CaO	10.53	10.07	10.33	10.70	9.04	10.12
	Na2O	2.75	3.68	2.41	2.56	6.69	2.80
	K2O	0.48	0.77	1.73	0.65	0.82	1.49
	P2O5	0.14	0.12	0.11	0.17	0.23	0.14
	LOI	2.43	3.57	3.50	2.91	4.95	2.91
	H2O	1.23	0.67	1.4	1.4	0.77	0.59
	total**	100.64	100.36	100.30	99.83	101.52	100.44
Trace Elements (ppm)	**Zn**	86	81	79	81	102	70
	Cu	92	90	178	105	105	96
	Ni	99	81	115	78	46	96
	Co	44	45	44	43	37	40
	Cr	321	337	335	234	109	296
	V	265	221	231	210	266	229
	Nb	6	4	4	11	11	9
	Z	82	73	68	87	109	94
	Y	25	23	21	23	30	25
	Sr	309	263	317	329	141	879
	Rb	6	16	16	13	37	25
	Ce	14	15	13	25	256	21
	Nd	10	11	10	15	17	15
	La	8	7	7	11	10	10
Colour		V. Dk grey	Dk grey	Grey	Dk grey	Dk grey	Dk grey-green
Amygdales			White			White	
Other							

Table IIa Continued:

Sample		**JG1-23**	**KV-100**	**KV-101**	**KV-102**	**KV-103**	**KV-105**
Major Elements							
(wt%)	**SiO2**	50.44	48.19	47.48	47.04	48.81	45.25
	TiO2	0.99	0.83	1.01	0.91	0.91	0.90
	Al2O3	15.54	14.58	15.15	14.17	14.91	14.46
	FeO*	9.73	9.29	10.37	10.04	9.53	9.63
	MnO	0.18	0.15	0.18	0.17	0.16	0.18
	MgO	7.11	6.64	7.00	9.80	7.30	9.18
	CaO	10.44	10.30	8.07	7.58	8.77	9.61
	Na2O	2.50	2.70	3.88	1.85	3.19	2.16
	K2O	0.55	1.91	1.62	2.30	1.09	1.03
	P2O5	0.14	0.14	0.18	0.16	0.15	0.17
	LOI	2.63	4.88	5.55	6.98	4.68	7.73
	H2O	0.55	0.68	1.27	0.39	1.56	0.37
	total**	100.80	100.30	101.75	101.38	101.07	100.67
Trace Elements							
(ppm)	**Zn**	84	76	85	86	83	84
	Cu	102	92	108	96	81	91
	Ni	132	80	59	57	82	64
	Co	49	43	41	40	42	43
	Cr	336	187	149	230	276	175
	V	250	207	244	248	215	226
	Nb	6	6	8	8	6	8
	Z	84	84	102	102	85	89
	Y	24	22	26	25	24	23
	Sr	271	299	293	394	353	384
	Rb	9	25	26	41	21	21
	Ce	18	22	23	20	17	18
	Nd	14	13	14	15	14	14
	La	8	9	10	9	10	14
Colour		Grey	Grey	Grey	Grey	Grey	Grey
Amygdales			White	White	White	White	White
Other							

Table IIa Continued:

Sample		**BF2-28**	**BF2-29**	**BF2-30**	****BF2-31**	**DB2-36**	**DB2-37**
Major Elements (wt%)	**SiO2**	42.96	44.13	46.04	49.99	46.58	53.04
	TiO2	1.29	1.19	1.04	1.01	1.12	1.14
	Al2O3	16.03	15.02	14.07	15.34	14.62	14.84
	FeO*	10.16	11.53	9.67	9.59	10.78	10.87
	MnO	0.18	0.20	0.06	0.18	0.16	0.22
	MgO	5.77	5.53	7.89	7.17	5.15	5.41
	CaO	3.17	4.83	5.37	10.26	5.11	2.08
	Na2O	5.56	4.44	1.60	2.98	4.67	2.05
	K2O	0.47	1.38	3.76	0.95	2.16	5.00
	P2O5	0.26	0.27	0.36	0.15	0.24	0.24
	LOI	8.74	8.65	7.51	2.99	7.49	4.95
	H2O	2.56	1.2	1.05	0.78	1.47	0.89
	total**	97.14	98.39	98.41	101.38	99.56	100.74
Trace Elements (ppm)	**Zn**	118	140	92	92	94	123
	Cu	31	28	17	94	33	57
	Ni	126	138	118	73	129	133
	Co	51	61	53	40	58	55
	Cr	33	43	29	31	31	29
	V	190	192	168	254	186	181
	Nb	10	9	8	8	9	8
	Z	210	197	168	80	185	194
	Y	26	26	21	24	22	24
	Sr	265	318	203	340	179	273
	Rb	48	55	65	21	67	91
	Ce	49	40	51	20	36	40
	Nd	27	22	28	13	22	23
	La	20	20	24	10	15	17
Colour		Lt Grey	Lt Grey	Lt Grey	Grey	Lt Grey	Lt Grey
Amygdales		White	White	White		White	White
Other							

**Karoo dolerite, for comparison purposes

Table IIb: Basalt Xenoliths Correlations

Sample	Correlation	Sample	Correlation
MW1-03	Mafika Lisiu	FS1-11	Maloti / Senqu / Mothae
MW1-05	Mafika Lisiu	PP-30	Mafika Lisiu
MW1-10	Maloti / Senqu / Mothae	PP-31	Mafika Lisiu
MW1-11	Maloti / Senqu / Mothae	PP-32	Mafika Lisiu
V1-02	Mothae or Oxbow	PP-33	Not Correlated
V1-03	Maloti / Senqu / Mothae	PP-36	Mafika Lisiu
V1-04	Maloti / Senqu / Mothae	UJ1-20	Mafika Lisiu
V1-05	Mothae or Oxbow	UJ1-22	Mafika Lisiu
V2-10	Maloti / Senqu / Mothae	UJ1-24	Mafika Lisiu
V6-19	Maloti / Senqu / Mothae	UJ1-25	Mafika Lisiu
V6-20	Mothae or Oxbow	UJ1-26	Mafika Lisiu
V6-21	Maloti / Senqu / Mothae	M3-05	Maloti / Senqu / Mothae
RV1-18	Maloti / Senqu / Mothae	M3-06	Maloti / Senqu / Mothae
RV1-19	Maloti / Senqu / Mothae	M4-08	Maloti / Senqu / Mothae
RV1-21	Maloti / Senqu / Mothae	M4-09	Mafika Lisiu
RV1-22	Mafika Lisiu	M4-10	Mafika Lisiu
WE1-60	Mafika Lisiu	JG1-14	Mafika Lisiu
WE1-61	Mafika Lisiu	JG1-15	Maloti / Senqu / Mothae
WE1-62	Mafika Lisiu	JG1-16	Mafika Lisiu
WE1-63	Mafika Lisiu	JG1-17	Mafika Lisiu
WE1-64	Mafika Lisiu	JG1-18	Mafika Lisiu
WE1-70	Maloti / Senqu / Mothae	JG1-19	Mafika Lisiu
WE1-71	Maloti / Senqu / Mothae	JG1-20	Mafika Lisiu
RSQ1-03	Mafika Lisiu	JG1-21	Maloti / Senqu / Mothae
RSQ1-10	Mafika Lisiu	JG1-22	Maloti / Senqu / Mothae
FN1-03	Mafika Lisiu	JG1-23	Mafika Lisiu
FN1-04	Mafika Lisiu	KV-100	Maloti / Senqu / Mothae
FN1-05	Maloti / Senqu / Mothae	KV-101	Maloti / Senqu / Mothae
FN1-07	Mafika Lisiu	KV-102	Mafika Lisiu – Maloti/Senqu
FN3-15	Maloti / Senqu / Mothae	KV-103	Mafika Lisiu
FN3-18	Maloti / Senqu / Mothae	KV-105	Mafika Lisiu
FN3-19	Maloti / Senqu / Mothae	BF2-28	Ventersdorp (Allanridge Formation)
FN3-20	Maloti / Senqu / Mothae	BF2-29	Ventersdorp (Allanridge Formation)
MK1-50	Evolved Karoo	BF2-30	Ventersdorp (Allanridge Formation)
MK1-53	Evolved Karoo	BF2-31	Karoo Dolerite
MK1-54	Evolved Karoo	DB2-36	Ventersdorp (Allanridge Formation)
MK1-55	Evolved Karoo	DB2-37	Ventersdorp (Allanridge Formation)

APPENDIX III: EROSION ESTIMATES

Table IIIa: Documented thickness and thinning rates of the KSG, utilized for method 1.

		Minimum	Maximum	Thinning Rate	Projected
Drakensberg Group (Lesotho Formation)*		700 m	1400 m[19]		Kimberley : 700 m[20]
	MSM	500 m	1000 m[1]		
	ML	200 m	400 m[1]		
'Stormberg' Group		200 m[21]	1100 m[3]	Molteno: 3-7 m/km[3]	
Beaufort Group		700 m[22]	7000 m[4]		Kimberley: 550 m[2] Finsch: 300 m[23]
	Tarkastad Subgroup	850 m	1900 m	6.5 m/km	
	Adelaide Subgroup	800 m	5000 m	20 m/km	
Ecca Group		900 m[24]	3000 m[6]	4-5 m/km[6]	Kimberley: 300 m[2] Finsch: 600 m[5]
Dwyka Group		~50 m[25]	800 m		Kimberley: 100 m
Total (no basalts)		1850 m	11900 m		Kimberley: 1900 m Koffiefontein: 2200 m
Total		2750 m	13700 m		

*Note: The thickness of the Lesotho Formation is only considered as the lavas of the Barkly East Formation are considered localized flows. Minimum thickness arbitrarily taken as ½ thickness of the Lesotho Remnant, thickness of the MSM units is estimated based on Marsh *et al.* (1997).

[19] Marsh *et al.,* 1997
[20] Hawthorne, 1975
[21] Visser, 1984; Johnson, 1991; 1994; Veevers *et al.,* 1994
[22] Johnson, 1976; 1994; Veevers *et al.,* 1994
[23] Visser, 1972
[24] Johnson, 1976; 1994; Johnson *et al.,* 1996
[25] Visser *et al.,* 1976-77; Visser *et al.,* 1990; Johnson, 1991; Johnson, 1994

Table IIIb: Erosion Estimates based on Method 1

Kimberlite	Country Rock	Youngest Stratigraphic Unit Represented by Xenoliths	Groups Present at the Time of Kimberlite Emplacement	Minimum Thickness	Maximum Thickness	Average Thickness
Melton Wold	Beaufort (basal)	Lesotho Formation	Beaufort, Lesotho	1500 m	8400 m	5000 m
Voorspoed	Ecca (middle)	Lesotho Formation	Upper Ecca, Beaufort, 'Stormberg', Lesotho	2150 m	11000 m	6575 m
Roberts Victor	Ecca (lower)	Lesotho Formation	Ecca, Beaufort, Lesotho	2400 m	11400 m	6900 m
West End	Transvaal Supergroup	Lesotho Formation	Complete Succession	2650 m	13300 m	7975 m
Record Stone Quarry	Ecca (basal)	Mafika Lisiu unit	Ecca, Beaufort, Mafika Lisiu	1800 m	10400 m	6100 m
Finsch	Transvaal Supergroup	Lesotho Formation	Complete Succession	2650 m	13300 m	7975 m
Markt	Ecca (basal)	Lesotho Formation	Ecca, Beaufort, Lesotho	2400 m	11400 m	6900 m
Frank Smith	Ecca (basal)	Lesotho Formation	Ecca, Beaufort, Lesotho	2400 m	11400 m	6900 m
Pampoenpoort	Ecca (upper)	Mafika Lisiu unit	Upper Ecca, Beaufort, Mafika Lisiu	1400 m	8900 m	5150 m
Uintjiesberg	Ecca (middle)	Mafika Lisiu unit	Upper Ecca, Beaufort, Mafika Lisiu	1500 m	8900 m	5200 m
Koffiefontein	Ecca (middle)	Adelaide Subgroup	Upper Ecca, Beaufort	1150 m	8500 m	4825 m
Monastery	Molteno (upper)	Lesotho Formation	Elliot, Clarens, Lesotho	850 m	2200 m	1525 m
Jagersfontein	Ecca (upper)	Lesotho Formation	Beaufort, Lesotho	1500 m	8400 m	4950 m
Kaal Vallei	Ecca (upper)	Lesotho Formation	Beaufort, Lesotho	1500 m	8400 m	4950 m
KKC	Ecca / Dwyka Contact	Adelaide Subgroup	Ecca, Beaufort	1600 m	10000 m	5800 m

Table IIIc: Erosion Estimates based on Method 1 and Extrapolated Thinning Rates

Kimberlite	**Ecca**			**Beaufort**			**'Stormberg'**		**Drakensberg****		**Min**	**Max**	Avg
	Min	Max	Value*	Min	Max	Value*	Min	Max	Min	Max			
Melton Wold		900 m[2, 5]	0	350 m[8]	1000 m[9]		0 m	0 m	700 m	1400 m	1050 m	2400 m	1725 m
Voorspoed		300 m[2]	0	180 m[1]	700 m[7]		50 m	200 m	700 m	1400 m	930 m	2300 m	1615 m
Roberts Victor		450 m[2]	400 m			650 m[8]	0 m	0 m	700 m	1400 m	1750 m	2450 m	2100 m
West End		600 m[2, 3]	600 m			300 m[3]	0 m	0 m	700 m	1400 m	1600 m	2300 m	1950 m
RSQ	300 m[4]	750 m[2]				550 m[4]	0 m	0 m	200 m	400 m	1050 m	1700 m	1375 m
Finsch			600 m[2, 3]			300 m[3]	0 m	0 m	700 m	1400 m	1600 m	2300 m	1950 m
Markt			800 m[2]	325 m[8]	1000 m[9]		0 m	0 m	700 m	1400 m	1825 m	3200 m	2510 m
Frank Smith			700 m[2]			450 m[8]	0 m	0 m	700 m	1400 m	1950 m	2950 m	2450 m
Pampoenpoort		700 m[2]	0	350 m[8]	1000 m[9]		0 m	0 m	200 m	400 m	550 m	1400 m	975 m
Uintjiesberg		700 m[2]	350 m	350 m[8]	1000 m[9]		0 m	0 m	200 m	400 m	900 m	1750 m	1325 m
Koffiefontein	300 m[5]	650 m[2]	650 m			700 m[8]	0 m	0 m	0 m	(6)			1350 m
Monastery		200 m[2,5]	0	~700 m[7]		0	200 m	300 m	700 m	1400 m	900 m	1700 m	1300 m
Jagersfontein		700 m[2]	0			750 m[8]	0 m	0 m	700 m	1400 m	1450 m	2150 m	1800 m
Kaal Vallei		250 m[2]	0	440 m[1]	700 m[1,7]		0 m	0 m	700 m	1400 m	1140 m	2100 m	1620 m
KKC	300 m[4]	750 m[2]				550 m[4]	0 m	0 m	0 m	(6)	850 m	1300 m	1075 m
Lushof		650 m[2]	250 m			350 m[8]	0 m	0 m	0 m	0 m		900 m	
Britstown Cluster		750 m[2]	0			375 m[8]	0 m	0 m	0 m	0 m		1125 m	
Hebron		700 m[2]	0			350 m[8]	0 m	0 m	0 m	0 m		1050 m	
Lovedale		750 m[2]	0			350 m[8]	0 m	0 m	0 m	0 m		1050 m	

*Thickness of the Group – value used for erosion estimate as it accounts for the present preserved thickness of the Group (estimated based on Ryan (1968) or relative position within Group), or is based on previous estimates, if empty, max and min values are used

** Minimum value for Drakensberg Group taken as just less than half of the thickness of the Lesotho Remnant, likely an overestimated value

[1] Based on thinning rates of Johnson, 1976; 1994; Johnson *et al.,* 1996

[2] Based on isopach studies of Ryan, 1968, isopachs include upper Dwyka + Ecca, therefore values are an overestimate of Ecca thickness

[3] Based on Visser, 1970

[4] Based on Hawthorne, 1975

[5] Present preserved thickness of the Group at this location

[6] Assuming Karoo basalt xenoliths were present in the upper levels of the kimberlite, the basalt layer was likely a thin veneer less than 100 m thick.

[7] Located near northern end of the basin, therefore thickness assumed to be equivalent to Johnson's (1976)

[8] Based on 1.5 m/km, E-W thinning rate inferred from Visser (1970) and Hawthorne (1975)

[9] E-W thinning rate in the southern part of the basin taken as 10 m/km (1/2 the documented SW-NE rate) for comparison with other rate (8)

Table IIId: Erosion Estimates based on Method 2

Kimberlite	Elevation (m asl)*	Country Rock	Youngest Stratigraphic Unit Represented by Xenoliths	Min Erosion	Max Erosion	Estimate
Melton Wold	1340	Adelaide (Abrahamskraal)	MSM Basalts	560 m	1660 m	1110 m
Voorspoed	1410	Ecca (Volksrust)	Mothae Basalts	490 m	1590 m	1040 m
Roberts Victor	1260	Ecca (Tierberg) / Dwyka	MSM Basalts	640 m	1740 m	1190 m
West End	1330		MSM Basalts	570 m	1740 m	1155 m
Record Stone Quarry	1220	Ecca (Prince Albert)	MSM Basalts	680 m	1080 m	880 m
Finsch	1550	Griqualand West Sequence	MSM Basalts	350 m	1450 m	900 m
Markt	1030	Ecca (Prince Albert)	Evolved Lesotho Basalts	870 m	1970 m	1420 m
Frank Smith	1080	Ecca (Prince Albert)	MSM Basalts	820 m	1920 m	1370 m
Pampoenpoort	1270	Ecca (Carnarvon, upper – Adelaide Contact)	Mafika Lisiu Basalts	630 m	1030 m	830 m
Uintjiesberg	1310	Ecca (Tierberg, upper)	Mafika Lisiu Basalts	590 m	990 m	790 m
Koffiefontein	1230	Ecca (Tierberg, upper)	Tarkastad Subgroup Sandstones	70 m	670 m	370 m
Monastery	1590	Molteno (upper)	MSM Basalts	310 m	1410 m	860 m
Jagersfontein	1410	Ecca (Tierberg) / Adelaide	MSM Basalts	490 m	1590 m	1040 m
Kaal Vallei	1360	Ecca / Adelaide	MSM Basalts	540 m	1640 m	1090 m
KKC	1230	Ecca / Dwyka	Tarkastad Subgroup Sandstones	120 m	670 m	395 m
Lushof	1150	Ecca	? Karoo Sedimentary Unit		750 m[26]	
Britstown Cluster	1120	Ecca			780 m[2]	
Hebron	1480	Ecca			420 m[2]	
Lovedale	1140	Ecca			760 m[2]	

* Elevation obtained from GPS readings and De Beers database (unpubl.).

[26] It is difficult to put a lower constraint on the erosion estimates for the LBH pipes because no sandstone xenoliths were analyzed, thus only a maximum value is estimated

REFERENCES

Allsopp, H.L. and Barrett, D.R. (1975). Rb-Sr age determinations on South African kimberlite pipes. *Physics and Chemistry of the Earth*, 9, 605-617.

Bangert, B., Stollhofen, H., Lorenz, V., Armstrong, R. (1999). The geochronology and significance of ash-fall tuffs in the glaciogenic Carboniferous-Permian Dwyka Group of Namibia and South Africa. *Journal of African Earth Sciences*, 29, 33-49.

Becker, G.F. (1904). Determination of rocks surrounding the Diamond pipes of Kimberley, South Africa. *In:* Reports on Determination of Rocks, Kimberley Diamond Mines, 1902-1905.

Beukes, N.J., (1970). Stratigraphy and sedimentology of the Cave Sandstone Stage, Karoo System. *In*: Haughton, S.H. (ed.), Proceedings of the 2nd IUGS Symposium on Gondwana Stratigraphy, 321-328.

Bordy, E.M., Hancox, P.J., Rubidge, B.S. (2004). Provenance study of the Late Triassic – Early Jurassic Elliot Formation, main Karoo Basin, South Africa. *South African Journal of Geology*, 107, 587-603.

Bordy, E.M., Hancox, P.J., Rubidge, B.S. (2005). The contact of the Molteno and Elliot formations through the main Karoo Basin, South Africa: a second order-sequence boundary. *South African Journal of Geology*, 108, 351-364.

Bowen, T.B., Julian, S.M., Bowen, M.P. and Eales, H.V. (1986). Volcanic rocks of the Wiwatersrand Triad, South Africa I: description, classification and geochemical stratigraphy. *Precambrian Research*, 31, 297-324.

Brown, R.W., Gallagher, K., Griffin, W.L., Ryan, C.G., de Wit, M.C.J., Belton, D.X., Harman, R. (1998). Kimberlites, accelerated erosion and evolution of the lithospheric mantle beneath the Kaapvaal craton during the mid-Cretaceous. *7th International Kimberlite Conference - Extended Abstracts*, 105-107.

Brown, R.W., Summerfield, M.A., Gleadow, J.W. (2002). Denudation history along a transect across the Drakensberg Escarpment of southern Africa derived from apatite fission track thermochronology. *Journal of Geophysical Research,* 107, 1-18.

Catuneanu, O. (2004). Retroarc foreland systems – evolution through time. *Journal of African Earth Sciences*, 38, 225-242.

Catuneanu, O, and Elango, H.N. (2001). Tectonic controls on fluvial styles: the Balfour Formation of the Karoo Basin, South Africa. *Sedimentary Geology,* 140, 291-313.

Catuneanu, O., Hancox, P.J. and Rubidge, B.S. (1998). Reciprocal flexural behaviour and contrasting stratigraphies: a new basin development model for the Karoo retroarc foreland system, South Africa. *Basin Research*, 10, 417-439.

Catuneanu, O., Hancox, P.J., Cairncross, B. and Rubidge, B.S. (2002). Foredeep submarine fans and forebulge deltas: orogenic offloading in the underfilled Karoo Basin. *Journal of African Earth Sciences,* 35, 489-502.

Catuneanu, O., Wopfner, H., Eriksson, P.G., Cairncross, B., Rubidge, B.S., Smith, R.M.H, Hancox, P.J. (2005). The Karoo basins of south-central Africa. *Journal of African Earth Sciences*, 43, 211-253.

Clement, C.R.(1975). The emplacement of some diatreme facies kimberlites, *Physics and Chemistry of the Earth* 9, 51–59.

Clement, C.R., (1982). A comparative geological study of some major kimberlite pipes in northern Cape and Orange Free State. PhD thesis (unpubl.), University of Cape Town, South Africa, 432 pp.

Clement, C.R. and Reid, A.M. (1989). The origin of kimberlite pipes: an interpretation based on the synthesis of geological features displayed by southern African occurrences. *In:* Ross, J., Jaques, A.L., Fergusan, J., Green, D.H., O'Reilly, S.Y., Danchin, R.V. and Janse, A.J.A. (Eds.), Kimberlites and Related Rocks, *Geological Society of Australia*, 14, 632–646.

Cole, D.I. (1992). Evolution and development of the Karoo Basin. *In*: de Wit, M.J., Ransome, I.G.D. (Eds.), Inversion Tectonics of the Cape Fold Belt, Karoo and Cretaceous Basins of Southern Africa. *A.A. Balkema, Rotterdam*, 87-89.

Davis, G.L. (1977). The ages and uranium contents of zircons from kimberlites and associated rocks. *Annual Report of the Director Geophysical Laboratory,* Carnegie Institution, 613-635.

Dawson, J.B. (1971). Advances in kimberlite geology, *Earth Science Reviews* 7, 187–214.

Dawson, J.B. (1980). Kimberlites and their Xenoliths. *Springer-Verlag, Berlin, Heidelberg, New York*, 255 pp.

Dickinson, W.R., Beard, L.S., Brakenridge, G.R., Erjavec, J.L., Ferguson, R.C., Inman, K.F., Knepp, R.A., Lindberg, F.A. and Ryberg, P.T. (1983). Provenance of North American Phanerozoic sandstones in relation to tectonic setting. *Bulletin of the Geological Society of America,* 94, 222-235.

Duncan, A.R., Erlank, A.J., Betton, P.J. (1984a). Appendix I: Analytical techniques and database descriptions. *Geological Society of South Africa, Special Publication*, 13, 389-395.

Duncan, A.R., Erlank, A.J. and Marsh, J.S. (1984b). Regional geochemistry of the Karoo igneous province. *Geological Society of South Africa, Special Publication*, 13, 355-388.

Duncan, R.A., Hooper, P.R., Rehacek, J., Marsh, J.S. and Duncan, A.R. (1997). The timing and duration of the Karoo igneous event, southern Gondwana. *Journal of Geophysical Research*, 102, 127-138.

Dunn, E.J. (1874). On the mode of occurrences of diamonds in South Africa. *QJGS*, 54-59.

Du Toit, A.L. (1906). Geological Survey of the Eastern Portion of Griqualand West. *11th Report of the Geological Commission, Cape Colony,* 89-176.

Du Toit, A.L. (1954). The Geology of South Africa, 3rd ed. *Oliver and Boyd, Edinburgh*, 611 pp.

Eales, H.V., Marsh, J.S. and Cox, K.G. (1984). The Karoo Igneous Province: an introduction. *Geological Society of South Africa, Special Publication*, 13, 1-26.

Edwards, R. (2005). Kimberley pipes, 4th Revision. De Beers Correspondence (unpubl.), Johannesburg, South Africa, 15 pp.

Encarnación, J., Fleming, T.H., Elliot, H. and Eales, H.V. (1996). Synchronous emplacement of Ferrar and Karoo dolerites and the early break-up of Gondwana. *Geology*, 24, 535-538.

Eriksson, P.G. (1984). A palaeoenvironmental study of the Molteno, Elliot and Clarens Formations in the Natal Drakensberg and northeastern Orange Free State. PhD thesis (unpubl.), University of Natal, South Africa, 209 pp.

Eriksson, P.G. (1985). The depositional environment of the Elliot Formation in the Natal Drakensberg and northeastern Orange Free State. *Transactions of the Geological Society of South Africa*, 88, 19-26.

Eriksson, P.G. (1986). Aeolian dune and alluvial fan deposits in the Clarens Formation of the Natal Drakensberg. *Transactions Geological Society of South Africa,* 80, 389–393.

Eriksson, P.G. (1987). A note on the red colouration in sedimentary rocks of the Molteno, Elliot and Clarens formations. *Annual Report of the Geological Survey of South Africa*, 21, 89-94.

Erlank, A.J., Marsh, J.S., Duncan, A.R., Miller, R.M.G., Hakesworth, C.J., Betton, P.J. and Rex, D.C. (1984). Geochemistry and petrogenesis of the Etendeka volcanic rocks from SWA/Namibia. *Geological Society of South Africa, Special Publications,* 13, 195-249.

Fiedler, K. and Adelmann, D. (1998). Provenance of Late Permian sediments of the Laingsburg subbasin (SW Karoo Basin, South Africa). *Journal of African Earth Sciences*, 27, Addendum, 3-4.

Field, M. and Scott Smith, B.H. (1999a). Textural and genetic classification schemes for kimberlites: a new perspective, *Proceedings of the 7th International Kimberlite Conference,* 1, 214–216.

Field, M. and Scott Smith, B.H. (1999b). Contrasting geology and near-surface emplacement of kimberlite pipes in southern Africa and Canada, *Proceedings of the 7th International Kimberlite Conference,* 1, 217–237.

Fitch, F.J. and Miller, J.A. (1984). Dating Karoo igneous rock by the conventional K-Ar and 40Ar/39Ar age spectrum methods. *Geological Society of South Africa, Special Publication*, 13, 247-266.

Galehouse, J.S. (1971). Point counting. *In*: Carver, R.E. (Ed.), Procedures in Sedimentary Petrology. *Wiley Interscience, New York*, 385-407.

Gauffre, F.X. (1993). Biostratigraphy of the Lower Elliot Formation (Southern Africa), and preliminary results on the Maphutseng dinosaur (Saurischia: Prosauropoda from the same Formation of Lesotho. *In*: S.G. Lucas and M. Morales (Eds.), The Nonmarine Triassic, Bulletin of the New Mexico Museum of Natural History, 3, 147-150.

Goddard, E.N., Trask, P.D., De Ford, R.K., Rove, O.N., Singewald, J.T. and Overbeck, R.M. (1970). Rock Color Chart. *Geological Society of America, Boulder, Colorado*.

Hancox, P.J. (1998). Stratigraphic, sedimentological and palaeoenvironmental synthesis of the Beaufort-Molteno contact in the Karoo Basin. PhD thesis (unpubl.), University of the Witwatersrand, South Africa, 380 pp.

Harger, H.S. (1905). The diamond pipes and fissures of South Africa. *Transactions of the Geological Society of South Africa,* VIII, 110-134.

Harger, H.S. (1909). The occurrence of diamonds in Dwyka conglomerate and amygdaloidal lavas; and the origin of Vaal River diamonds. *Transactions of the Geological Society of South Africa,* 139-158.

Harger, H.S. (1913). Some Features associated with the Denudation of the South African Continent. *Annual Proceedings of the Geological Society of South Africa*, XXII-XXXIX.

Harris, C., Marsh, J.S., Duncan, A.R. and Conrey, R.M. (1990). The petrogenesis of the Kirwan basalts of Dronning Maud Land, Antarctica. *Journal of Petrology,* 31, 341-369.

Hawthorne, J.B. (1975). Model of a kimberlite pipe, *Physics and Chemistry of the Earth,* 9, 1–15.

Haycock, C.A., Mason, T.R., Watkeys, M.K. (1997). Early Triassic palaeoenvironements in the eastern Karoo Foreland Basin, South Africa. *Journal of African Earth Sciences*, 24 (1/2), 79-94.

Herbert (2004). The geology of the Letseng Kimberlite. BSc Honours thesis (unpubl.), Rhodes University, South Africa, 76 pp.

Ingersoll, R.V., Bullard, T.F., Ford, R.I., Grimm, J.P., Pickle, J.D. and Sares, S.W. (1984). The effect of grain size on detrital modes: a test of the Gazzi-Dickinson point-counting method. *Journal of Sedimentary Petrology,* 54, 103-116.

Johnson, M.R. (1976). Stratigraphy and sedimentology of the Cape and Karoo sequences in the Eastern Cape Province. PhD Thesis (unpubl.), Rhodes University, South Africa, 276 pp.

Johnson, M.R. (1991). Sandstone petrography, provenance and plate tectonic setting in Gondwana context of the southeastern Cape – Karoo Basin. *South African Journal of Geology*, 94, 137-145.

Johnson, M.R. (Editor)(1994). The Lexicon of South African Stratigraphy. Part 1: Phanerozoic Units. *Geological Survey of South Africa Handbook,* 56 pp.

Johnson, M.R., Van Vuuren, C.J., Hegenberger, W.F., Key, R., and Shoko, U. (1996). Stratigraphy of the Karoo Supergroup in southern Africa: an overview. *Journal of African Earth Sciences*, 23, 3-15.

Kingsley, C.S. (1977). Stratigraphy and Sedimentology of the Ecca Group in the Eastern Cape Province, South Africa. PhD Thesis (unpubl.), University of Port Elizabeth, South Africa, 240 pp.

Kramers, J.D., Roddick, J. C. M. and Dawson, J. B. (1983). Trace element and isotope studies on veined, metasomatic and "MARID" xenoliths from Bultfontein, South Africa. *Earth and Planetary Science Letters,* 65, 90-106.

Le Roex, A.P. and Reid, D.L. (1978). Geochemistry of Karoo dolerite sills in the Calvinia District, Western Cape Province, South Africa. *Contributions Mineralogy Petrology,* 66, 351-360.

Le Roex, A.P., Bell, D.R. and Davis, P. (2003). Petrogenesis of Group I kimberlites from Kimberley, South Africa, Evidence from bulk-rock geochemistry. *Journal of Petrology*, 44, 2261-2286.

Letsale, B.M. (1998). The geology of the Uintjiesburg kimberlite and its xenoliths. BSc Honours Thesis (unpubl.), Rhodes University, South Africa, 64 pp.

Lindgren, W. (1905). Determination of rocks from Kimberley, South Africa. *In*: Reports on Determination of rocks, Kimberley diamond mines, 1902-1905.

Lock, B.E., Paverd, A.L. and Broderick, T.J. (1974). Stratigraphy of the Karoo volcanic rocks of the Barkley East district. *Transactions of the Geological Society of South Africa*, 77, 117-130.

Lorenz, V. (1973). Formation of maar-diatreme volcanoes and its relevance to the formation of kimberlite diatremes. *1st International Kimberlite Conference, Cape Town, South Africa, Extended Abstracts*, 203-205.

Lorenz, V. (1975). Formation of phreatomagmatic maar–diatreme volcanoes and its relevance to kimberlite diatremes, *Physics and Chemistry of the Earth,* 9, 17–29.

Lorenz, V. (1985). Maars and diatremes of phreatomagmatic origin, *Transactions of the Geological Society of South Africa,* 88, 459–470.

Lorenz, V. (1993). On the phreatomagmatic origin of kimberlite and lamproite diatremes. *IAVCEI International Volcanological Congress, Canberra, Australia, Abstracts*.

Lorenz, V., Zimanowski, B., Büttner, R., and Kurszlaukis, S. (1999). Formation of kimberlite diatremes by explosive interaction of kimberlite magma with groundwater: field and experimental aspects, *Proceedings of the 7th International Kimberlite Conference*, 2, 522–528.

Mambali, A.F. (1998). Melton Wold kimberlite: Petrography, geochemistry, xenoliths and model of genesis. BSc Honours thesis (unpubl.), Rhodes University, South Africa, 53 pp.

Marsh, J.S. (1987). Basalt geochemistry and tectonic discrimination within continental flood basalt provinces. *Journal of Volcanology and Geothermal Research,* 32, 35-49.

Marsh, J.S. (1998). Geochemical stratigraphy in basalts of the Mohale Dam – Katse dam areas, Lesotho. Report on Contract LHDA 1009, Mohale Tunnel: Sampling and testing of cores. Lesotho Highlands Tunnel Partnership (Mohale) (unpubl.). Rhodes University, Grahamstown, 21 pp.

Marsh, J.S. and Eales, H.V. (1984). Chemistry and petrogenesis of igneous rocks of the Karoo Central area, southern Africa. *Geological Society of South Africa, Special Publication*, 13, 27-67.

Marsh, J.S., Hooper, P.R., Rehacek, J., Duncan, R.A. and Duncan, A.R. (1997). Stratigraphy and age of Karoo basalts of Lesotho and implications for correlations within the Karoo Igneous Province. *In*: Mahoney, J.J., Coffin, M.F. (Eds.), Large Igneous Provinces: Continental, Oceanic, and Planetary Flood Volcanism. *Geophysical Monograph 100. American Geophysical Union, Washington DC*, 247–272.

Matthews, J.W. (1887). Incwadi Yami, or Twenty Years' Personal Experiences in South Africa. *New York.*

Mitha, V.R. (2006). An insight into magma supply to the Karoo Igneous Province: a geochemical investigation of Karoo dykes adjacent to the northwestern sector of the Lesotho volcanic remnant. MSc thesis (unpubl.), Rhodes University, South Africa, 164 pp.

Mudge, M.R. (1968). Depth control of some concordant intrusions. *Bulletin of the Geological Society of America,* 79, 315-332.

Munsell Soil Color Chart (1971). *Munsell Color Company, INC., Baltimore, Maryland.*

Naidoo, P., Stiefenhofer, J., Field, M. and Dobbe, R. (2004). Recent advances in the geology of the Koffiefontein mine, *Lithos*, 76, 161-182.

Norrish, K. and Hutton. J.T. (1969). An accurate X-ray spectrographic method for the analysis of a wide range of geological samples. *Geochemica et Cosmochimica Acta,* 33, 431-453.

Partridge, T.C. and Maud, R.R. (1987). Geomorphic evolution of southern Africa since the Mesozoic. *South African Journal of Geology,* 90, 179-208.

Pettijohn, F.J., Potter, P.E. and Siever, R. (1987). Sand and Sandstone. *2nd Edition. Springer Verlag, New York, U.S.*A., 553 pp.

Phillips, D., Kiviets, G.B., Barton, E.S., Smith, C.B., Viljoen, K.S., and Fourie, L.F. (1999). $^{40}Ar/^{39}Ar$ dating of kimberlites and related rocks: problems and solutions. *Proceedings of the 7th International Kimberlite Conference*, 2, 677-687.

Rambula, T. (2005). Karoo-age xenoliths in the Kimberley kimberlites – implications for post-Cretaceous erosion in South Africa. BSc Honours thesis (unpubl.), University of the Witwatersrand, South Africa, 34 pp.

Rastall, R.H. (1906). The petrography of the rocks surrounding the diamond-pipes of the Kimberley district. Internal De Beers report (unpubl.), 40 pp.

Riley, T.R., Curtis, M.L., Leat, P.T., Watkeys, M.K., Duncan, R.A., Millar, I.L. and Owens, W.H. (2006). Overlap of Karoo and Ferrar magma types in Kwazulu-Natal, South Africa. *Journal of Petrology*, 47, 541-566.

Roberts. M.A. (1997). The geology of the Voorspoed kimberlite and its xenoliths. BSc Honours thesis (unpubl.), Rhodes University, South Africa, 105 pp.

Robey, J.V.A. (1976). Aspects of the geochemistry of the dolerites and basalts of the northeastern Cape Province, South Africa. M.Sc. thesis (unpubl.), Rhodes University, South Africa, 174 pp.

Robey, J.V.A. (1981). Kimberlites of the central Cape Province, Republic of South Africa. PhD thesis (unpubl.), University of Cape Town, South Africa, 261 pp.

Rogers, A.W. and Du Toit, A.L. (1909). Kimberlite and Allied Pipes and Fissures in Carnarvon and Victoria West. *14th Annual Report of the Geological Commission, Cape Colony,* 98-108.

Rubidge, B.S. (1995). Biostratigraphy of the *Eodicynodon* Assemblage Zone. *In:* Rubidge, B.S. (Ed.), Biostratigraphy of the Beaufort Group (Karoo Supergroup). *SACS Biostratigraphic Series, Council for Geoscience,* Pretoria, South Africa, 1, 3-7.

Rubidge, B.S., Hancox, P.J., Catuneanu, O. (2000). Sequence analysis of the Ecca – Beaufort contact in the southern Karoo of South Africa. *South African Journal of Geology*, 103, 81-96.

Ryan, P.J. (1968). Stratigraphic and Paleocurrent Analysis of the Ecca Series and Lowermost Beaufort Beds in the Karroo Basin of South Africa. PhD Thesis (unpubl.), University of the Witwatersrand, South Africa, 210 pp.

Skinner, E.M.W. and Marsh, J.S. (2004). Distinct kimberlite pipe classes with contrasting eruption processes. *Lithos*, 76, 183-200.

Skinner, E.M.W., Smith, C.B., Viljoen, K.S. and Clark, T.C. (1992). The petrography, tectonic setting and emplacement ages of kimberlites in the southwestern border region of the Kaapvaal Craton, Prieska area, South Africa. *Proceedings of the 5th International Kimberlite Conference*, 80-97.

Smith, C.B. (1990). A review of the stratigraphy and sedimentary environments of the Karoo basin of South Africa. *Journal of African Earth Sciences,* 10, 117-137.

Smith, C.B. and Kitching, J.W. (1997). Sedimentology and vertebrate taphonomy of the *Trytylodon* Acme Zone, a reworked palaeosol in the Lower Jurassic Elliot Formation, Karoo Supergroup, South Africa. *Palaeogeography, Palaeoclimatology, Palaeoecology,* 131, 29-50.

Smith, C.B., Allsopp, H.L., Kramers, J.D., Hutchinson, G., and Roddick, J.C. (1985). Emplacement ages of Jurassic-Cretaceous South African kimberlites by the Rb-Sr method on phlogopite and whole rock samples. *Transactions of the Geological Society of South Africa,* 88, 149-169.

Smith, C.B., Clark, T.C., Barton, E.S., and Bristow, J.W. (1994). Emplacement ages of kimberlite occurrences in the Prieska region, southwest border of the Kaapvaal Craton, South Africa. *Chemical Geology (Isotopic Geosciences Section),* 113, 149-169.

Sparks, R.S.J., Baker, L., Brown, R.J., Field, M., Schumacher, J., Stripp, G. and Walters, A. (2006). Dynamical constraints on kimberlite volcanism. *Journal of Volcanology and Geothermal Research*, 155, 18-48.

Turner, B.R. (1983). Braidplain deposition of the Upper Triassic Molteno Formation in the main Karoo (Gondwana) Basin, South Africa. *Sedimentology*, 30, 77-89.

Turner, B.R. (1999). Tectonostratigraphical development of the Upper Karoo foreland basin: orogenic unloading versus thermally-induced Gondwana rifting. *Journal of African Earth Sciences,* 28, 215-238.

Van Lente, B., Wickens, D.V., Flint, S., Worden, R. (2003). Petrographic evolution of the early S.W. Karoo foreland basin, South Africa. *British Sedimentological Research Group Annual Meeting*, Leeds, 1 pp.

Veevers, J.J., Cole, D.I. and Cowan, E.J. (1994). Southern Africa: Karoo basin and Cape Fold Belt. *In:* Veevers, J.J. and Powell, C.M.A. (Eds.), Permian-Triassic Pangean Basins and Foldbelts along the Panthalassan Margin of Gondwanaland. *Geological Society of America,* Boulder*, Colorado*, Memoir 184, 223-279.

Viljoen, J.H.A. (1990). K-bentonites in the Ecca Group of the south and central Karoo Basin. *Abstracts Geocongress '90, Geological Society of South Africa, Cape Town,* 576-579.

Visser, J.N.J. (1972). Sedimentêre insluitsels van Karoo-ouderdom in kimberliet van die Finsch-diamantmyn. *Tydskrif vir Natuurwetenskappe,* 32-36.

Visser, J.N.J. (1984). A review of the Stormberg Group and Drakensberg volcanics in southern Africa. *Palaeontologia Africana,* 25, 5-27.

Visser, J.N.J. (1986). Lateral lithofacies relationships in the glaciogene Dwyka Formation in the western and central parts of the Karoo Basin. *Transactions of the Geological Society of South Africa*, 89, 373-383.

Visser, J.N.J. (1997). Deglaciation sequences in the Permo-Carboniferous Karoo and Kalahari basins of southern Africa: a tool in the analysis of cyclic glaciomarine basin fills. *Sedimentology*, 44, 507-521.

Visser, J.N.J., Loock, J.C., van der Merwe, J., Joubert, C.W., Potgieter, C.D., McLaren, C.H., Potgieter, G.J.A., van der Westhuizen, W.A., Nel, A. and Lemmer, W.M. (1976-77). The Dwyka Formation and Ecca Group, Karoo sequence, in the northern Karoo Basin, Kimberley – Britstown area. *Annual Reports of the Geological Survey of South Africa*, 12, 143-176.

Visser, J.N.J., Vonn Brunn, V. and Johnson, M.R. (1990). Dwyka Group. *In:* Johnson, M.R. (Ed.), Catalogue of South African Lithostratigraphic Units. *South African Committee Stratigraphy*, 2-15 – 2-17.

Visser, J.N.J., van Niekerk, B.N. and van der Merwe, S.W. (1997). Sediment transport of the Late Palaeozoic glacial Dwyka Group in the south-western Karoo Basin. *South African Journal of Geology*, 100, 223-236.

Wagner, P. A. (1914). The diamond fields of South Africa. *Johannesburg, Transvaal Leader*.

Williams, A. F. (1932). The Genesis of Diamonds. *London, Ernest Benn Ltd.*